University of Windsor

Scholarship at UWindsor

2008

Examining the effect of Plk4/Sak levels on the transcript profiles of other genes

Alan James Morettin
University of Windsor

Follow this and additional works at: https://scholar.uwindsor.ca/etd

Examining the Effect of Plk4/Sak Levels on the Transcript Profiles of other Genes

by

Alan James Morettin

A Thesis
Submitted to the Faculty of Graduate Studies
Through Biological Sciences
in Partial Fulfillment of the Requirements for
the Degree of Master of Science at the
University of Windsor

Windsor, Ontario, Canada

2008

Author's Declaration of Originality

I hereby certify that I am the sole author of this thesis and that no part of this thesis has been published or submitted for publication.

I certify that, to the best of my knowledge, my thesis does not infringe upon anyone's copyright nor violate any proprietary rights and that any ideas, techniques, quotations, or any other material from the work of other people included in my thesis, published or otherwise, are fully acknowledged in accordance with the standard referencing practices. Furthermore, to the extent that I have included copyrighted material that surpasses the bounds of fair dealing within the meaning of the Canada Copyright Act, I certify that I have obtained a written permission from the copyright owner(s) to include such material(s) in my thesis and have included copies of such copyright clearances to my appendix.

I declare that this is a true copy of my thesis, including any final revisions, as approved by my thesis committee and the Graduate Studies office, and that this thesis has not been submitted for a higher degree to any other University of Institution.

ABSTRACT

The aberrant regulation of cell cycle checkpoints can potentially initiate cellular transformation to an oncogenic state that leads to tumor formation. Many families of cell cycle regulators are present to ensure that normal cellular growth and replication occurs, including the polo-like kinases (Plk). Plk4 (Sak), the newest and most structurally divergent member of the Plks has been implicated to play crucial roles in centrosome dynamics and mitotic progression. Plk4 heterozygous mouse embryonic fibroblasts (MEFs) present a number of phenotypic differences, in comparison to their wild type counterparts that may contribute to the increased incidence of tumor formation observed in heterozygous Plk4 mice. Microarray technology was employed to investigate transcriptional differences between the wild type and heterozygous Plk4 MEFs. Furthermore, transcriptional and protein differences were examined in the Plk4 MEFs in response to DNA damaging agents, to explore a possible role for Plk4 in the DNA damage pathways.

ACKNOWLEDGEMENTS

I would like to thank my supervisor, Dr. John Hudson for giving me the opportunity to pursue a Master's thesis in his laboratory. His guidance was invaluable in my pursuing my Master's thesis.

I am also grateful to my committee members, Dr. William Crosby and Dr. Siyaram Pandey, as well as Dr. Huiming Zhang, my committee chair for taking the time to read my thesis, as well as for their valuable input in my Master's career.

I would like to thank my family and friends for all of their help and support throughout this process.

I would also like to thank Hudson lab member's past and present for all of the good times we had together. It would have been very difficult to get through this process without your help and support. A special thanks to Anna Kozarova for her assistance during my master's project.

TABLE OF CONTENTS

IV.   RESULTS

V.   DISCUSSION

LIST OF TABLES

LIST OF FIGURES

Chapter 1

Review of Literature

General Introduction

The progression of the cell cycle is tightly regulated to ensure proper integrity of

the DNA information and to provide that the genetic material is passed on to viable,

normal daughter cells. The integrity of the genetic material is protected by cell cycle

checkpoints (Elledge, 1996). These checkpoints halt the cell cycle if the DNA has been

damaged or mutated in response to genotoxic stress. Aberrant regulation or loss of one of

these checkpoints can results in errors in DNA replication or in chromosomal

segregation, leading to aneuploidy or polyploidy, predisposing cells to genetic instability

(Xie *et al.*, 2005). This genetic instability can lead to uncontrollable, rapid cellular

proliferation which can eventually form cancerous tumors. The cell cycle is tightly

controlled, with built-in redundancies that are designed to ensure fidelity. The focus of

my research is on Plk4, a member of the polo like kinase (Plk) family of serine/threonine

kinases, which have been shown to control a multitude events throughout the cell cycle

(Xie *et al.*, 2005).

Polo like Kinase Family

The polo like kinases (Plks) are an evolutionary conserved family of cell cycle

regulators (Dai, 2005). The founding member of the Plk family, Polo was first discovered

in *Drosophila melanogaster* (Sunkel *et al*, 1988) and was shown to be serine/threonine

kinase crucial for mitosis (Glover *et al*, 1993). Mutations in the Polo gene lead to

abnomalities in spindle pole formation leading to abnormal mitotic division (Glover *et al*,

1998). Subsequently homologues have been characterized in simple single celled organisms such as yeast to more complex organisms such as mammals. The family, as a whole, plays key roles in the regulation of the cell cycle and DNA damage pathways. The budding yeast, *Saccharomyces cerevisae*, and the fission yeast, *Schizosaccharomyces pombe* (Ohkura *et al.*, 1995), contain one Plk homologue, Cdc5 (Golsteyn *et al.*, 1996), and Plo1 (Ohkura *et al.*, 1995) respectively. *Drosophila* contains two Plk homologues, Polo (Fenton and Glover, 1993) and Plk4 (Lowery *et al.*, 2005), while the nematode, *Caenohabditis elegans* contains three Plk homologues, Plc1, Plc2 (Ouyang *et al.*, 1999), and Plc3 (Chase *et al.*, 2000). Both *Xenopus laevis* and mammals contain four Plk homologues. In *Xenopus,* Plx1 (Kumagai and Dunphy, 1996), Plx2 (Duncan *et al.*, 2001), Plx3 (Duncan *et al.*, 2001), and Plx4 (unpublished data) have all been identified while in mammals, Plk1 (Golsteyn *et al.*, 1994), Snk/Plk2 (Donohue *et al.*, 1994), Prk/Fnk/Plk3 (Donohue *et al.*, 1995) and Sak/Plk4 (Fode *et al.*, 1994) have been characterized. The increase in number of Plk members in more complex organisms is likely a reflection of the need for tighter controls for cell cycle regulation inherent with multicellularity. Plks possess many unique functions throughout the cell cycle including events critical for cell division, centrosome duplication and maturation, DNA damage checkpoint activation, mitotic onset, bipolar spindle formation, Golgi fragmentation and assembly, chromosome segregation, and cytokinesis (Dai, 2005).

Plk Structure

The Plk family consists of catalytic domain at the N-terminus and a one or two polo box domains at the C-terminus of the protein (Dai, 2005) (Figure 1). The catalytic
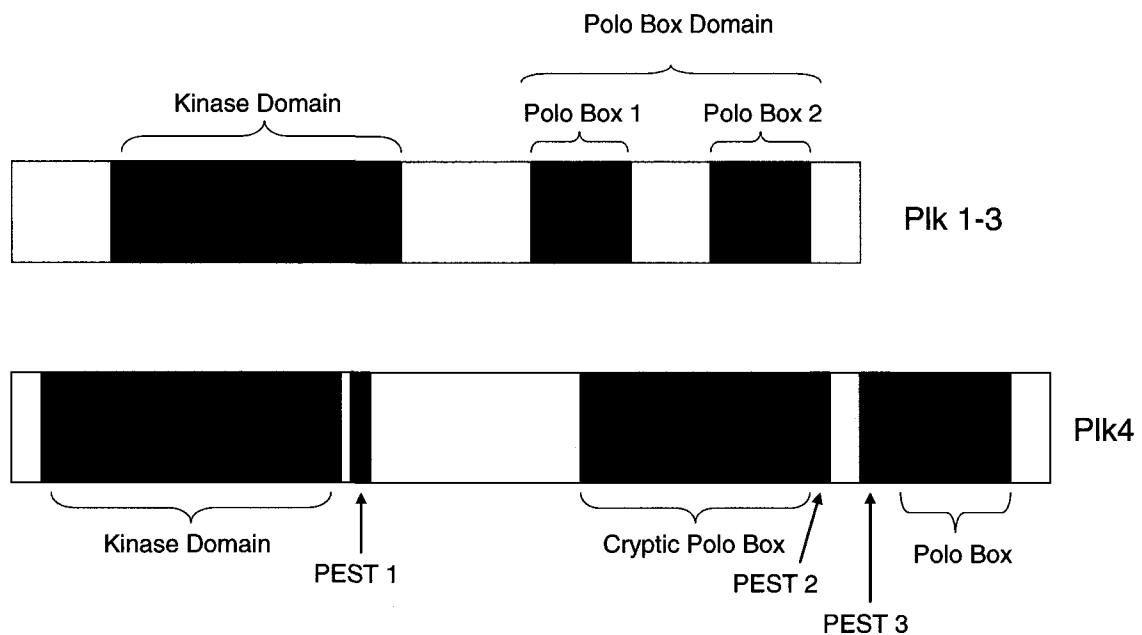
Figure 1: Structural Comparison between Plk4 and of other Plk Family Members

Members of the Plk family all contain a highly homologous kinase domain at the N-terminus and one or two polo box domains at the C-terminus of the protein. Plk4 differs from the other Plks as it contains only one polo box domain. Upstream of Plk4s polo box domain is also a region depicted as the cryptic polo box domain. In addition, Plk4 as contains three PEST sequences associated with reduced protein stability.

domain of the Plks contains their kinase activity and is highly homologous in all Plks.

The polo box domain located at the C-terminus of the protein has been shown to regulate

cellular functions (Seung *et al.*, 2002), subcellular localization (Elia *et al.*, 2003), and

provide a docking site for protein-protein interaction (Reynolds *et al.*, 2003). Plk4 differs

from the other Plks in respect to the polo box domain as it contains only one domain.

Upstream of the polo box domain, Plk4 contains a cryptic polo box domain, which along

with the polo box domain serves as self association domains (Leung *et al.*, 2002). In

addition, Plk4 contains 3 PEST sequences which are commonly associated with reduced

protein stability and this is the case with Plk4 as it displays a short half life of only two to

three hours in non-synchronized cells (Fode *et al.*, 1996) (Figure 1). Though Plk4

contains significant sequence homology to the other Plks in its kinase domain, Plk4

appears to have diverged from a primordial polo-like kinase early in the radiation of

metazoans in respect to the rest of its structure (Hudson *et al.*, 2001).

Plk Expression and Localization Profiles

    a) Unicellular organisms and invertebrates: The mRNA and protein levels of the Plk

family are regulated in a cell-cycle dependent manner. The yeast Plks, Cdc5 and Plo1, in

Saccharomyces cerevisiae and *Schizosaccharomyces pombe* respectively, both localize

to the spindle pole bodies, although the timing of localization differs within the cell cycle.

Cdc5 localization to the spindle pole bodies occurs in G_1 and persists until late mitosis

(Song *et al.*, 2000). Conversely, Plo1 localizes to the spindle pole bodies at the G_2/M

transition when Cdc2 is active and subsequently dissociates from the spindle pole bodies

during anaphase upon Cdc2 inactivation (Mulvihill *et al.*, 1999). Both yeast Plk

homologues also localize to the cytokinetic ring structures, and play a role in cytokinesis. Cdc5 localizes to the septin ring during G_2 and remains activated until late mitosis (Sakchaisri et al., 2004), whereas Plo1 localizes to the medial ring structures when they are formed (Bahler et al., 1998).

The *Drosophila* Plk homologue, polo localizes to the centrosomes during the G_2/M transition and then associates with the nuclear membrane until its breakdown. During prometaphase, polo localizes to the kinetochores and prior to cytokinesis at the mid-part of the central spindle, a structure essential for cytokinesis (Moutinho-Santos et al., 1999).

In all organisms within the Animal kingdom, Plk homologues follow similar patterns of subcellular localization (Glover, 2005) with localization of the protein a reflection of the different role the respective protein plays throughout the cell cycle. In the following sections I will discuss this for Plks1-3. Plk4 will be discussed in detail individually.

b) Mammalian Plks: In humans Plk1 expression increases from late S phase onward and peaks in mid mitosis at which point Plk1 activity is greatest. Plk1 is then targeted for degradation by the anaphase promoting complex in late mitosis. Plk1 expression levels are high in proliferating tissue such as the testis, spleen and thymus (Golsteyn et al., 1994). Plk1 localizes to many cellular structures throughout the cell cycle, in accordance with the many functions Plk1 performs. Plk1 localizes to the nucleus and cytoplasm during G_2, though its localization is specifically targeted to the centrosomes. In early mitosis, Plk1 is present at the centrosome and kinetochores, while in late mitosis Plk1 localizes to the spindle midbody (Golsteyn et al., 1995). The polo box domain is essential

for targeting Plk1 to these subcellular structures as well as to interacting partners throughout the cell cycle (Elia *et al.*, 2003).

Whereas Plk2 displays significant homology to Plk1, its function and tissue distribution differ greatly. Plk2 has been identified as an early response gene with mRNA levels peaking in response to mitogens. Plk2 primarily functions as a regulator of cell proliferation in G_1 (Simmons *et al.*, 1992). Upon its activation at the G_1/S transition, Plk2 localizes to the centrosomes, indicating a role for Plk2 in centriole duplication (Warnke *et al.*, 2004). A role for Plk2 later in the cell cycle may also be plausible. In response to genotoxic stress causing mitotic spindle damage, Plk2 expression was able to prevent mitotic catastrophe (Burns *et al.*, 2003). Whereas no Plk1 activity was detected in the brain, Plk2 is constitutively expressed in the post-mitotic neurons of the brain indicating Plk2 mediates phosphorylation of proteins within the neurons (Kauselmann *et al.*, 1999).

Similarly to Plk2, Plk3 was identified as an immediate early response gene with mRNA levels peaking after the addition of mitogens (Donohue *et al.*, 1995). Like Plk2, Plk3 also displays a broad distribution of tissue specificity (Holtrich *et al.*, 2000). Plk3 expression is relatively low during mitosis, G_1, the G_1/S transition, and peaks during late S phase and G_2 (Ouyang *et al.*, 1997). Discrepancies have emerged over the localization pattern of Plk3 throughout the cell cycle. Previous work has shown that Plk3 localization is polo-box mediated and that Plk3 localizes to the centrosomes, spindle poles, and the spindle midbody (Jiang *et al*, 2006). In contrast, Zimmerman and Erikson, 2006 found that Plk3 localized exclusively to the nucleolus and suggested a role for Plk3 in the G_1/S transition. In this study, Plk3 expression was undetectable during mitosis. Similar to Plk2, Plk3 is also expressed in post-mitotic neurons with a possible role in synaptic plasticity

(Kauselmann *et al.*, 1999). Interestingly, Plk3 has also been implicated to have a role in cellular adhesion (Holtrich *et al.*, 2000).

Plks and Mitotic Entry

The transition from G_2 to mitosis is a crucial junction in the cell cycle. Aberrant regulation of this cellular checkpoint can lead to genomic instability and promote oncogenesis. Members of the Plk family play crucial roles at the G_2/M cellular checkpoint to promote entry into mitosis. Plk1 has been implicated to perform numerous functions to promote mitotic entry within the cell. For mitotic entry to occur, the Cyclin B/Cyclin Dependent Kinase 1(Cdk1) complex must become activated. Plk1 promotes mitotic entry by activating cyclin B/Cdk1 at three levels. Firstly, Plk1 is able to phosphorylate Cdc25C in its nuclear export signal sequence promoting its nuclear translocation and activation (Roshak *et al.*, 2000, Toyoshima *et al.*, 2002). Therefore, Cdc25C is able to dephosphorylate Cdk1 promoting the activation of the cyclin B/Cdk1 and mitotic entry (Gauthier *et al.*, 1991). Secondly, Plk1 phosphorylates both Wee1 and Myt1, both CyclinB/Cdk1-inhibiting kinases. In the fission yeast, *Saccharomyces pombe*, Wee1 is known to phosphorylate Thr14 and Tyr15 on Cdc2, the fission yeast homologue of Cdk1. Though in mammals, Wee1 phosphoryation only occurs on Tyr15 (McGowan *et al.*, 1993). Phosphorylation of Wee1 by Plk1 leads to Wee1 enhanced association with the SCF/beta-TrCp E3 ubiquitin ligase, inducing its degradation (Watanabe *et al.*, 2004). Phosphorylation of Thr14 by Myt1 is the additional phosphorylation that serves to inhibit the activity of Cdk1 (Lui *et al.*, 1997). Thirdly, Plk1 phosphorylates cyclin B at the centrosomes in prophase, this being the first site where cyclin B/Cdk1 is actually

phosphorylated. Though discrepancy remains whether this phosphorylation by Plk1 of cyclin B triggers its nuclear import or whether the cyclin B/Cdk1 complex is activated in a different manner.

Plx1, the *Xenopus laevis* homologue of Plk1 is shown to stimulate activation of cyclin B/Cdc2 complex and regulate mitotic entry through a positive feedback loop. Plx1 phosphorylates and activates Xenopus polo-like kinase-kinase 1 (xPlkk1). Subsequently, xPlkk1 phosphorylates and activates Plx1 (Qian *et al.*, 1998). Activated Plx1 can subsequently phosphorylate and activate Cdc25C which dephosphorylates Thr14 and Try15 on cdc2 promoting mitotic entry (Qian *et al.*, 2001).

Whereas the role of Plk1 in mitotic entry has been well described, the role of the other Plks at the G_2/M checkpoint remains to be elucidated. As Plk2 primarily regulates G_1/S progression, it doesn't appear to play a role in mitotic entry (Simmons *et al.*, 1992). Although Plk3 does not appear to play a role in mitotic entry, in response to DNA damage Plk3 positively regulates p53 activity to halt progression of the cell from G_2 to mitosis (Xie *et al.*, 2001).

Plks and their Role in Mitotic Exit and Cytokinesis

Plks have been shown to play roles in both exit from mitosis and cytokinesis. For mitotic exit to occur, the inactivation of Cdk1 is required. In budding yeast, inactivation of Cdk1 occurs after the metaphase/anaphase transition, which differs from mammalian cells, where downregulation of Cdk1 occurs at the metaphase/anaphase transition (Clute and Pines, 1999). The downregulation of Cdk1 promotes exit from mitosis, and in budding yeast requires the cooperation of the FEAR (Cdc Fourteen Early Anaphase

Release) (Stegmeier *et al.*, 2002) and MEN (Mitotic Exit Network) pathways (Bardin and Amon, 2001) and Cdc5 plays an important role in regulating both of these pathways. Although the role which Cdc5 plays in regulating has yet to be described, it is assumed that Cdc5 coordinates between the FEAR and MEN pathways via phosphorylating regulatory components in each pathway (Lee *et al.*, 2005). Cdc5 and additional components of the MEN pathway are also required for proper actin ring formation at the mother-bud-neck, the site of cytokinesis (Jimenez *et al.*, 1998).

In fission yeast, Plo1 has been implicated in two events regulating cytokinesis. First, Plo1 localizes to the site of cytokinesis, and this localization is important for the placement and organization of the actin-based medial ring (Bahler *et al.*, 1998). Secondly, Plo1 activity correlates with the initiation of septin formation which regulated by the septin initiation network (SIN) (Gruneberg and Nigg, 2003). The SIN and MEN networks contain structurally related proteins that perform similar functions in each pathway. Like Cdc5, the functional significance of Plo1 role in the SIN pathway has yet to be determined.

In *Drosophila*, polo has also been implicated as having a role in cytokinesis as it directs the function of the Pavarotti-KLP (Pav-KLP) family of motor proteins. This family of proteins plays a role in organizing the central spindle in anticipation of cytokinesis (Glover, 2005). Polo and Pav-KLP interact and both co-localize to the central part of the spindle (Liu *et al.*, 2004). Interestingly, studies have revealed that proteins including Polo, Asp (Wakefield *et al.*, 2001), and γ-TuRC (Sampaio *et al.*, 2001) are involved in the organization of the centrosomes and the early mitotic spindles also

perform roles in cytokinesis. It is hypothesized that Polo may phosphorylate these substrates at both the beginning and conclusion of mitosis (Glover, 2005).

In *Xenopus*, the transition from metaphase to anaphase and therefore exit from mitosis requires the activity of Plx1 since inhibition of Plx1 prevents the metaphase to anaphase transition (Qian *et al.*, 1999). The requirement for Plx1 activity suggests that Plx1 may control the anaphase-promoting complex/cyclosome (APC/C). Three possible mechanisms have been hypothesized; first, Plx1 may activate the APC/C through direct phosphorylation of several APC/C subunits (Kotani *et al.*, 1998). Secondly, Plx1 may regulate the activators or inhibitors of the APC/C (Reimann *et al.*, 2001), or thirdly, Plx1 could activate the APC/C and prevent premature inactivation of the APC/C (Brassac *et al.*, 2000). Additionally, the inactivation of Plx1 may be required for the completion of cytokinesis to occur (Qian *et al.*, 1999).

Like Plx1, Plk1 may be involved both directly and indirectly in the activation of the APC/C. Activation of the APC/C may occur through direct phosphoryation of APC/C subunits along with the phosphorylation of the cyclin B/Cdk1 complex (Golan *et al.*, 2002). Indirectly, Plk1 is responsible for activating the APC/C by inducing the destruction of APC/C inhibitor "Early mitotic inhibitor 1" (Emi1) (Moshe *et al.*, 2004). Similar to other Plk homologues, Plk1 has also been implicated to play a role in cytokinesis. Although the exact role that Plk1 plays in cytokinesis is unknown, Plk1 has been shown to interact with and phosphorylate cytokinetic proteins. Plk1 phosphorylates the kinesin-like motor protein CHO1/MKLP-1 (Lee *et al.*, 1995), NudC (a component of the dynaction complex Zhou *et al.*, 2003), the mitotic kinesin-like protein 2 (MKlp2) (Neef et *al.*, 2003), and the Rho exchange factor ECT2 (Niiya *et al.*, 2005). Though the

functional significance of some of these interactions remains to be elucidated, phosphorylation of NudC and MKlp2 by Plk1 are indispensible for the execution of cytokinesis. To date, Plk2 and Plk3 have not been implicated in mitotic exit or cytokinesis.

Plks and their Role in DNA Damage Pathways

The cellular response to DNA damage by genotoxic stress is crucial, as failure to repair any damage in the genetic material can produce aneuploidy leading to uncontrolled cellular growth and oncogenesis. In response to genotoxic stress, cell cycle checkpoints are employed to repair damage that has occurred to the DNA or to initiate apoptosis if the damage is irreparable. Plks have been implicated to play crucial roles in the DNA damage pathways.

In response to DNA damage, the DNA damage sensor proteins, ataxia-telangiectasia mutated (ATM) or ataxia-telangiectasia and Rad3-related (ATR) become activated (Bakkenist et al., 2003). Activation of ATM or ATR in response to DNA damage inhibits the function of Plk1 (van Vugt et al., 2001). The inhibition of Plk1 by ATM or ATR is mediated by the ATM/ATR downstream effector kinase checkpoint kinase 1 (Chk1). Experimentally it has been observed that the inhibition of Plk1 is rescued in Chk1-depleted cells exposed to UV radiation (Tang et al., 2006). Inhibition of Plk1 in response to DNA damage prevents it from promoting mitotic entry in the presence of genomic instability. Subsequently, Plk1 also binds to and phosphorylates the tumor suppressor p53 inhibiting its function, thus preventing p53 mediated pro-apoptotic pathways. Expression of ATM is able to attenuate Plk1 interaction with p53 (Ando et al.,

11

2004). Whereas Plk1 is able to negatively regulate p53 function, Plk3 positively regulates

the transcriptional function of p53. In response to DNA damage, ATM phosphorylates

Plk3 activating its kinase ability and Plk3 then phosphorylates p53 on a different residue

from Plk1, promoting p53 mediated G_2/M cell cycle arrest and apoptosis (Xie *et al.*,

2001).

In addition, Plk3 has been implicated to play a role in DNA damage repair. Plk3

is able to regulate the activity of DNA polymerase δ (pol δ), a major enzyme in DNA

damage repair (Hubscher *et al.*, 2002). Plk3 phosphorylates pol δ on p125, the major pol

δ subunit on Ser60. Though the functional significance of this interaction remains to be

elucidated, it is speculated that since Plk3 phosphorylates p125 in its nuclear localization

signal, this phosphorylation controls the subcellular localization of pol δ (Xie *et al.*,

2005).

Plk2 may also play a role in DNA damage pathways. In response to ionizing

radiation, mRNA transcript levels of Plk2 were shown to increase. This response was

deemed to be p53 dependent as based on luciferase assay data; a candidate site for a

radiation response element was mapped to the Plk2 promoter containing a p53 binding

motif (Shimizu-Yoshida *et al.*, 2001). A subsequent study showed that p53 indeed

regulates Plk2 in response to genotoxic stress. In response to mitotic spindle damage,

Plk2 is activated in a p53 dependent manner and this activation prevents mitotic

catastrophe (Burns *et al.*, 2003) (Figure 2).

Figure 2: Role of Plks in the DNA damage Pathways

In response to either ultraviolet radiation (UV) or ionizing radiation (IR), the DNA

damage sensor proteins ataxia telangiectesia and Rad3 related (ATR) and ataxia

telangiectesia mutated (ATM) become activated, respectively. In response to either UV

or IR damage, Plk1 is either inhibited by ATR or ATM. Subsequently, ATR activates

checkpoint kinase 1 (Chk1), or ATM activates checkpoint kinase 2 (Chk2). Normally,

Plk1 activates cell division cycle 25c (Cdc25c) promoting G_2/M transition. Since Plk1 is

inhibited by either ATR or ATM, Cdc25c activity is inhibited by Chk1 or Chk2 in

response to UV or IR, respectively. In response to IR, ATM also activates Plk3, which

activates DNA polymerase δ, promoting DNA repair. In addition, Plk3 can activate Chk2

and p53, while Chk2 can also activate p53. The activation of p53 inhibits progression of

the cell cycle from G_2 to mitosis. Plk2 activity is also initiated by p53 in response to

DNA damage. The role that Plk4 may play in the DNA damage pathways remains to be

elucidated. Plk4 interacts with ATM, ATR, Chk1, Chk2, p53, and Cdc25c, though the

functional significance of these interactions remains to be described. Black arrows denote

activation, red bars denote inhibition.

Ultarviolet
Radiaton

Ionizing
Radiation

DNA Damage

DNA
Repair

ATR

ATM

Chk1

Plk1 → Chk2 ← Plk3 → Polδ

Cdc25c

p53 → Plk2

Plk4???

G₂ ——→ M
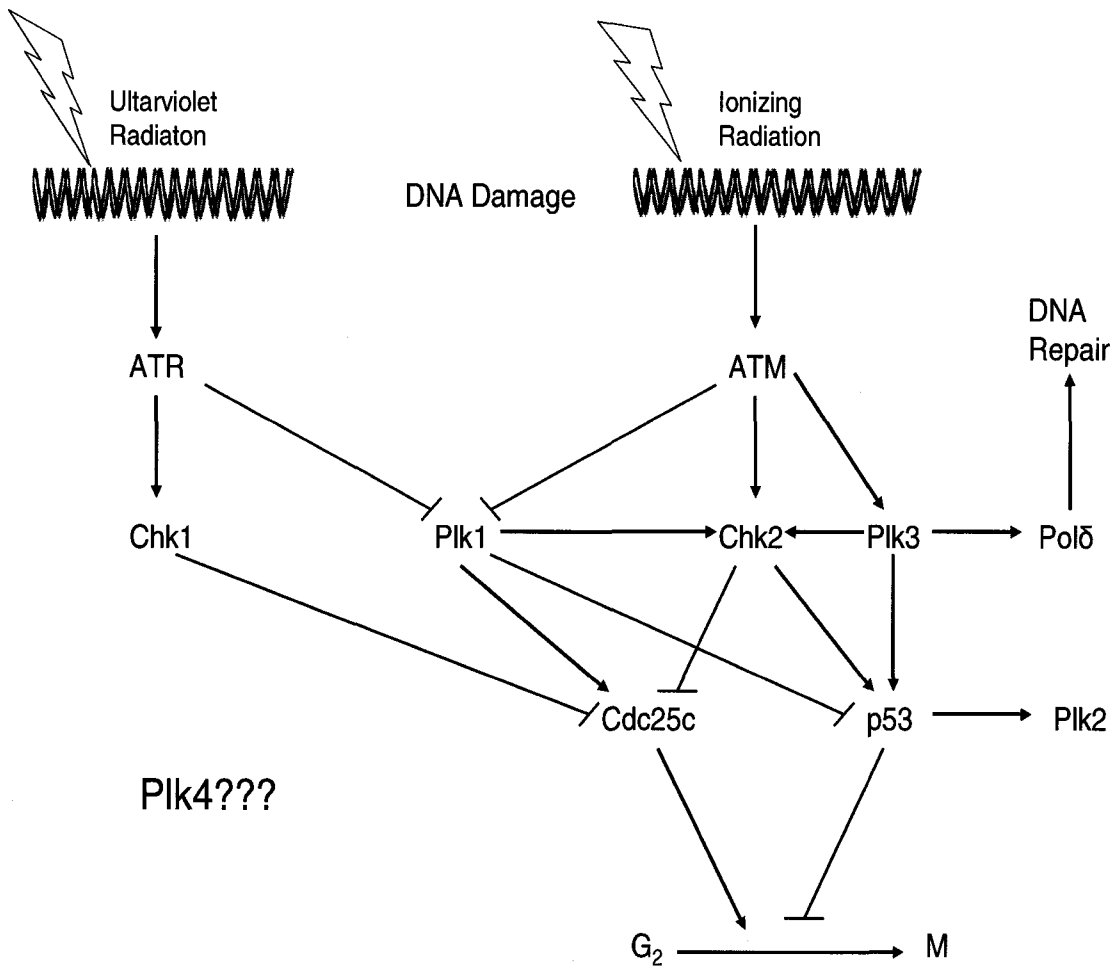
Plks and the Centrosomes

The centrosome plays a major role in organizing the microtubule cytoskeleton of the cell and is the organizational centre of an astral array of microtubules that participate in cellular functions including intracellular trafficking, cell motility, cell adhesion, and cell polarity. In proliferating cells, the centrosomes participate in the assembly and organization of the mitotic spindle, their spatial orientation, and cytokinesis (Azimzadeh and Bornens, 2007).

The centrosome consists of two centrioles with an orthogonal arrangement linked together at their proximal regions by a matrix consisting of proteins of the pericentrin family (Nigg, 2007; Dawe *et al.*, 2007). The centrosomes replicate once during the cell cycle with each centrosome consisting of a mother/daughter centriole. During G_1, centriolar disengagement occurs through the actions of separase (Tsou and Stearns, 2006). Though the orthogonal arrangement is lost, the centrioles are still connected by a tether of microfilaments (Bahe *et al.*, 2005). In S phase, a procentriole grows from the existing centriole at an orthogonal angle through the activity of several centriolar proteins. The procentriole continues to grow till G_2 until it reaches full maturity. Subsequently, the tether of filaments connecting the two mother centrioles together is severed to allow the centrosomes to enable spindle formation and chromosome segregation during mitosis (Mayor *et al.*, 2000).

The centrosome has also been implicated in playing a role in DNA damage checkpoint control (Fletcher and Muschel, 2006). Centrosome inactivation has been observed to be part of the DNA damage control system seen in *Drosophila*. In response to DNA damage, centrosome function was abrogated causing spindle defects and

subsequent failure in chromosomal segregation. These results indicated that centrosome inactivation is a checkpoint independent and mitosis-specific response to genotoxic stresses (Sibon *et al.*, 2000). Additionally, in mammalian cell lines, centrosomal segregation is inhibited in G_2 in response to DNA damage. Centrosomal segregation is controlled by the protein kinase Nek2 whose activity is inhibited by DNA damage (Fletcher *et al.*, 2004). Interestingly, Plk1 can interact with and phosphorylate Nek2 promoting centrosomal segregation. However, in response to DNA damage the activity of Plk1 is inhibited, therefore preventing Nek2 from promoting centrosomal segregation. The inhibition of centrosome segregation occurs in an ATM/ATR dependent manner (Zhang *et al.*, 2005).

Members of the Plk family have been implicated to play additional crucial roles in the centrosome cycle. In fission yeast, loss of function of Plk1 homologue, Plo1 leads to mitotic arrest where the chromosomes are condensed with only a monopolar spindle present (Ohkura *et al.*, 1995). In contrast, in budding yeast, Cdc5 may be required for microtubule nucleation, though Cdc5 activity is not essential for the establishment of bipolar spindles (Lee *et al.*, 2005). In *Drosophila*, Plk homologue polo is required for the recruitment of two crucial centrosomal components: CP190 and γ-tubulin. In polo mutants, CP190 and γ-tubulin are unable to localize specifically to the centrosomes, instead they scatter throughout the mitotic spindles (Dai and Cogswell, 2003). A similar inability to recruit γ-tubulin to the centrosomes has also been observed in mammalian cell lines (Lane and Nigg, 1996). In addition, polo is required to phosphorylate and activate centrosomal protein Asp which is required for microtubule nucleation (Avides *et al.*, 2001). Asp mutants present mitotic spindles with highly unfocused poles and a high

mitotic index. In polo mutants, Asp is still able to localize to the centrosomes, though its activity is negligible. In polo and asp double mutants, there is a substantial increase in mitotic index (Gonzalez *et al.*, 1998). Polo is also required for the nucleation of microtubules by centrosomes. The chaperone protein heat shock protein 90 (Hsp90) is required to ensure the stability of polo. Inhibition of Hsp90 results in inactivation of polo kinase activity, thereby abolishing the nucleation of the microtubules (de Carcer *et al.*, 2001). In *Xenopus* it is also assumed that Plx1 regulates centrosome separation and maturation by recruiting proteins to the centrosomes. This assumption is supported by the finding that inhibition of Plx1 results in monopolar spindles with α-tubulin not localizing to the centrosomes (Qian et *al.*, 1998).

In mammalian cells, centrosome maturation is also dependent on Plk1, which phosphorylates Nlp, a centrosome protein. This allows Nlp to be removed from the centrosomes and for the recruitment of microtubule nucleation scaffolding (Casenghi *et al.*, 2003). In addition, Plk1 plays a role in centrosome separation as depletion of Plk1 leads to monopolar spindles and eventually mitotic arrest (Lane and Nigg, 1996). Plk1 may also regulate spindle formation as it has been shown to phosphorylate α-, β-, γ-tubulins and the tubulin stabilizing protein TCTP (Feng *et al.*, 1999) (Yarm, 2002). Interestingly, it has been shown that Plk1 does not need to be bound to the centrosomes to perform its centrosomal functions. Hanisch *et al.*, 2006 showed that delocalized Plk1 can still contribute to centrosome maturation, separation and spindle formation but not chromosome segregation.

Plk2 kinase activity is required for initiation of centriole duplication at the G_1/S transition. Previous work has shown that overexpression of a catalytically inactive form

of Plk2 blocks centriole duplication (Warnke *et al.*, 2004). Subsequently, inhibition of

Plk2 through siRNA also blocked centriole duplication. Alternatively, overexpression of

Plk2 causes an increase in centrosome number. Plk1 has also been described to be

required for centriole duplication (Liu and Erikson, 2002). Though in contrast to Plk2,

kinase activity of Plk1 is not required for initition of centriole duplication at the G_1/S

transition (Warnke *et al.*, 2004). Whereas Plk2 initiates centrosome duplication, Plk1

ensures centrosome maturation (van de Weerdt and Medema, 2006). To date, no evidence

has been presented implicating Plk3 with a role in centriole duplication or centrosome

function.

Plks and Oncogenesis and Tumor Development

Since Plks are crucial cell cycle regulators, aberrant regulation of their function

may contribute to oncogenesis, designed as a shift to cellular proliferation stimulating

signals to encourage uncontrollable cellular growth. This uncontrolled cell growth will

eventually lead to tumor formation and cancer (Eckerdt *et al.*, 2005). Plk1 expression

and activity are tightly controlled throughout the cell cycle, though Plk1 mRNA and

protein levels have been found to be significantly increased in proliferating cells (Wolf *et al.*, 2000). Plk1 is over expressed in tumor cell lines, indicating that Plk1 could lead to

enhanced cellular proliferation and eventually cell transformation (Simizu and Osada,

2000). Elevated Plk1 levels are also found in a number of cancers including non-small-

cell lung cancer, head/neck squamous cell carcinomas, esophageal carcinoma,

oropharyngeal carcinomas, melanomas, breast cancer, ovarian cancer, pancreatic cancer,

prostate carcinomas and papillary carcinomas (Eckerdt *et al.*, 2005). Increased levels of

Plk1 have also been correlated with severity of diagnosis and patient prognosis (Kneisel *et al.*, 2002).

The ability of Plk1 to induce oncogenesis may be due to its capacity to interact with several tumor suppressor genes. Plk1 is able to to bind to the DNA binding domain of p53 (Ando *et al.*, 2004) and phosphorylate a residue which blocks p53's transcriptional activity inhibiting its proapoptotic function (Xie *et al.*, 2001). In contrast, p53 activity is significantly stabilized in Plk1-depleted cells (Liu and Erikson, 2003).

Checkpoint kinase 2 (Chk2), another tumor suppressor protein also interacts with Plk1. A Chk2 mutant lacking catalytic activity has been shown to contribute to increased risk of breast cancer (Meijers-Heijboer *et al.*, 2002). Chk2 and Plk1 both colocalize at the centrosomes in early mitosis, and to the mid-body in late mitosis (Tsvetkov *et al.*, 2003). In response to ionizing radiation, Plk1 can phosphorylate Chk2 at Thr-68, a site normally phosphorylated by ATM. The phosphorylation of Chk2 by ATM usually activates Chk2 which then phosphorylates BRCA1 which inhibits the activity of Plk1 (Ree *et al.*, 2003). Though the physiological significance of Plk1's phosphorylation of Chk2 remains to be elucidated, it is believed the Plk1 phosphorylation of Chk2 may contribute to a crosstalk between the DNA damage pathways and mitotic regulation (Matsuoka *et al.*, 2000). A network of tumor suppressor proteins is in place to suppress the oncogenic functions of Plk1, inhibiting its ability to promote mitosis and cell growth. Therefore, in response to DNA damage, it requires the loss of function of numerous tumor suppressor proteins to promote oncogenesis. It is believed that Plk1 function is inhibited in two ways in response to DNA damage. If damage occurs within interphase, Plk1 activity is inhibited in an ATM/ATR dependent manner through the activity of either Chk1 or BRCA1. In

response to DNA damage occurring within mitosis, Plk1 is inhibited through an ATM/ATR independent manner, through the activation of retinoblastoma protein (RB) by p53 (Eckerdt *et al.*, 2005) (Figure 3).

While Plk2 expression has yet to be correlated with the progression or suppression of tumor formation in any cancer, through its actions in the cell cycle, Plk2 may play a crucial tumor suppressor role. In response to DNA damage, the activity of Plk2 is transcriptionally up-regulated in a p53 dependent manner. This activation is able to prevent mitotic catastrophe following mitotic spindle damage by activating the spindle checkpoint (Burns *et al.*, 2003). The activation of the spindle checkpoint prevents the completion of mitosis which can contribute to genomic instability and the promotion of oncogenesis.

In contrast to Plk1, Plk3 expression is negatively correlated with the development of cancer. Plk3 mRNA levels are either undetectable or down-regulated in lung carcinomas (Li *et al.*, 1996), head/neck squamous cell carcinomas (Dai *et al.*, 2000), and in carcinogen-induced rat colon tumors (Dai *et al.*, 2002). Furthermore, ectopic expression of Plk3 decreases cellular proliferation in fibroblasts (Dai *et al.*, 2000), while over expression of a catalytically active form of Plk3 induces chromatin condensation, rapid cell cycle arrest and eventual apoptosis (Conn *et al.*, 2000; Wang *et al.*, 2002). These observations indicate a tumor suppressor role for Plk3 though, to the contrary, Plk3 along with Plk1 were both found to be over expressed in malignant epithelial ovarian tumors, with over-expression correlating with an enhanced mitotic index and decreased patient survival (Weichert *et al.*, 2004).

In contrast to Plk1 during the cell cycle, which mediates oncogenic cellular transformation, Plk3 inhibits mitosis in the presence of damage to the genome. Plk3 activation in response to DNA damage is mediated in an ATM-dependent fashion. Plk3 can in turn activate tumor suppressor proteins like Chk2, which subsequently inhibit the mitotic-promoting functions of Plk1, or p53 which initiates apoptotic pathways (Xie *et al.*, 2001). Therefore, Plk3 function maybe crucial to inhibiting the progression of cells to an oncogenic state.

Polo-like Kinase 4 (Plk4)/Sak

Plk4 or Sak (*S*nk/Plk-*a*kin *k*inase), was first identified in a screen of a murine lymphoid cDNA library for wheat germ agglutinin (WGA) resistant clones and was found to be a putative protein-serine/threonine kinase. Due to its expression pattern and sequence similarity with *Drosophila* polo, it was suggested that Plk4 played a role in cell cycle regulation (Fode *et al.*, 1994). Murine Plk4 is located on chromosome 3 while the human homologue is found on chromosome 4q28 (Swallow *et al.*, 2005). In mice, two isoforms have been identified while only a single isoform of the product protein found in humans. The Plk4-a and Plk4-b variants differ in respect to the C-terminus end. Plk4-a encodes a 925 amino acid (aa) protein while Plk4-b encodes a 464 aa protein. The first 416 aa of Plk4-a and Plk4-b are identical while at the C-terminus end Plk-a region encodes 509 aa and Plk-b encodes 48 aa. Murine Plk4 has 15 coding exons and both the Plk-a and Plk-b variant are encoded for by a single gene. Human Plk4 differs from the murine Plk4-a in that contains a 34 aa insertion adjacent to exon 5 that is found in the murine Plk4-b variant (Hudson *et al.*, 2000).

Figure 3: Interactions between Plks and Tumor Suppressor Proteins

Members of the Plk family interact with tumor suppressor proteins and have been

implicated in the progression or inhibition of oncogenesis. Plk1 activity is either inhibited

directly or indirectly by ataxia telangiectesia and Rad3 related (ATR), ataxia

telangiectesia mutated (ATM), checkpoint kinase 1 (Chk1), checkpoint kinase 2 (Chk2),

Breast cancer 1 gene (BRCA1), Retinoblastoma protein (pRb) and p53. The inhibition of

Plk1 activity is in response to activation of the DNA damage or mitotic spindle

checkpoints. Whereas Plk1 promotes progression through the cell cycle, Plk2 and Plk3

suppress the cell cycle in response to damage. Loss of function of one or more of these

tumor suppressor proteins, can lead to aberrant regulation of the cell cycle and the

progression of oncogenesis. Though the exact function of Plk4 as a tumor suppressor or

oncogene has yet to be determined, the fact that heterozygous Plk4 mice develop tumors

at a rate higher than wild type litters, supporting the notion that Plk4 plays a significant

role in these oncogenic pathways. Black arrows denote activation; red bars denote

inhibition.
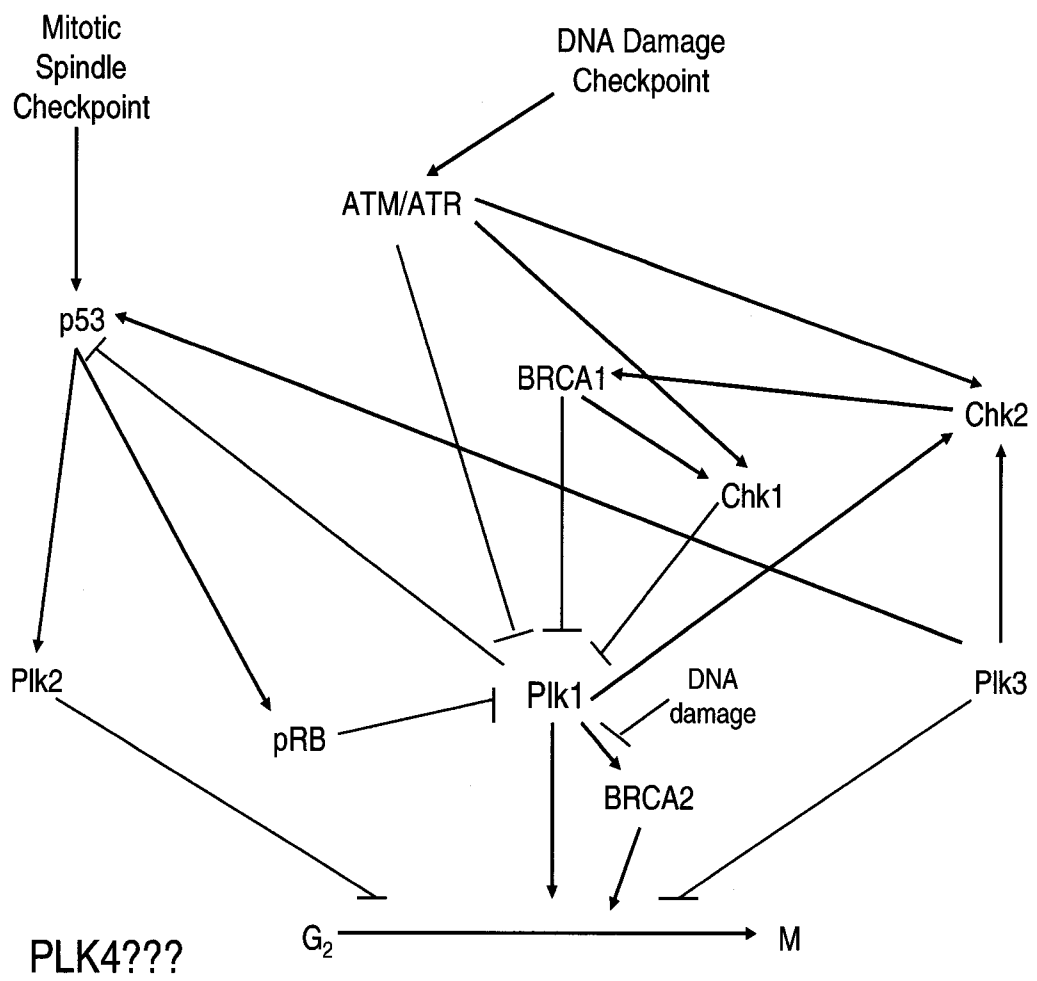
Plk4 Expression Profile and Localization

Like Plk1, Plk4 mRNA and protein levels are regulated in a cell cycle dependent

manner with Plk4 expression low in G1, increasing during DNA replication and G2 and

peaking during cytokinesis. Plk4 is targeted for ubiquitination by the anaphase promoting

complex (Fode *et al.*, 1996). Plk4 expression is also highest in rapidly proliferating

tissues, such as the testis, spleen, and thymus (Fode *et al.*, 1994). Differing views have

emerged concerning the localization of Plk4 during the cell cycle. Previous work has

shown that Plk4 localized to the nucleolus and perinuclearly in G2, and to the

centrosomes in early mitosis. During anaphase, Plk4 localized throughout the cell and in

telophase to the cleavage furrow (Hudson *et al*, 2001). This pattern of localization was

supported by (Martindill *et al*, 2007) where Plk4 showed a similar localization pattern

and was shown to phosphorylate the developmental protein Hand1, controlling its

nucleolar release. In contrast, Habedanck *et al*, 2005 showed Plk4 localized exclusively

to the centrosomes throughout the cell cycle. In support of this finding, Bettencourt-Dias

et al, 2005 working with *Drosophila melangastor* cells showed Plk4 localization to the

centrosomes throughout the cell cycle. Among the other Plk family members, both of the

polo box domains are necessary for subcellular localization (Jang *et al.*, 2002), but in

Plk4 there is debate whether the polo box domain itself is sufficient for localization.

Previous work has shown that the polo box itself is sufficient for localization of Plk4,

though a truncated mutant lacking both the polo box and cryptic polo box region reduced

the efficiency of Plk4 for localization (Leung *et al.*, 2002). In contrast, an additional

study has shown that the polo box region itself is not sufficient for localization

(Habedanck *et al*, 2005).

Plk4 and the Centrosomes

Plk4 has been identified as a key regulator of centriole duplication. Over-expression of Plk4 leads to centrosome amplification through the generation of numerous progeny centrioles from a parental centriole (Habedanck *et al.*, 2005; Kleylein-Sohn *et al.*, 2007). Conversely, inhibition of Plk4 activity leads to inhibition of centriole formation in *Drosophila* cells and subsequently the formation of basal bodies and flagella (Habedanck *et* al., 2005; Bettencourt-Dias *et al.*, 2005). In the initial studies, both kinase activity and presence of the cryptic polo box domain of Plk4, which is necessary for localization to the centrosome were required to induce amplification. The necessity of the kinase domain indicates that Plk4 may be required to target key substrates that are involved in the centrosome cycle. It was also observed that over expression of a catalytically inactive form of Plk4 could induce some centrosome amplification, albeit through a different mechanism that likely involves cell division failure through a dominant-negative method of action (Habedanck *et al.*, 2005). Over expression of Plk4 produces a phenotype reminiscent of a flower, with progeny centrioles arranged around the parental centriole like petals. Plk4 appears to localize to the parental centriole at the G_1/S transition, and this localization initiates multiple centriole duplication sites around the parental centriole. In addition, the localization of Plk4 to the parental centriole initiates that rapid recruitment of centriole proteins hSas6, CPAP, Cep135 and γ-tubulin to the parental centriole (Kleylein-Sohn *et al.*, 2007). Whether Plk4 interacts with or phosporylates any of these proteins to recruit them to the parental centriole remains to be elucidated. These proteins along with CP110 provide the foundation for procentriole formation. Plk4 appears to be the upstream regulator required for initiation of centriole

duplication and the recruitment of other proteins. Inhibition of hSas-6, CPAP, Cep135, CP110 or γ-tubulin *via* siRNA suppresses Plk4's ability to induce centriole formation (Kleylein-Sohn *et al.*, 2007). Therefore, the activity of Plk4 is likely tightly regulated within the cell cycle since aberrant activity would produce centriole over duplication. The kinase responsible for activating Plk4 function or the counteracting phosphatase responsible for suppressing Plk4 activity remains to be identified.

It is noted that cyclin-dependent kinase 2 (Cdk2) has been implicated as having a role in centrosome duplication and that inhibition of Cdk2 activity suppresses centrosome duplication (Matsumoto *et al.*, 1999). Interestingly, over-expression of Plk4 requires the activity of Cdk2 to produce centrosome amplification, while a catalytically inactive Cdk2, or the presence of the Cdk2 inhibitor p27 suppresses Plk4-induced centrosome amplification. Conversely, Cdk2 requires Plk4 activity to perform its role in centrosome duplication, indicating Cdk2 and Plk4 in their respective functions cooperate (Habendanck *et al.*, 2005).

Interestingly, the over-expression phenotype of Plk4 is similar to the phenotype observed in heterozygous Plk4 MEFs. The heterozygous MEFs present a phenotype of increased centrosomal amplification, multipolar spindle formation and subsequent mitotic failure (Ko *et al.*, 2005). It is plausible that reduced Plk4 activity in the heterozygous MEFs can cause cellular division failure from aberrant centrosome segregation or abnormal mitotic spindle formation (Habendanck *et al.*, 2005). The findings within heterozygous MEFs are likely due a reduced gene dose of Plk4.

In contrast, depletion of Plk4 in human cells by siRNA causes a step by step reduction in centriole number resulting in the presence of monopolar spindles during

mitosis (Habedanck *et al.*, 2005). Additionally, inhibition of Plk4 *via* siRNA leads to an increased mitotic index and an increase in apoptotic cells (Bettencourt-Dias *et al.*, 2005). In *Drosophila* cells, inhibition of Plk4 leads to the failure of several centrosomal proteins, γ-tubulin, CP190 and Cnn to localize to the centrosomes. Additionally, cells lacking γ-tubulin at the spindle poles also had no detectable pericentrin-like protein (D-PLP). In contrast, inhibition of polo did not affect D-PLP presence at the spindle poles. Although inhibition of Plk4 leads to a reduction and failure in centrosome number and centriole formation, in contrast inhibition of polo doesn't reduce centrosome number or affect centriole formation. Interestingly, inhibition of Plk4 and a reduction in centrosome number did not effect cell cycle progression. However, Plk4 null *Drosophila* adults were uncoordinated and eventually died as a result of a failure to produce basal bodies, a centriolar derived structure in the sensory neurons (Bettencourt-Dias *et al.*, 2005).

Plk4 Role in Mitosis

Plk4 plays a crucial role in regulating centrosome dynamics, although whether Plk4 plays any additional roles in the cell cycle remains to be elucidated. Experimental evidence suggests a role for Plk4 in promoting mitotic entry since Plk4 interacts with two key genes in the G_2/M transition. Plk4 interacts with and phosphorylates Cdc25C (Bonni *et al.,* 2008) and interacts with cyclin B (Hudson *et al.*, unpublished data), though the functional significance of these interactions remains to be described. Plk4 may also play a role in promoting mitotic exit. In Plk4 null mice where embryonic lethality is observed, high levels of cyclin B are observed in anaphase and telophase cells (Hudson *et al.*,

2001). This is indicative of cells arresting late in mitosis. Therefore, Plk4 may play a crucial role in the APC/C dependent destruction of cyclin B.

Plk4 Role in DNA Damage Pathways

As with the other Plk family members, Plk4 may also play a role in the DNA damage pathways since Plk4 has been shown to interact with p53 (Swallow *et al.*, 2005) and Plk4 expression is repressed in a p53 dependent manner in response to DNA damaging agents (Li *et al.*, 2005). It was determined that p53 repression of Plk4 activity occurred through the recruitment of a histone deacetylase (HDAC) transcription repressor. In addition, Plk4 repression through RNA interference allowed p53-induced apoptosis to occur, while Plk4 overexpression attenuated p53-mediated apoptosis. Though a direct role for Plk4 in DNA damage pathways has yet to be described, Plk4 has been shown to interact with various sensor, transducer and effector proteins including ATM, ATR, Chk1, Chk2, and members of the Cdc25 phosphatase family (Hudson *et al.*, unpublished data). Therefore, it is plausible that Plk4 may play a substantive role in the cellular response to genotoxic stresses.

Plk4 Null Mice

To study the role of Plk4 in embryogenesis and to determine the effect of loss of Plk4 function in mice, a Plk4 null allele was generated by replacing exons 1 and 2 with a Neo gene deleting the start of translation (Hudson *et al.*, 2001). It was discovered that Plk4 null mice arrested at approximately 7.5 days post coitum after gastrulation had occurred. Formation of the neural plate was evident but somite development and neural

tube formation failed to occur (Hudson *et al.*, 2001; Swallow *et al.*, 2005). An examination at 8.5 days found that Plk4 null embryos were smaller than both wild type and heterozygous embryos with the embryonic and extra embryonic structures that were reduced in size. Null embryos showed an increased number of cells present in mitosis indicating a block or delay in mitosis which was confirmed by phosphorylated histone H3 detected six times more frequent in null embryos. Outgrowths from E2.5 blastocysts were compared, and Plk4 null outgrowths were smaller and DNA synthesis was reduced in comparison to the wild type. As seen with embryos at E8.5, 68% of Plk4 null outgrowths were positive for phosphorylated histone H3 compared to only 17% of wild type outgrowths indicating an anaphase block had occurred in the nulls (Hudson *et al.*, 2001). Plk4 null blastocysts also displayed an increased number of cells present with a dumbbell morphology indicating a block in telophase (Hudson *et al.*, 2001; Swallow *et al.*, 2005). Plk4 null embryos also presented a high number of cells with a late mitotic delay leading to a high apoptotic rate.

Plk4 was the first member of the polo like kinase family to be studied by germline mutation; whereas experimental data indicates that Plk4 is required for embryonic development, a study by Ma *et al.*, 2003 showed that in contrast Plk2 null mice were not embryonic lethal. Plk2 null mice were smaller than their littermates and show a slight delay in skeletal development. In addition, Plk2 null mice were all fertile and show comparable survival rates to their heterozygous and wild type littermates (Ma *et al.*, 2003). These results indicated that although Plk2 may play an essential role in cell cycle progression, it is not essential for embryonic development. To date, no germline

mutations of Plk1 or Plk3 have been devised to assess the functional significance of these genes in an animal system.

Plk4 Mouse Embryonic Fibroblasts (MEFs)

Consistent with the embryonic lethality observed with Plk4 null embryos, the establishment of Plk4 null MEFs was unsuccessful indicating the Plk4 is not only necessary for embryonic development but also for cell viability (Hudson et al 2001; Ko *et al.*, 2005). In contrast, Plk2 null MEFs are viable though they are delayed in entering S phase (Ma *et al.*, 2003).

Plk4 heterozygous MEFs are viable though they exhibit a slower growth rate compared to wild type MEFs (Ko *et al.*, 2005). Plk4 heterozygous MEFs presented a number of mitotic defects including abnormal spindle number as well as abnormal chromosomal number and segregation. The percentage of MEFs with greater than three centrosomes was significantly increased in heterozygous Plk4 MEFs, while the presence of more than one microtubule organizing centres (MTOC) was observed in approximately one-third of Plk4 heterozygous MEFs in interphase (Ko *et al.*, 2005; Swallow *et al.*, 2005). A similar phenotype is observed in MEFs deficient in p53 or p21 with an incidence of centrosome amplification similar to that of Plk4 heterozygous MEFs (Carroll *et al.*, 1999). Tatapore *et al.* showed that in p53 null MEFs there was an increase in centrosome and MTOC number. Plk4 heterozygous MEFs contain mRNA and protein levels at about 50% the level found in wild type MEFs (Swallow *et al.*, 2005).

Cancer Development in Plk4 Heterozygous Mice

Plk4 heterozygous mice are healthy and fertile and show no abnormal defects early in development (Hudson *et al.*, 2001; Ko *et al.*, 2005). On the other hand, aged Plk4 heterozygous mice (18-24 months) developed primary hepatocellular (HCC) liver tumors at a frequency of 50% in comparison with only 3% in wild type mice. These liver tumors were typically multifocal indicating a predisposition to tumor development throughout the liver. Further examination showed that the hepatocytes presented a high mitotic index and nuclear atypia. Tumor development in heterozygous mice was also observed in the lung with papillary adenocarcinomas discovered in the periphery of the lung parenchyma. In addition, a few heterozygous mice developed large soft tissue tumors of the axilla and upper chest wall (Ko *et al.*, 2005).

A two-thirds partial hepatectomy was employed to study the molecular basis why Plk4 heterozygous mice were predisposed to mitotic errors. This method was employed to induce dormant hepatocytes back into the cell cycle. It was shown that 44 hours after partial hepatectomy, Plk4 heterozygous hepatocytes had a significantly higher incidence of tri- or tetrapolar spindles leading to abnormal mitosis. Introduction of hepatocytes in S phase was delayed by four hours in heterozygotes as seem by the persistence of Cdk2 activity and the delay of phosphorylation of Rb. Subsequently, entry into mitosis was delayed in heterozygous Plk4 livers as observed by the persistence of cyclin B1, and phosphorylated Cdk1. Seven days post hepatectomy, heterozygous hepatocytes were poorly organized, though normal liver mass was restored and no difference in the survival rate was observed in both wild type and heterozygotes,. Six months post partial hepatectomy, 70% of heterozygous mice displayed hepatocellular dysplasia with nuclear

atypia as well as disorganization in the normal liver architecture, while wild type livers were normal. Twelve months post partial hepatectomy, all heterozygous Plk4 mice presented abnormal liver histology with 37% developing HCC tumors that were multifocal in nature with a high degree of aberrant mitotic errors. The majority of the wild type Plk4 mice had normal liver architecture. These studies reasoned that some hepatocytes in heterozygote livers with abnormal spindle morphology escaped programmed cell death and passed this phenotype to subsequent generations of hepatocytes leading to the increased development of liver tumors in the Plk4 mice (Ko *et al.*, 2005).

The results observed in heterozygous mice are consistent with the observation that the Plk4 gene is present on human chromosome 4q28, a syntenic region that frequently undergoes rearrangement in hepatocellular carcinomas. It was determined that the increased incidence of hepatomas in Plk4 heterozygous mice resulted from haploinsufficiency and that the Plk4 gene dosage is crucial for suppression of carcinogenesis (Ko *et al.*,2005).

Plk4 Role in Oncogenesis

In contrast to heterozygous Plk4 mice where a reduced gene dose of Plk4 was correlated with tumor development, Plk4 was found to be over expressed in colorectal cancers. Similar over expression in colorectal cancers is observed with Plk1. Expression of both Plk1 and Plk4 increased with the age of the patient, and interestingly, the expression profiles of Plk1 and Plk4 correlated with each other (Macmillan *et al.*, 2001).

Few interacting partners of Plk4 have been identified therefore it has been difficult to determine the function that Plk4 may play in the progression or suppression of oncogenesis. Like Plk1, Plk4 expression is transcriptionally repressed by a p53 mediated pathway (Li *et al.*, 2005). Although the characterization of this repression has yet to be characterized in response to DNA damage, it provides evidence that the functions of Plk4 may impact upon oncogenic properties. In contrast, heterozygous Plk4 MEFs display a phenotype typified by multiple centrosomes, multipolar spindles and mitotic failure (Ko *et al.*, 2005). This phenotype was similar to that observed following over expression of a catalytically inactive Plk4 mutant. The results suggest that reduced Plk4 activity can cause occasional cellular division failure as a result of aberrant centrosome duplication and subsequent mitotic spindle malformation. This cell division failure can lead to either aneuploidy or polyploidy, which could in turn contribute to the incidence of tumors in heterozygous mice (Habendanck *et al.*, 2005).

Experimental Approach

The use of microarrays is an established technique in the field of molecular biology which allows for the large-scale examining of the expression profiles of thousands of genes within a genome. Microarrays allow for the characterization of global expression patterns between a reference and one or multiple experimental conditions. The advent of microarray technology has provided researchers with an invaluable tool to elucidate the function of genes in cellular processes. For the purpose of my experimentation, microarray technology was employed to examine cellular variations of transcript levels based of Plk4 gene dosage in mouse embryonic fibroblasts.

Microarray employs the principle that a given cDNA molecule will bind to its complement on a DNA template from which it has originated (Southern *et al.*, 1999). Two types of microarrays technologies are being employed: oligonucleotides and spotted cDNA arrays. Oligonucleotides are short synthetic sequences of DNA often between twenty to sixty base pairs in length which are representative of a single gene or a family of gene splice variants (Lipshutz et *al.*, 1999). Spotted arrays or complementary DNA (cDNA) arrays contain expressed sequence tags (ESTs) which are small pieces of a DNA sequence generally between 200 to 500 nucleotides long in length that are generated by sequencing either one or both ends of an expressed gene (Duggan *et al.*, 1999). Oligo arrays differ from spotted arrays in the way they are manufactured. Oligonucleotide arrays are produced by printing short oligonucleotide sequences directly onto the array surface. Oligo arrays can be synthesized by photolithographic synthesis, where light and light-sensitive masking agents are used to build one nucleotide sequence at a time across an array surface. Spotted arrays probes are synthesized prior to deposition on the array surface and are then "spotted" onto glass. Spotted arrays are usually synthesized by means of a robotic arm, which contains an array of pins or needles which deposits DNA probes on the designated location on the array surface. For the purpose of the present study, cDNA microarrays were employed.

Spotted arrays are scanned *via* a microarray scanner at two wavelengths to produce images for data analysis: 532nm which causes excitation of the Cy3 fluor which emits a wavelength of 570nm in the green part of the visual spectrum and 635nm which causes the excitation of Cy5 which emits a wavelength of 670nm in the red part of the visual spectrum. Differences in gene expression between the reference and experimental

states are measured based on the visual intensities emitted by the Cy3 and Cy5 dyes which represent the amount of mRNA transcript per a specific gene that hybridized to the array. A visual representation of yellow represents equal hybridization of a gene for both the reference and experimental cDNA and therefore equal mRNA expression. While a predominantly red visualization represent that for a gene in the experimental condition, there were more mRNA transcripts present and therefore it was upregulated. A predominantly green visualization represents that the gene in the reference condition presented more mRNA transcripts present and is downregulated (Figure 4).

532nm Excitation 635nm

570nm Emission 670nm

Cy 3

Cy 5

Composite Image

Computational Analysis
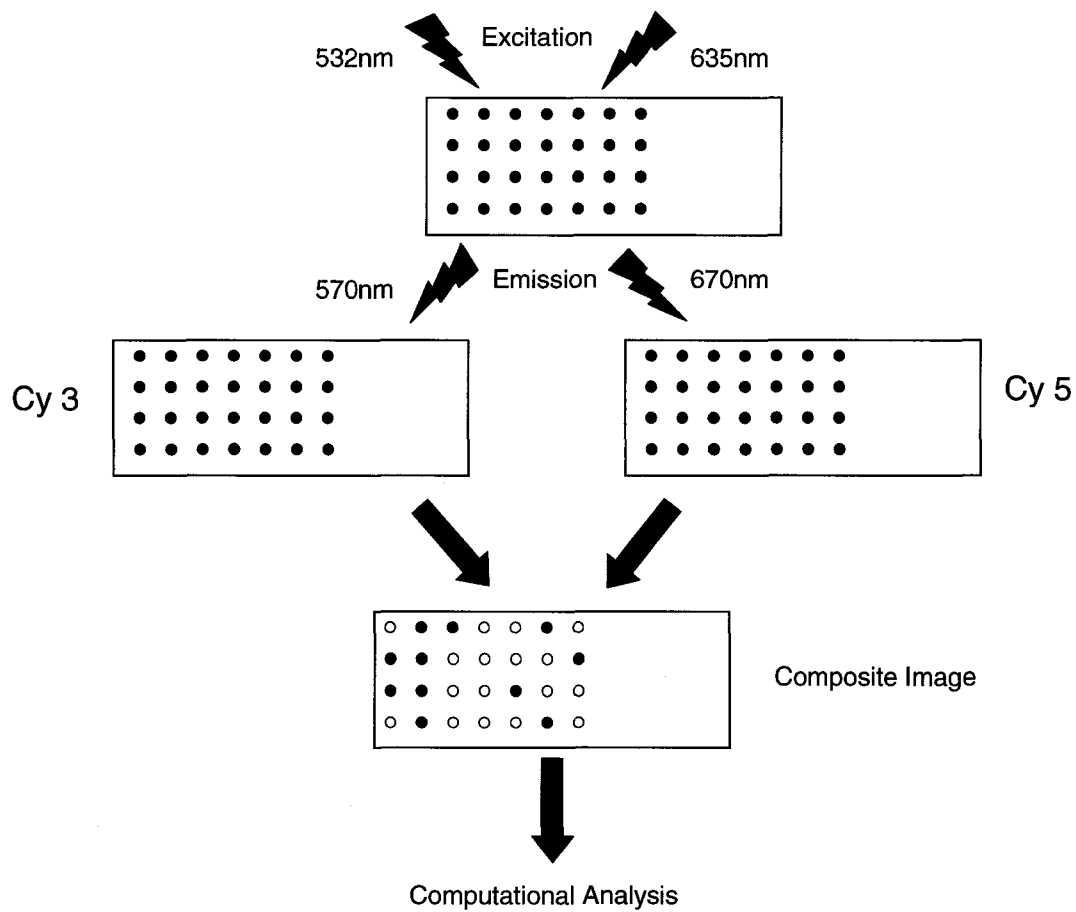
Figure 4: Composite View of Cy3 and Cy5 Labeled Microarray

The wild type Cy3 labeled cDNA is scanned at 532nm causing the Cy3 fluor to emit at 570nm, while the heterozygous Cy5 cDNA is scanned at 635nm causing an emission at 670nm. A composite image is produced by the Scanarray software using the Cy3 and Cy5 scanned images. A predominately green spot indicates increased transcript expression in wild type Plk4 MEFs, while a predominately red spot indicates increased transcript expression in heterozygous Plk4 MEFs. A yellow spot indicates equal transcript expression between wild type and heterozygous Plk4 MEFs.

Chapter 2

Objectives of the Study

Significant phenotypic differences are observed between wild type and heterozygous Plk4 mice and mouse embryonic fibroblasts (MEFs), although the exact mechanisms by which these phenotypic differences occurs has yet to be fully elucidated. The aim of this study was firstly, to provide a general survey of differences in the transcript profile between wild type and heterozygous MEFs using microarray technology. Secondly, Plk1, Plk2, and Plk3 have been implicated to play substantive roles in the cell cycle response to DNA damage. Hence, it is plausible that Plk4 also plays a significant role in the DNA damage pathways. Therefore, transcriptional and protein difference were examined in wild type and heterozygous MEFs in response to both ionizing and ultraviolet radiation.

Chapter 3

Materials and Methods

Establishment of Primary Mouse Embryonic Fibroblasts (MEFs)

Mouse embryonic fibroblast cell lines were established by sacrificing a pregnant female mouse 12.5 days post coitum by carbon dioxide (CO_2) asphyxiation. The uterine horns were removed and washed with 70% ethanol. Each embryo was separated from the placenta and placed in 1ml of Hanks Balanced Salt Solution (HBSS) (Sigma). The embryos were minced with a razor blade until they were pipettable. The resulting cell/tissue solution was suspended in 1ml 10X Trypsin (Sigma) and placed in an incubator at 37°C with 5% CO_2 for 15 minutes. 10ml of MEF media (Dulbecco's Modified Eagles Medium (DMEM; Sigma) containing 20% Fetal Bovine Serum (FBS; Sigma), 1% penicillin-streptomycin (Gibco) and 250 ug/ml gentamicin (Gibco)) were added to the MEF suspension and transferred to a 50 ml falcon tube. Tissue was allowed to settle to the bottom of the tube and the supernatant was transferred to a 15 ml falcon tube and subjected to centrifugation at 100 x g for five minutes. The supernatant was removed and the resulting pellet was suspended in 10 ml of MEF media and plated on a 10 cm tissue culture dish and placed in an incubator at 37°C with 5% CO_2.

When the MEFs reached confluency, they were washed once with HBSS, trypsinized with 1 ml 10X Trypsin (Sigma) for 5 min at room temperature, resuspended in fresh MEF media, pelleted by centrifugation at 100 x g for five minutes and split at a ratio of 1 to 10, with 200 ul kept for genotyping. MEFs were allowed to reach 80% confluency, and then were frozen down. Briefly, MEFs were washed once with HBSS, trypsinized with 1ml 10X Trypsin (Sigma) for 5 min at room temperature, resuspended in

fresh MEF media, pelleted by centrifugation at 100 x g for five minutes and resuspended in 1ml of cold MEF freezing media (MEF media containing 10% dimethyl sulfoxide (DMSO) (Sigma)). MEFs were kept at -80°C for 3 days and then transferred to liquid nitrogen for long term storage.

MEF Genotyping

Isolation of DNA from MEFs was performed by adding 620 ul Proteinase K buffer (50mM Tris, 100mM EDTA, 100mM NaCl, 1% SDS) and 30 ul of 20 mg/ml Proteinase K (Roche). The solution was placed in a 55°C water bath overnight. A 1:1 ratio of water saturated phenol (Sigma) and chloroform (Sigma) was added and the solution was placed on a Nutator Mixer (Becton-Dickinson) for 1hr. The solution was centrifuged in a table top microcentrifuge (Jouan) at 4000 x g for 10 min. The aqueous phase of the resulting mixture was transferred to an eppendorf tube containing 650 ul of isopropanol and centrifuged at 4000 x g to pellet the DNA. The DNA was washed with 70% ethanol and resuspended in 100 ul of deionized water.

PCR genotyping established whether the MEFs were Plk4 wild type or heterozygous. Primers F25 (5'-GCCCCCACTAAGACGAC-3') and VEC523 (5'-AGCTGGGGCTCGACTAG-3') amplified a wild type band at 316bp while primers F25 and PR436 (5'-TGCTAGTAAATAATCCGACAGG-3') amplified a mutant band at 403bp (Hudson *et al.*, 2001).

RNA Isolation

RNA isolation was performed using the RNeasy Mini Kit (Qiagen). Briefly, MEF cells were grown asynchronously to a confluency of 80% and washed twice with HBSS (Sigma) before trypsinization with 10X Trypsin (Sigma). Cells were then pelleted at 100 x g for 5 min in a 15ml falcon tube and washed twice with HBSS in the falcon tube and spun at 100 x g for 3 min. After the second HBSS wash, cells were lysed with the addition of 600 ul lysis buffer and the lysates were homogenized with a Qiashredder (Qiagen) spin column and spun in a microcentrifuge (Juoan) at 4000 x g for 2 mins. 75% ethanol was added to the homogenized lysate to precipitate the total RNA. The solution was placed in an RNeasy Mini Column where the RNA was bound to the column. The RNA was washed three times in the column to get rid of any contaminants and then eluted with Diethyl Pyrocarbonate (DEPC) water. A spectrophotometer reading at A_{260} was performed to estimate the concentration of the RNA. To confirm the integrity and quality of the RNA, a sample was run on the 2100 Bioanalyzer (Agilent) using the RNA 6000 Nano Assay Kit. The RNA was flash frozen in liquid nitrogen and placed in the -80°C freezer until ready for use.

Microarray

Three plates of either wild type or heterozygous MEFs were pooled for RNA isolation as described. RNA was sent to the University Health Network (UHN) Microarray Centre in Toronto were the microarray experiments were performed. The samples were labeled using the UHN's standard indirect labeling protocol. Briefly, 10

micrograms of total RNA sample was used and following reverse transcription to cDNA labeled with Cyanine dyes Cy3 and Cy5 (Amersham Bioscience). Wild type Plk4 cDNA was labeled with Cy3 while heterozygous Plk4 cDNA labeled with Cy5. The labeled samples were hybridized to a Mouse 22.4K microarray chip containing 22 400 features. Hybridization was performed on an Advalytix Slidebooster (Advalytix) using DIG easy hybridization solution. The arrays were scanned using an Agilent G2565BA scanner and quantified using ArrayVision v.8.0 (Imaging Research Inc.).

Synthesis of Complementary DNA (cDNA)

RNA isolation was performed by the method stated previously. The quality of the RNA was examined using the bioanalyzer with the RNA used for reverse transcription if the RNA integrity number was greater than 8.0. Reverse transcription (RT) was performed to convert the total RNA isolated from the MEFs into cDNA. Complementary DNA was synthesized using 5 ug of total RNA, 1ul 0.5ug/ul oligo (dT) $_{12-18}$ primer (Invitrogen), 1ul 10mM dNTPs (Invitrogen) to a value of 12ul with DEPC water. The mixture was incubated at 65°C for five minutes in a heating block and then placed on ice for 2 minute. 4ul of 5X First-Strand Reaction Mix (Invitrogen) and 2ul 0.1M dithiothreitol (DTT) of were added to the mixture and incubated in a heating block at 42°C for 2 minutes. 1 ul of Superscript II Reverse Transcriptase was added and the reaction was incubated at 42°C for 50 minutes for first strand synthesis. The reaction was terminated by incubating the mixture in a heating block at 70° for 15 minutes. The cDNA was stored at -20°C until use.

Polymerase Chain Reaction (PCR)

i) Plk4

All forward and reverse primers for PCR were designed to span intron/exon

boundaries to prevent amplification of contaminating genomic DNA in the cDNA

mixture. The primers for Plk4 (5- AGGGAAGCTAGGCACTTCATG-3'; 5-

GGAAGACCACCTTTTGAC-3') yielded a PCR product of 310 bp. PCR was performed

in a 20 ul reaction mixture containing 2 ul of cDNA template, 2.5 ul of 10X PCR buffer,

4.625mM $MgCl_2$, .5mM of dNTPs, 1 ul each of forward and reverse primers and 2.5 U of

Hot Star Taq DNA Polymerase (Qiagen). PCR was performed using a Tpersonal

(Biometra) programmable thermal cycler as follows: denaturation at 95°C for 15 minutes,

then 38 to 42 cycles of denaturation at 94°C for 30 seconds, annealing at 48°C for 30

seconds and extension at 72°C for 60 seconds. Completed PCR reactions were cooled to

4°C and aliquots resolved by electrophoresis on a 2% tris-acetate-EDTA (TAE) agarose

gel at 85 V for 85 minutes and visualized by ethidium bromide staining. Gels were

imaged using a Chemi Genius Bio Imaging System (Perkin Elmer) using the Gene Snap

software. All PCR products were run and imaged using the same methodology and

equipment.

ii) Glyceraldehyde 3-phosphate dehydrogenase (GAPDH)

Oligonucleotide primers for GAPDH (5'-GCTGAGTATGTCGTGGAGTCT-3';

5'-CAGAGCTGAACGGGAAGCTC-3') yielded a product of 410 bp. PCR was

performed in a 20 ul reaction mixture containing 1 ul of cDNA template, 2.5 ul of 10X

PCR buffer, 4.625mM $MgCl_2$, .5mM of dNTPs, .5 ul each of forward and reverse primers

and 1 U of Hot Star Taq DNA Polymerase (Qiagen). PCR was performed using a programmable thermal cycler as follows: denaturation at 95°C for 15 minutes, then 28 to 32 cycles of denaturation at 94°C for 30 seconds, annealing at 57°C for 40 seconds and extension at 72°C for 40 seconds. PCR reactions were cooled to 4°C and aliquots resolved on a 2% agarose gel.

iii) Prohibitin

The primers for prohibitin (5'-CGTATCTACACCAGCATTGGC-3'; 5'-TGTGGTGGAAAAGGCTGAGC -3') yielded a product of 301 bp. PCR was performed in a 20 ul reaction mixture containing 2 ul of cDNA template, 2.5 ul of 10X PCR buffer, 2.0mM MgCl2, .5mM of dNTPs, .75 ul each of forward and reverse primers and 2.5U of Hot Star Taq DNA Polymersae (Qiagen). PCR was performed using a programmable thermal cycler as follows: denaturation at 95°C for 15 minutes, then 32 to 36 cycles of denaturation at 94°C for 30 seconds, annealing at 55°C for 30 seconds and extension at 72° for 30 seconds. PCR reactions were cooled to 4°C and aliquots resolved on a 2% agarose gel.

iv) SAP30 Binding Protein (SAP30BP)

The primers for SAP30BP (5'-CCAGAAGCTCTACGAGCGGAA-3'; 5'-TGGTCTGAAGACTCCTACTATGAG-3') yielded a product of 190 bp. PCR was performed in a 20 ul reaction mixture containing 2 ul of cDNA template, 2.5 ul of 10X PCR buffer, 2.75mM $MgCl_2$, .5mM of dNTPs, 1 ul each of forward and reverse primers and 2.5 U of Hot Star Taq DNA Polymerase (Qiagen). PCR was performed using a

programmable thermal cycler as follows: denaturation at 95°C for 15 minutes, then 38 to 42 cycles of denaturation at 94°C for 30 seconds, annealing at 57°C for 30 seconds and extension at 72°C for 30 seconds. PCR reactions were cooled to 4°C and aliquots resolved on a 2% agarose gel. .

v) WNT-Inducible Signaling Pathway Protein 1 (Wisp1)

The primers for Wisp1 (5'-GCCTAATCACAGATGGCTGTG-3'; 5'-CAATAGGAGTGTGTGCACAGGTG-3') yielded a product of 150 bp. PCR was performed in a 20 ul reaction mixture containing 2 ul of cDNA template, 2.5 ul of 10X PCR buffer, 1.5mM MgCl$_2$, .5mM of dNTPs, 1ul each of forward and reverse primers and 2.5U of Hot Star Taq DNA Polymerase (Qiagen). PCR was performed using a programmable thermal cycler as follows: denaturation at 95°C for 15 minutes, then 36 to 40 cycles of denaturation at 94°C for 60 seconds, annealing at 54°C for 60 seconds and extension at 72°C for 60 seconds. PCR reactions were cooled to 4°C and aliquots resolved on a 2% agarose gel.

Densitometry

Densitometry was performed using the Gene Tools software from Perkin Elmer. Briefly, the program identified the correct gel lanes associated with the samples run using an algorithm. Subsequently, any unwanted lanes were deleted. Next, using a predetermined algorithm, the computer identified bands on the gel and was allowed to assign intensity values for the bands to eliminate any bias. Unwanted bands not necessary for analysis were removed.

TdT-Mediated dUTP Nick-End Labeling (TUNEL) Assay

Wild type and heterozygous MEFs were plated on glass coverslips at 70%

confluency in six well plates. MEFs were exposed to 40 mJ/cm^2 ultraviolet radiation.

MEF media was removed and the cells were washed twice with 1X phosphate buffer

saline (PBS). Cells were fixed in 4% paraformaldehyde in PBS at 4°C, 0hr, 1hr, 2hr, 4hr,

6hr, and 8hr post radiation. Cells were permeabilized in 0.2% Triton X-100 (Sigma) in

PBS and washed twice in 1X PBS. Cells were equilibrated in Equilibration buffer for 10

minutes at room temperature. Equilibration buffer was removed and the cells were

incubated with rTdT incubation buffer (88% equilibration buffer, 10% nucleotide mix,

2% rTdT enzyme) for 60 minutes at 37°C in the dark to label apoptotic cells with

fluorescien-12-dUTP. Cells were washed with 2X Sodium Salt Citrate (SCC) (20X SCC

in deionized water) 15 minutes at room temperature to terminate the labeling reaction.

Cells were washed three times with 1X PBS at room temperature for 5 minutes. Cells

were stained with 5ug/ml of propidium iodide (PI) in 1X PBS to stain the nuclei of the

cells. Subsequently, cells were washed three times with deionized water. Excess water

was removed from the cover slips, one drop of Anti-Fade solution (Molecular Probes)

was added and the cover slips were mounted on glass slides. Cells were viewed at high

magnification at red fluorescence at 620 nm for propidium iodide and green fluorescence

at 520 nm for fluorescien-12-dUTP. 200 cells per slide were counted to analyze the

number of apoptotic cells and three trials were performed. DNase I was used as a positive

control to induce DNA fragmentation indicative of apoptosis.

Exposure of MEFs to DNA Damaging Agents

Wild type and heterozygous MEFs were exposed to ultraviolet light (UV) at 40

mJ/cm^2 using a GS Gene Linker UV Chamber (Biorad) or ionizing radiation (IR) of 25

Gy using a RX-650 Cabinet X-ray System (Faxitron) and RNA was isolated from the

MEFs at desired time points.

SDS-PAGE

MEFs were exposed to either ultraviolet or ionizing radiation and then lysed 6

hours post radiation. Cells were lysed with 1ml lysis buffer (50 mM Tris-Cl, 100 mM

Nacl, 500 mM EDTA, 1% Triton-X) on ice for 20 min. Lysates were spun in a

microcentrifuge at 4000 x g for 20 min at 4°C to remove cellular debris. A Bradford

assay was performed to find out protein concentration. 2X loading dye containing 5% β-

mercaptoethanol was added to 30 ug of lysates, and the samples were boiled for 5 min.

The lystates were loaded onto either an 8% or 15% protein gel and subjected to SDS-

PAGE for 48 minutes at 200V.

Western Blot Analysis

After SDS-PAGE, the proteins were transferred onto a PVDF membrane

(Millipore) using a semi-dry transfer apparatus (Biorad) at 12V for 45 minutes. The

membrane was then blocked with Tris-buffer saline and Tween (TBST) buffer with 1%

blotto to block non-specific protein binding for 1hour at room temperature with gentle

agitation. The membrane was washed three times with TBST for 5 minutes at room

temperature. The membrane was then incubated with the desired primary antibody

(Appendix A) in TBST with 1% blotto for 1 hour at room temperature; then washed three times with TBST for 5 minutes. The membrane was incubated with the appropriate horseradish peroxidase secondary antibody (Appendix A) in TBST with 1% blotto for 45 minutes at room temperature; then again washed three times with TBST for 5 minutes. 1 ml of Supersignal West Femto Maximun Sensitivity Substrate (Pierce) was added to the membrane and the reaction between the horseradish peroxidase and its substrate was allowed to occur for 5 minutes. The proteins were then visualized by chemiluminescence.

Stripping of Western Blots for Re-probing

Stripping of Western blots was used to remove any bound primary and secondary from the blot so that other primary antibodies could be tested. Stripping buffer (100 mM β-mercaptoethanol, 2% SDS, 62.5 mM Tris-Cl at pH 6.7) was prewarmed to 50°C and added to the blot for 25 minutes at 50°C with gentle agitation. The stripping buffer was removed and the blot was incubated with prewarmed TBST for 25 minutes at 50°C. The blot was washed with water and then incubated with the desired primary antibody.

Chapter 4

Results

Comparison between Transcript Profiles in Wild Type and Heterozygous Plk4

MEFs using Microarray.

A number of phenotypic differences have been observed between wild type and

heterozygous Plk4 MEFs including that heterozygous MEFs exhibit a growth rate

approaching ½ that of their wild type counterparts (Ko *et al.*, 2005). In addition,

heterozygous MEFs present an increase in the number of cells with multiple centrosomes

which have the potential to lead to abnormal chromosome alignment and segregation (Ko

et al., 2005). These abnormalities have been proposed as a mechanism that leads to

genomic instability and the observed increase incidence of tumor development in aged

heterozygous Plk4 mice in comparison to the wild types. Therefore, it was of interest to

study the effect of lower Plk4 levels on the expression pattern of other genes. We

measured the global transcriptional differences between wild type and heterozygous

MEFs using microarray technology using RNA samples isolated from both Plk4 wild

type and heterozygous MEFs using three microarray replicates were performed. The

experiments were performed at the University Health Network (UHN) Microarray facility

using Mouse 22.4k cDNA arrays using an indirect labeling methodology. Scanned TIFF

images of both the Cy3-labeled and Cy5-labeled were received from UHN and analysis

was performed.

Quantification of results was performed using ScanArray Express v.3.0 (Perkin

Elmer). Cy3-labeled and Cy-5 labeled images were loaded on the ScanArray Express

Software producing a composite image of the array (Figure 5). A QuantArray microarray

gene annotation file was obtained from the University Health Network (UHN)

Microarray Centre website indicating the identification of each spot on the array

(http://www.microarrays.ca/products/glists.html). Using the template obtained from the

gene list, a grid overlay was designed of the microarray spots and was aligned with the

scanned image. Quantification was performed by the ScanArray Express software to

measure the intensity of the hybridization of both the Cy3 and Cy5 labeled samples to its

complement on the chip. Locally Weighted Scatter Plot Smoother (LOWESS)

normalization was performed to account for any intensity dependent effects that may

occur when differences in log ratio values are observed (Quackenbush, 2001). The

resulting quantification and normalization of the data produced a data file that allowed

transfer to "The Institute for Genomic Research" (TIGR) TM4 microarray data analysis

suite for further analysis. Further normalization and filtering of the data was performed

using the TIGR Microarray Data Analysis System (MIDAS) application. Analysis of all

microarray data sets for the different microarray experiments (ex. Wild type Plk4 MEFs

vs Heterozygous Plk4 MEFs) were performed independently. Initial filtering of the data

was performed. Spots were removed from downstream analysis if an intensity value for

either the Cy3-labeled or Cy5-labeled spot were invalid (an intensity less than 1). Next,

flag filtering was performed to remove invalid spots from further analysis. For example,

if the Cy-3 or Cy5 samples had an intensity of 0 non-saturated pixels within a spot, the

spot was removed. Subsequently, background filtering was employed. If the background-

corrected intensity of a spot was greater than or equal to the background intensity for

both the Cy3 and Cy5 labeled samples than the spot was kept in the data set for further

downstream analysis.

Wild Type MEFs
Cyanine 3

Heterozygous MEFs
Cyanine 5
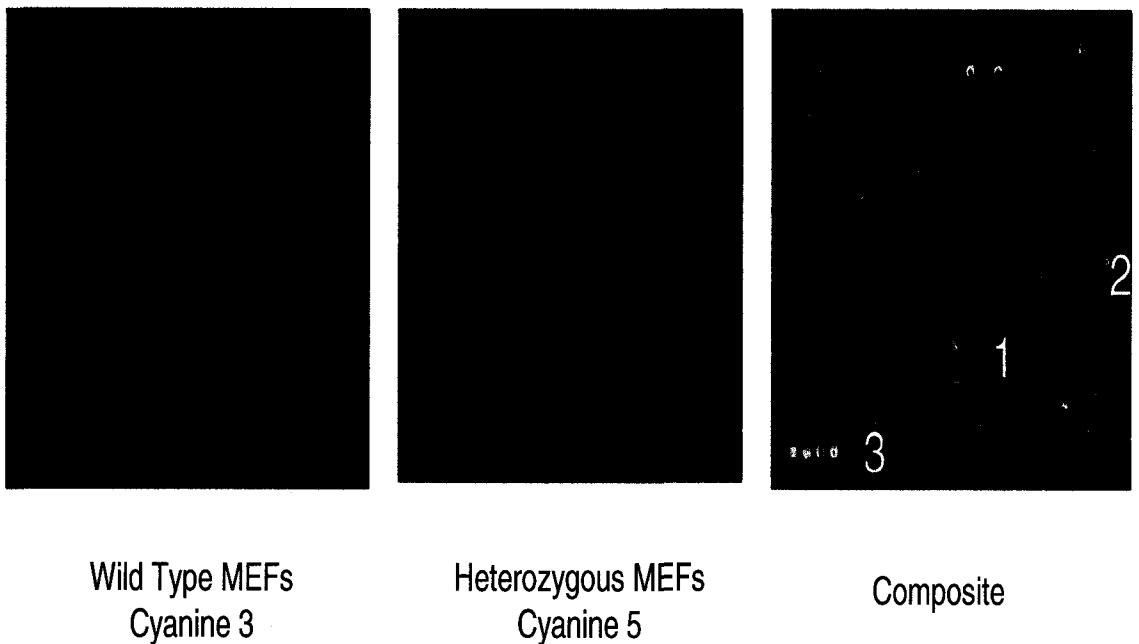
Composite

Figure 5: Composite View of Cy3 and Cy5 Labeled Microarray

The wild type Cy3 labeled cDNA was scanned at 532nm causing the Cy3 fluor to emit at

570nm, while the heterozygous Cy5 cDNA was scanned at 635nm causing an emission at

670nm. A composite image was produced by the Scanarray software using the Cy3 and

Cy5 scanned images. 1) A predominately green spot indicated increased transcript

abundance in wild type Plk4 MEFs, 2) while a predominately red spot indicated increased

transcript abundance in heterozygous Plk4 MEFs. 3) A yellow spot indicated equal

transcript levels between wild type and heterozygous Plk4 MEFs

Locfit (LOWESS) normalization was performed with specific parameters set. Block LOWESS normalization was applied to the data set meaning that only spots within a certain block or grid on the microarray chip contribute to the bias of the spots intensity. A smoothing parameter was established at 33 percent to compute the normalization of each spot using the LOWESS algorithm. These computations were performed by MIDAS with the input that the Cy3 labeled sample (wild type MEFs) was the reference or the control and the Cy5 labeled sample (heterozygous MEFs) was the experimental value. Next, standard deviation regularization parameters were established ensuring that all spots within each block or grid of the microarray chip have the same standard deviation with the Cy3 labeled sample being the reference. Spots were then filtered from the further analysis based on the raw intensity of the hybridization. The cutoff raw intensity was set at 10000 with any spots with intensity lower than this threshold removed from any further analysis.

The normalized and filtered data set was loaded into TIGR Multiexperiment Viewer (MEV) for clustering analysis. For clustering, the filtered data from all three chips was loaded into MEV simultaneously for clustering to occur. The data set was clustered using K-Means clustering. K-means clustering divides the filtered data into clusters based on the principle that genes within a cluster are closely related. Genes were divided into ten different clusters. Within each cluster, genes having a log ratio value greater than 1 or less than -1 on each microarray chip were identified. Genes having a log ratio greater than 1 represented genes in the heterozygous MEFs that have at least a two fold increase in gene expression. As the wild type MEFs was used as the control, genes with a log ratio greater than 1 were classified as up-regulated in the heterozygous MEFs.

While, a log ratio less than -1 represented genes in the wild type MEFs that have at least a two fold increase in gene expression or are down-regulated in the heterozygous MEFs.

From the microarray data, 9 genes were identified as having at least a two fold decrease in transcript profile in the heterozygous MEFs or were down-regulated in the heterozygous MEFs when compared to the wild-type control (Table 1) (Appendix J), while 146 genes were identified as having at least a two fold increase in transcript profile in the heterozygous MEFs (Table 2) (Appendix K). Cellular function for each gene was identified using annotation data from the Pubmed database or the Online Mendelian Inheritance in Man (OMIM) database.

Confirmation of Microarray Results Using RT-PCR

To confirm the validity of the microarray results, qualitative RT-PCR was employed. Three genes classified as having increased transcript profiles in the heterozygous MEFs were examined: Wnt1 inducible signaling pathway protein 1 (Wisp1), Sap30 Binding Protein (SAP30BP), Prohibitin (PHB).

a) Wisp1 Expression in Heterozygous Plk4 MEFs

Wisp1 over expression has been implicated in cellular morphological transformation (Xu *et al.*, 2000) as well as and tumor formation in hepatocellular carcinomas (Cervello *et al.*, 2004). In addition, over expression of other Wnt pathway proteins have also been implicated in tumor formation. I speculate that over expression of Wisp1 and other Wnt pathway proteins could contribute to tumor formation in heterozygous Plk4 mice. To confirm the validity of the microarray results, RT-PCR was

performed to compare Wisp1 expression rates in wild type and heterozygous Plk4 MEFs, and subsequently densitometry was performed to measure the quantitative differences. RNA was isolated from both wild type and heterozygous MEFs and a reverse transcription reaction was performed to produce first strand cDNA. PCR primers for Wisp1 were designed to amplify a product of 150 base pair, while PCR primers for glyceraldehyde 3-phosphate dehydrogenase (GAPDH), amplified a product 410 base pairs in length and was used as an internal loading control. PCR products amplified from cDNA taken at three times points for both Wisp1 and GAPDH, were performed and terminated the PCR in the linear part of the PCR amplification curve. The PCR products were resolved on a 2% agarose gel to view their difference in relative abundance in the wild type and heterozygous MEFs (Figure 6a).

Densitometry was performed using the Gene Tools software. Intensity values were assigned to the bands for Wisp1 and GAPDH by the software to eliminate any bias. To determine the relative expression of Wisp1 in the heterozygous MEFs compared to wild type, first the ratio of the value for Wisp1 to GAPDH was taken for each individual time point. Next, the ratio of GAPDH to Wisp1 was determined for the wild type time points. The ratio of Wisp1 to GAPDH for the heterozygous time points was multiplied by the ratio of GAPDH to Wisp1 to determine the relative expression of Wisp1 in the heterozygous MEFs to the Wisp1 in the wild type MEFs (Appendix B). Densitometry was performed for three individual trials of RT-PCR for Wisp1. The relative expression for Wisp1 over the three trials was calculated along with the standard error of the mean. For the three trials of Wisp1, the average change in expression of Wisp1 over the three PCR time points was between 1.36 and 1.48 times greater level of transcriptional

Table 1: Down-regulated Genes in Heterozygous Plk4 MEFs

Developmental
Procollagen, type III, alpha 1
Procollagen, type V, alpha 2
Oral-facial-digital syndrome 1 gene homolog
Procollagen, type I, alpha 2

Metabolism
Stearoyl-Coenzyme A desaturase 2

Unknown Function
Mus musculus mVL30-1 retroelement mRNA sequence
Transmembrane protein 34
Mus musculus 0 day neonate cerebellum cDNA
Hypothetical protein LOC639390

54

Table 2: Up-regulated Genes in the Heterozygous Plk4 MEFs

Cell Cycle
Casein kinase II
Protein phosphatase 1F (PP2C domain containing)
Squamous cell carcinoma antigen recognized by T-cells 1
Origin recognition complex, subunit 4-like
Inhibitor of DNA binding 2
Protein phosphatase 5
Prohibitin
Cyclin dependent kinase 8
Phosphatidylinositol 3-kinase
Pituitary tumor-transforming 1
Heterogeneous nuclear ribonucleoprotein C
heme binding protein 2
TVMSFG fibroblast growth factor receptor 1 precursor
Neuropilin

DNA Methylation
SET domain ERG-associated histone methyltransferase
SAP30 binding protein

Developmental
Sal-like 3
Transducin-like enhancer of split 1
T-cell factor 4
Inositol 1,4,5-triphosphate receptor 5
Procollagen, type VI, alpha 3
Fetal Alzheimer antigen
WNT1 inducible signaling pathway protein 1
T-box transcription factor Tbx15
Nuclear factor I/X
Thrombospondin 2
Osteopontin
Fukuyama type congenital muscular dystrophy homolog
Nuclear receptor co-repressor 1

DNA Repair
Thymine DNA glycosylase
Uracil-DNA glycosylase
MutS homolog 6

Table 2: Up-regulated Genes in the Heterozygous MEFs

Metabolism
N-acylsphingosine amidohydrolase (acid ceramidase) like
Leucyl/cystinyl aminopeptidase
Galactose-4-epimerase
L-2-hydroxyglutarate dehydrogenase
Fatty acid desaturase 3
Carbohydrate sulfotransferase 2
Stearoyl-Coenzyme A desaturase 1
CCR4 carbon catabolite repression like 4
protein kinase, cAMP dependent regulatory, type I beta

Transcriptional/Translational Regulation
Transcription factor A
Zinc finger protein 689
Transmembrane and tetratricopeptide repeat containing 2
GLIS family zinc finger 3
Phenylalanine-tRNA synthetase 2
Glutamyl-prolyl-tRNA synthetase
Protein kinase, cAMP dependent regulatory, type I beta
Highly similar to CBP_MOUSE CREB-binding protein
Tetratricopeptide repeat domain 1
Cysteinyl -tRNA synthetase
Negative elongation factor B

Cellular/Ion Transport
Protein kinase, cAMP dependent regulatory, type I beta
Pleckstrin
Calcium binding and coiled coil domain 1
Aquaporin-1
Solute carrier family 6
Exocyst complex component 3
Protein-coupled receptor 19
Solute carrier family 39
Frequenin homolog
Serine Hydrolase like
Solute carrier family 14
Translocator of inner mitochondrial membrane
ATPase, Ca++ transporting, plasma membrane 2
Transient receptor potential cation channel, subfamily M member 7

Table 2: Up-regulated Genes in the Heterozygous MEFs

Miscellaneous Cellular Functions

Thyroid hormone receptor interactor 11
Smg-6 homolog
Talin 2
Tomoregulin1
Syntaxin 18
Channel-interacting PDZ domain protein
Inositol hexaphosphate kinase 1
Multiple PDZ domain protein
Myosin heavy chain 10
CDC42 effector protein (Rho GTPase binding) 2
Zinc finger protein 507
Zinc finger protein 689
Ring finger protein 11
GC-rich sequence DNA-binding factor homolog candidate isoform 1
Villin
3-phosphoglycerate dehydrogenase
Olfactory receptor 202
Discs, large homolog 5
2'-phosphodiesterase
Heat shock protein 1
Similar to crooked neck protein
Oxysterol binding protein like protein 9
Mitochondrial ribosomal protein L50
Proteasome (prosome, macropain) 26S subunit, non-ATPase
Coiled Coil domain containing 131
WD repeat domain 50

Spetex-2E protein
Zinc Finger Protein 451
aarF domain containing kinase 1(Adck1)
AHNAK nucleoprotein
Arginine/serine-rich coiled-coil 1
HD domain containing 3 (Hdcc3)
Myotubularin related protein 7
NICE-5 protein

46 additional genes came up as being down-regulated th there present cellular function is unknown or there are classified as hypothetical proteins

expression in the heterozygous Plk4 MEFs than in the wild type (Figure 6b). The average

log ratio from the three microarray chips for Wisp1 was 1.64 corresponding to an average

3.28 change increase in expression for Wisp1 in the heterozygous MEFs. Though the

change in expression appears to differ substantially from the microarray data to the RT-

PCR data, differences are most likely attributed to the fact that the MEFs used for the

microarray experiments were different MEFs than the MEFs used for the RT-PCR

experiments.

b) SAP30-Binding Protein Expression in Heterozygous Plk4 MEFs

Preliminary data shows that methylation of the Plk4 gene in heterozygous mice

occurs at a substantially higher rate than in wild type mice. Therefore, it is hypothesized

that the transcriptional repression of Plk4 in heterozygous mice contributes to the

increased incidence of tumorigenesis within these mice. Since SAP30BP binds SAP30

(Li *et al.*, 2004), a component of the SIN3 histone deactylase complex, it is plausible that

the increased methylation status of Plk4 heterozygous mice could be contributed to a

complex that includes SAP30BP.

RNA was isolated from both wild type and heterozygous Plk4 MEFs and a

reverse transcription reaction was performed to produce cDNA. PCR primers for

SAP30BP amplified a product of 190 base pairs, while GAPDH, used as an internal

loading control amplified a product of 410 base pairs. PCR products were run at three

time points for both SAP30BP and GAPDH, while amplification was in the linear part of

the PCR amplification curve except for cycle 42 for SAP30BP which became saturated.

PCR products were run on a 2% agarose gel to view the differences in the transcript

Figure 6: Wisp1 Transcript Expression in Heterozygous Plk4 MEFs

a) RT-PCR was performed over three PCR time points to measure the relative

quantitative difference in the transcript expression of Wisp1 in wild type and

heterozygous Plk4 MEFs. GAPDH was used as an internal loading control. b)

Densitometry was performed to measure the raw intensity of each band. Values for

Wisp1 were normalized to GAPDH and the relative mean expression over three PCR

trials was graphed. The average increase in transcript expression for Wisp1 in

heterozygous Plk4 MEFs was between 1.36 to 1.48 greater than in wild type Plk4 MEFs.

(NB WT: Wild Type; HET: Heterozygous)

A

GAPDH 410 bp

Wisp1 150 bp

B

Comparison between Transcript Profiles for Wisp1 in Wild Type and Heterozygous PLK4 MEFs
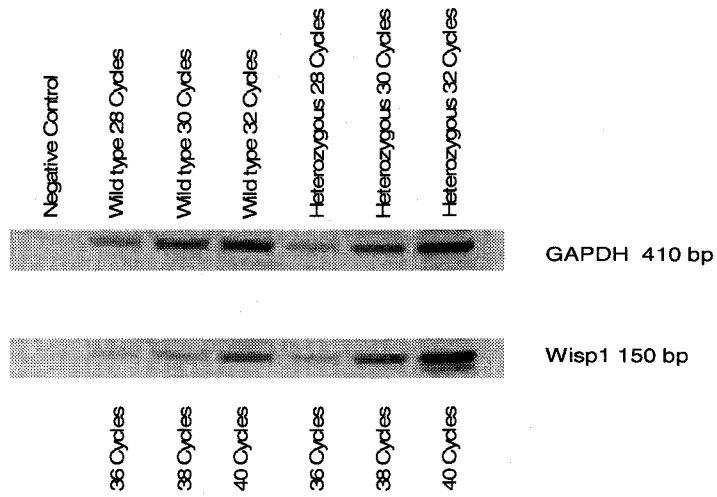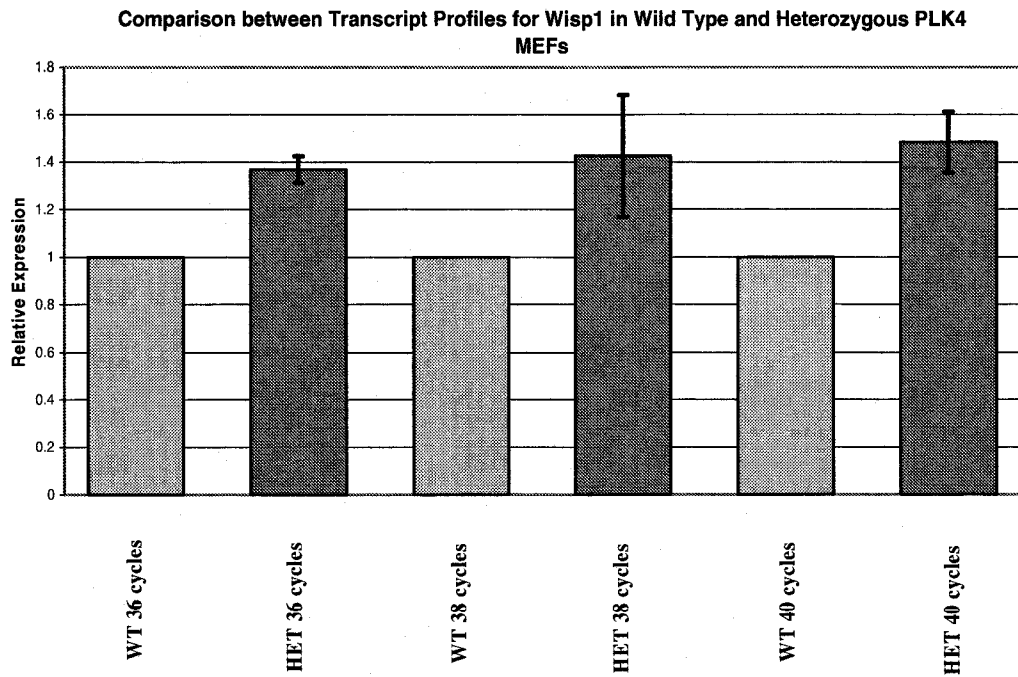
Wisp1 Transcript Profile in Wild Type & Heterozygous MEFs over Three PCR cycles

profiles of SAP30BP in wild type and heterozygous Plk4 MEFs (Figure 7a).

Densitometry was used to quantify the differences in transcript expression of SAP30BP. The same rationale was used to determine the relative expression of SAP30BP in the heterozygous MEFs compared to the wild type MEFs as with Wisp1. The ratio of SAP30BP to GAPDH was determined for both wild type and heterozygous SAP30 at the three different PCR time points. Next, in the wild types, the ratio of GAPDH to SAP30BP was determined. This value was multiplied with the SAP30BP to GAPDH value for heterozygous SAP30 to get the relative expression in relation to wild type SAP30BP (Appendix C). Densitometry was performed on three individual RT-PCR trials for SAP30BP. The average relative expression and standard average of the mean was calculated for the three RT-PCR trials. For the three trials of SAP30BP, the average change in expression of SAP30BP over the three PCR time points was between 1.36 and 1.81 times greater level of transcriptional expression in the heterozygous Plk4 MEFs than in the wild type (Figure 7b). The average log ratio for the three microarray chips was 1.49 corresponding to an average increase in expression of 2.98 in the heterozygous Plk4 MEFs. Similar to Wisp1, MEFs from different embryos were used for both the microarray and the RT-PCR experiments. These differences possibly could contribute to the variation in change of expression between the microarray and the RT-PCR. Also, the relative expression of SAP30BP decreases in the heterozygous MEFs over the three PCR time points due to a result that the PCR product was becoming saturated, and therefore not in the linear part of the PCR product amplification curve.

c) Prohibitin Expression in Heterozygous Plk4 MEFs

Prohibitin (PHB) has been implicated to play a role in cellular senescence (Rastogi *et al.*, 2006). Since mouse embryonic fibroblasts are primary cell lines, they eventually stop dividing and take a senescent phenotype of flattened morphology and increased granularity. In heterozygous Plk4 MEFs, the senescent phenotype is observed at an earlier passage than in the wild types. Therefore, it is plausible that increased prohibitin expression in heterozygous Plk4 MEFs contributes to this observed earlier senescent phenotype.

RNA was isolated from both wild type and heterozygous Plk4 MEFs and a reverse transcription reaction was performed to produce cDNA. PCR primers for PHB multiplied by the ratio of PHB to GAPDH for the heterozygous time points to determine the relative expression of PHB in the heterozygous Plk4 MEFs to the wild type MEFs (Appendix D). Densitometry was performed for three individual PCR experiments and the average of the relative expression and standard error of the mean were calculated. Over three PCR trials, the average mean transcript expression of prohibitin in heterozygous MEFs was between 1.83 and 2.37 times greater than in the wild type Plk4 MEFs (Figure 8b). The average log ratio for the three microarray experiments for prohibitin was 1.52 corresponding to an increase in transcript expression of 3.04 times greater in the heterozygous MEFs. Similar to Wisp1 and Sap30BP, MEFs from different mice were used for the RT-PCR experiments than for the microarray, possibly explaining a reason for the variance in the results.

A

GAPDH 410 bp

SAP30BP 190 bp

B
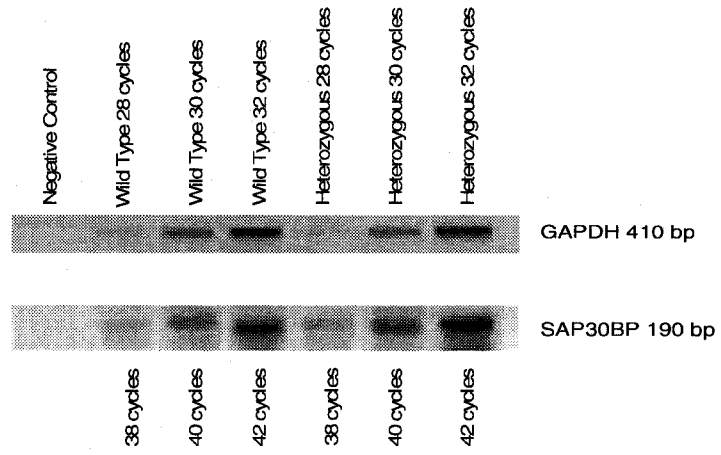
Comparison between Transcript Profiles of SAP30BP in Wild Type & Heterozygous Plk4 MEFs
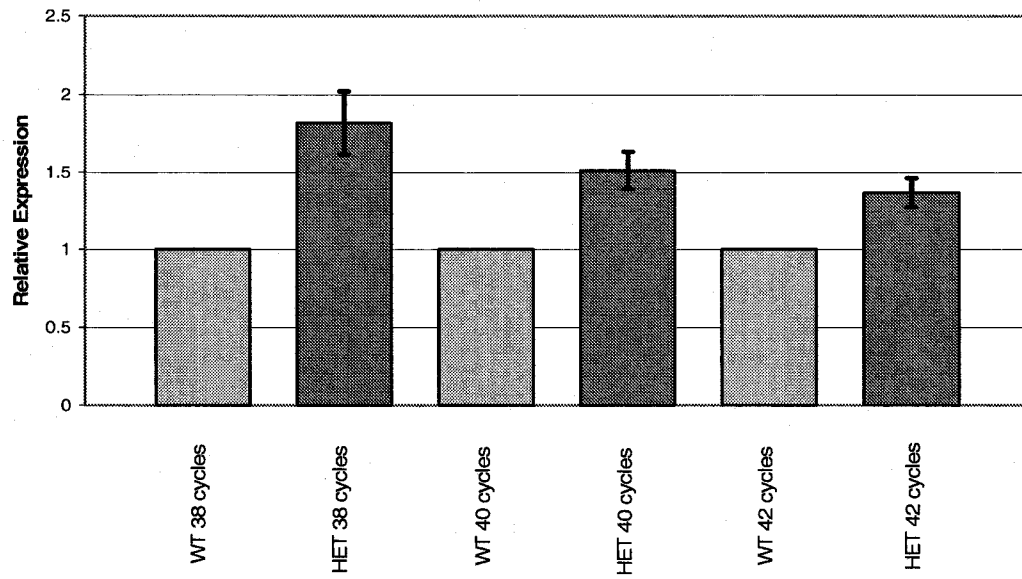
Comparison of Transcript Profiles of SAP30BP over Three PCR Time Points

A

Negative Control
Wild Type 28 cycles
Wild Type 30 cycles
Wild Type 32 cycles
Heterozygous 28 cycles
Heterozygous 30 cycles
Heterozygous 32 cycles

GAPDH 410 bp

Prohibitin 301 bp

32 cycles
34 cycles
36 cycles
32 cycles
34 cycles
36 cycles

B
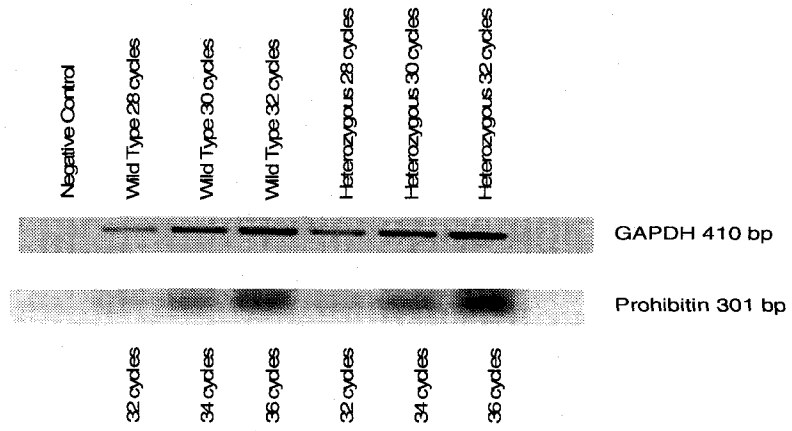
Comparison between Transcript Profiles of Prohibitin in Wild Type & Heterozygous Plk4 MEFs
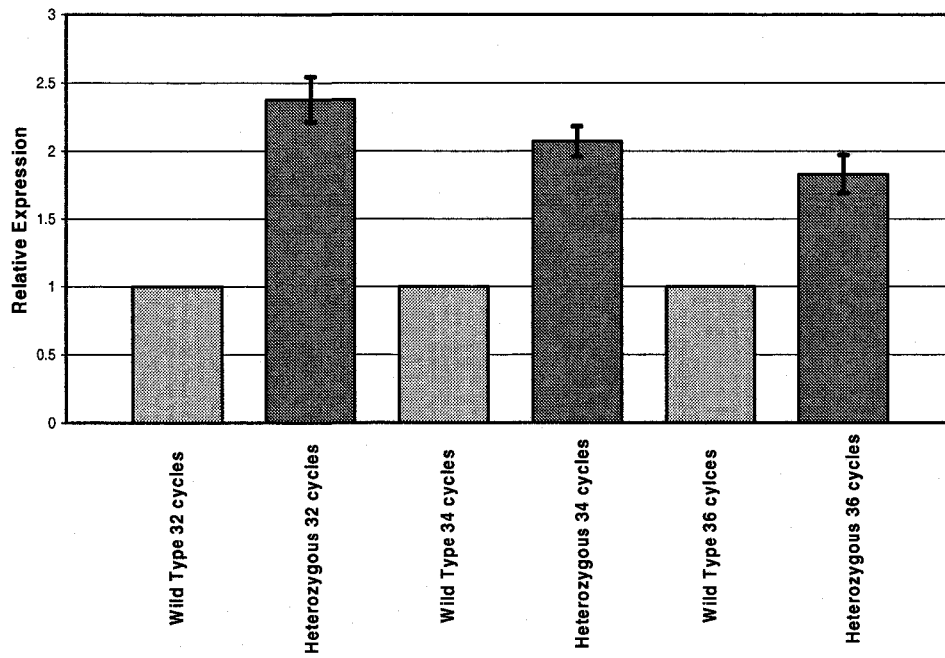
Prohibitin Transcript Profiles in Wild Type & Heterozygous MEFs over Three PCR Time Points

The Effect of Ionizing and Ultraviolet Radiation on the Plk4 Transcript Profile in MEFs

Though it is not yet known whether Plk4 plays a crucial role in response to DNA damaging agents, Plk4 has shown to interact with crucial DNA damage proteins including p53 (Swallow *et al.*, 2005), Cdc25c (Bonni *et al.*, 2008), ATM, ATR, Chk1 and Chk2 (Hudson *et al*, unpublished data). Subsequently, it was of interest to analyzeis the effect of DNA damaging agents on the transcript profile of Plk4, and whether there exist a difference in transcript expression between wild type and heterozygous MEFs.

Wild type and heterozygous MEFs were exposed to 25 Gy IR or 40 mJ/cm^2 UV. RNA was isolated at various time points and RT-PCR was performed to visualize if there were differences in transcript expression. PCR primers for Plk4 amplified a PCR product of 310 base pairs, while GAPDH, used as an internal loading control amplified a product 410 base pairs. PCR products were amplified at three time points in the linear range of the PCR amplification curve. PCR products were run on a 2% agarose gel to visualize differences between the wild type and heterozygous Plk4 MEFs in response, first to IR then to UV.

Densitometry was performed to quantitate the transcriptional difference between wild type and heterozygous Plk4 MEFs. The control with no exposure was used as a base line with the subsequent time points normalized back to it. Densitometry for both wild type and heterozygous samples was done separately and differences were visualized using a graph. Briefly, for each time point post exposure to DNA damage, and each PCR cycle time point, a ratio of Plk4 to GAPDH was determined. Then for the control with no exposure, a ratio of GAPDH to Plk4 was determined. The relative expression was

determined by multiplying the Plk4 to GAPDH ratio for time points post exposure to the

ratio of GAPDH to Plk4. Densitometry was performed for three individual PCR

reactions. The average relative expression was determined along with the standard error

of the mean. Subsequently, the values for the heterozygous MEFs were normalized back

to the wild type MEFs as RNA levels in the wild type MEFs are expressed twice as much

as in heterozygous MEFs (Swallow *et al.*, 2005).

In response to IR, the Plk4 transcript profile of the wild type MEFs stays constant

until one hour post exposure when levels declined to between 60-70% relative to the

control. These levels continue to remain at this decreased level 24 hours post irradiation

(Figure 9a) (Appendix E). Similarly, for the heterozygous MEFs in response to IR, the

Plk4 transcript profile remains constant till one hour post exposure, until a similar decline

in transcript expression is observed. Between 2 and 24 hours post irradiation, the Plk4

transcript levels were between 60-70% relative to the control (Figure 9b) (Appendix F).

When a comparison between wild type and heterozygous MEFs at the first PCR time

point is observed, there is no comparable difference between Plk4 transcript profiles

(Figure 9c). When a comparison of the Plk4 transcript profile at the second PCR time

point is examined, the differences in transcript profile 2 hours post exposure for both the

wild type and heterozygous MEFs is 70-90% relative to the control (Figure 9d). At the

third PCR time point, observable differences between wild type and heterozygous

transcript profile appear (Figure 9e). The difference for the heterozygous MEFs for all

time points is within the standard error relative to the control. This is most likely due to

the PCR amplification being in the non-linear part of the amplification curve. Subsequent

differences are noticed between wild type and heterozygous transcript profile. At one

Figure 9: Effect of Ionizing Radiation on the Transcript Profile of Plk4 in Wild Type and Heterozygous MEFs

Wild type and heterozygous MEFs were exposed to 25 Gy ionizing radiation (IR), and RNA was isolated at various time points post exposure. RT-PCR was performed to measure the relative quantitative difference in Plk4 expression after exposure in both wild type and heterozygous MEFs. GAPDH was used as an internal loading control. PCR cycles for GAPDH were 28, 30, 32 cycles while for Plk4 38, 40, 42 cycles. Within each time post IR exposure, PCR products over three PCR cycles is shown corresponding to the number of cycles for GAPDH and Plk4 a) For wild type MEFs, in response to IR, Plk4 transcript levels remain constant until 1hr post radiation when a reduction in levels is observed to between 60-70% relative to the control. b) Similarly, for heterozygous MEFs, Plk4 transcript levels remained constant until 1hr post radiation when a decrease to 60-70% relative to the control was observed. c) Densitometry was performed to measure the raw intensity for each band. Values for Plk4 were normalized to GAPDH, and subsequently values for the heterozygous MEFs were normalized to the wild type to determine the mean relative expression over the three PCR time points. For the first PCR time point, there is no comparable difference between the wild type and heterozygous Plk4 transcript levels. d) At the second PCR time point, the difference in transcript levels between wild type and heterozygous is minimal. e) At the third PCR time point, differences are apparent between the transcript profiles of Plk4 in wild type and heterozygous MEFs. (NB WT: Wild Type; HET: Heterozygous)

A
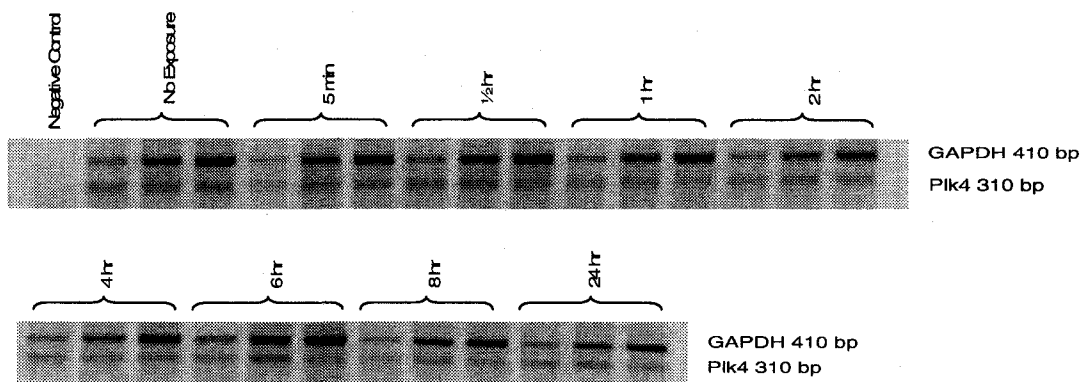
B
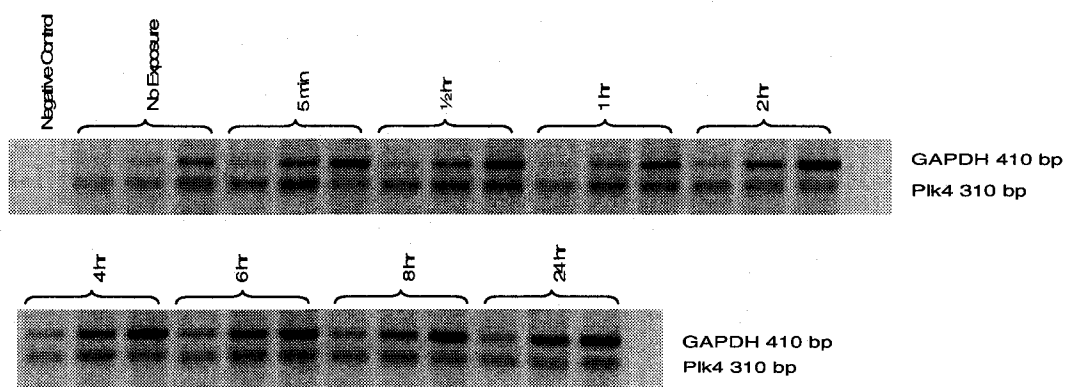
C

Comparison of Plk4 Transcript Levels in Wild Type & Heterozygous MEFs after Exposure to
25 Gy Ionizing Radiation: First PCR Time Point

Time After Exposure to Ionizing Radiation
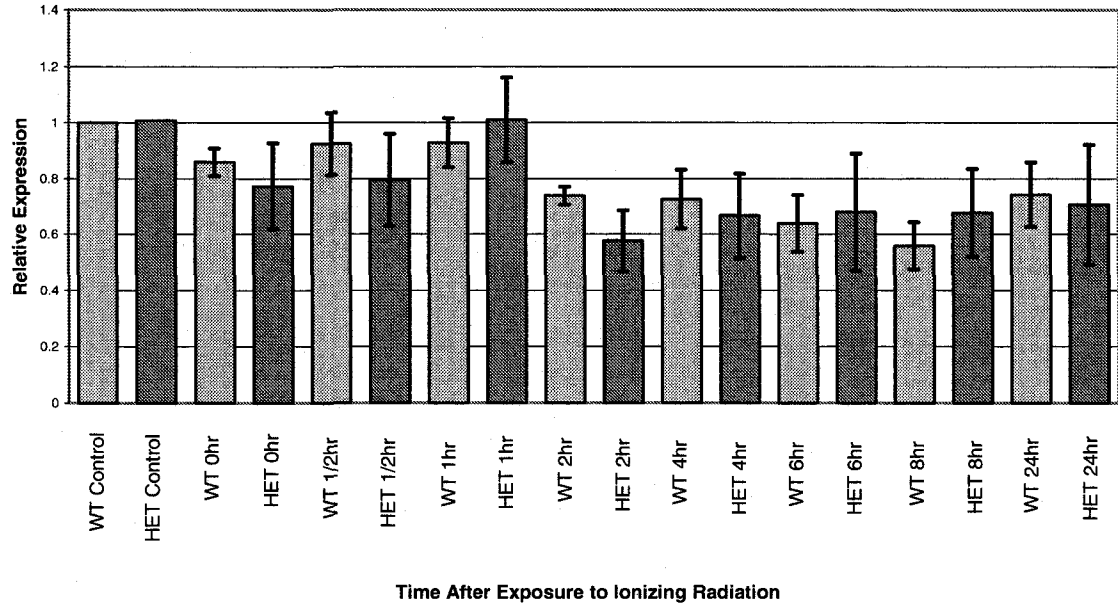
D

Comparison of Plk4 Transcript Levels in Wild Type & Heterozygous MEFs after Exposure to
25 Gy Ionizing Radiation: Second PCR Time Point

Time Point after Exposure to Ionizing Radiation
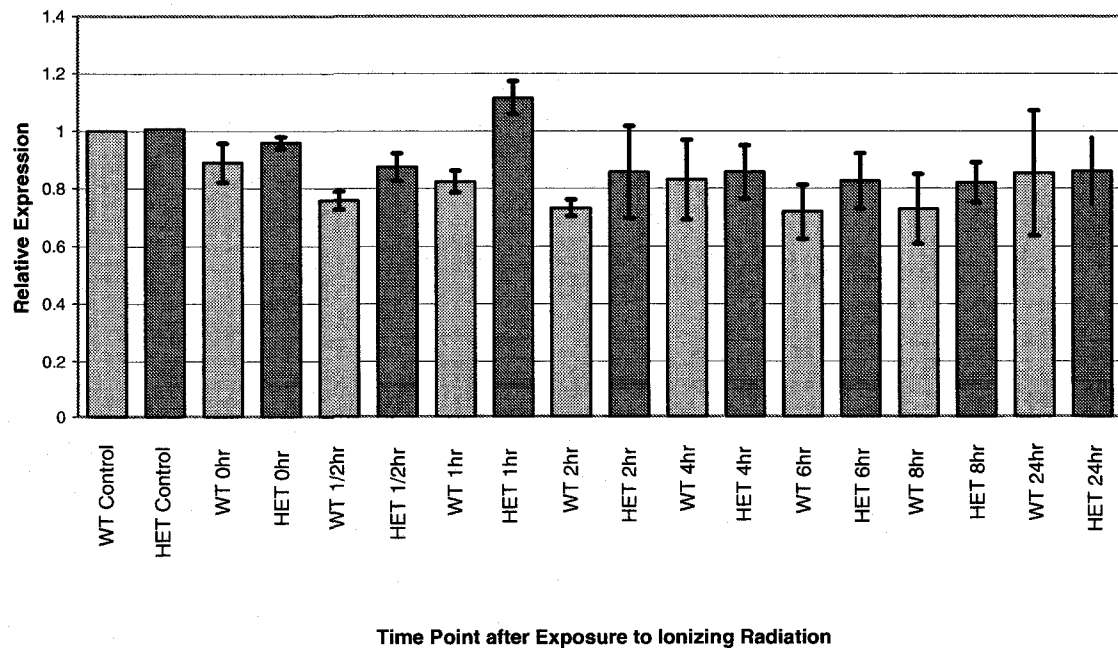
E

Comparison of Plk4 Transcript Levels in Wild Type & Heterozygous MEFs after Exposure to 25 Gy Ionizing Radiation: Third PCR Time Point

Time Point after Exposure to Ionizing Radiation
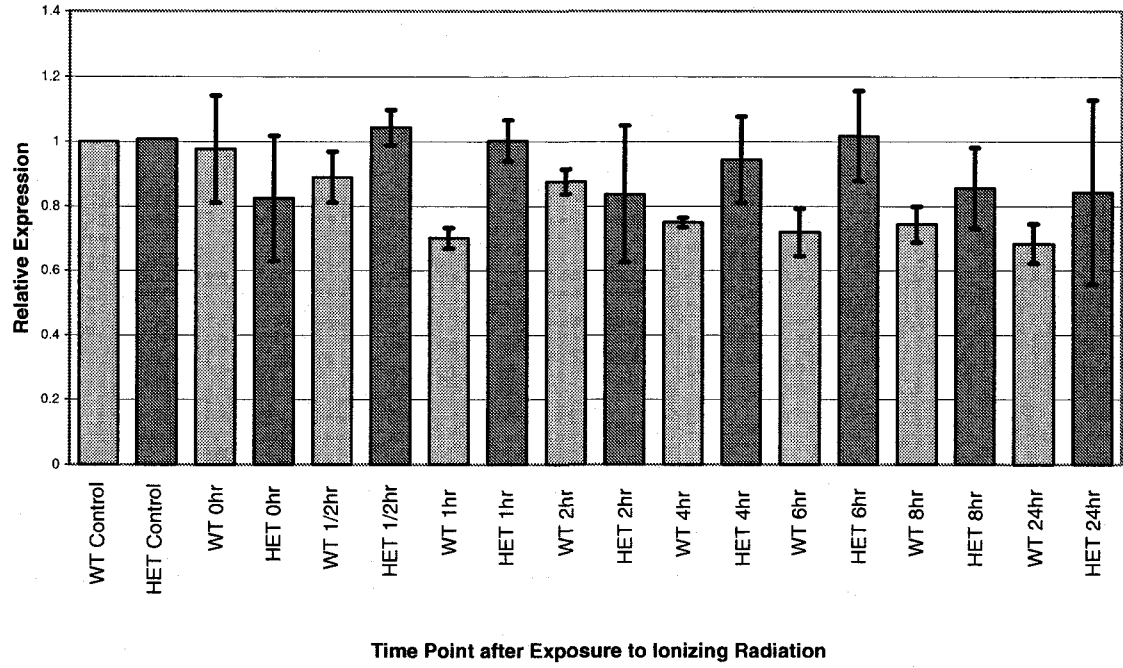
hour to 24 hours post exposure to IR, the transcript profile is 70-90% relative to the control. Most likely, in correlation with the first PCR time point, levels of Plk4 for both the wild type and heterozygous MEFs drop to around 70% relative to the control.

Upon exposure to UV, there is a striking difference in transcript profile levels of Plk4 between wild type and heterozygous MEFs. In the wild types, upon exposure to UV, levels of Plk4 are undetectable. At 2 hours post UV exposure levels reappear to the level of the control, then increase to 40% greater expression than is observed in the control (Figure 10a) (Appendix G). Unfortunately, at a dosage of 40 mJ/cm^2, the majority of cells undergo apoptosis, so levels of Plk4 at 24 hours were unable to be determined. In contrast, upon exposure to UV, no levels of Plk4 were detected in the heterozygous MEFs at any time (Figure 10b) (Appendix H). Similarly, to the wild type MEFs, the heterozygous MEFs undergo apoptosis prior to 24 hours post exposure. The results for the wild type and heterozygous Plk4 transcript profiles are consistent across all three PCR time points (Figure 10c,d,e). In the heterozygous MEFs in response to UV, the levels of Plk4 are undetectable. Therefore, it is plausible that since there is only one dose of the Plk4 gene in heterozygous MEFs, that Plk4 is transcribed at such low levels that it is undetectable by the conditions of PCR that were run. Since levels of wild type Plk4 increased relative to the control 4 to 8 hours post UV exposure, it could be hypothesized that Plk4 plays a dispensable role in apoptosis.

The Effect of Ionizing and Ultraviolet Radiation on Plk4 Protein Levels in MEFs

As RNA transcript levels do not necessarily correlate with protein levels, Plk4 protein levels in wild type and heterozygous MEFs were examined to determine if there

Figure 10: Effect of Ultraviolet Radiation on the Transcript Profile of Plk4 in Wild Type and Heterozygous MEFs

Wild type and heterozygous MEFs were exposed to 40mJ/cm^2 ultraviolet radiation (UV), and RNA was isolated at various time points post exposure. RT-PCR was performed to measure the relative quantitative difference in Plk4 expression after exposure in both wild type and heterozygous MEFs. GAPDH was used as an internal loading control. PCR time points for GAPDH were 28, 30, 32 cycles while time points for Plk4 were 38, 40, 42 cycles. Within each time post UV exposure, PCR products over three PCR cycles is shown corresponding to the number of cycles for GAPDH and Plk4a) In response to UV, Plk4 transcript levels in wild type MEFs decrease to undetectable levels immediately after exposure. At 2hrs post exposure, Plk4 levels start to continually increase to levels greater than observed in the control. b) In contrast, levels of Plk4 are completely undetectable in heterozygous MEFs upon exposure to UV through to 8hrs post exposure. c) Densitometry was performed to measure the raw intensity for each band. Values for Plk4 were normalized to GAPDH, and subsequently values for the heterozygous MEFs were normalized to the wild type to determine the mean relative expression over three PCR time points and the results were graphed. For all three PCR time points (c, d, e), both wild type and heterozygous Plk4 levels decrease after exposure to UV. But at two hours, levels of Plk4 in wild type MEFs increase and continue to increase to levels greater than control, while heterozygous Plk4 levels remain undetectable. (NB WT: Wild Type; HET: Heterozygous)

A
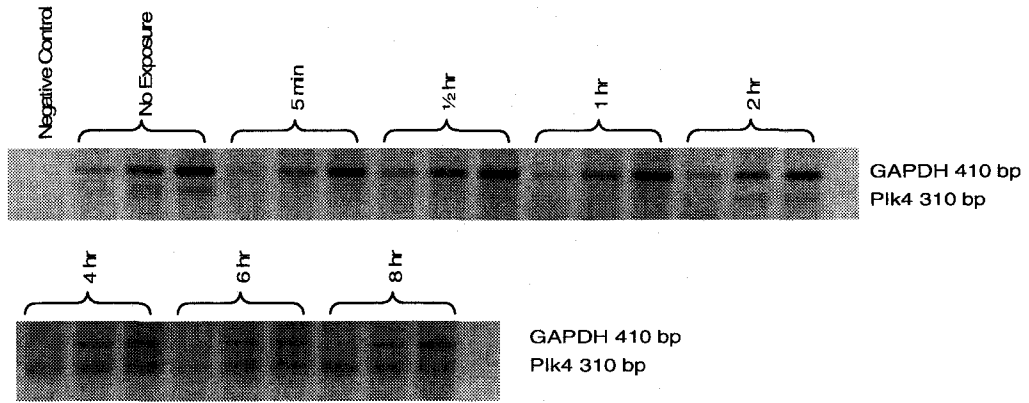
B
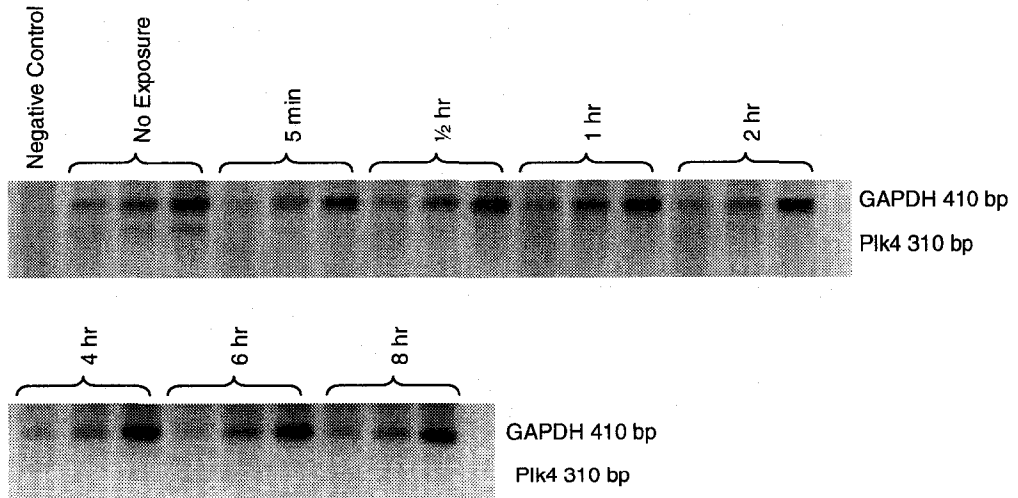
C

Comparison between Wild Type and Heterozygous PLK4 MEFs after Exposure to 40mJ/cm2 Ultraviolet Radiation: First Time Point

Time after Exposure to Ultraviolet Radiation
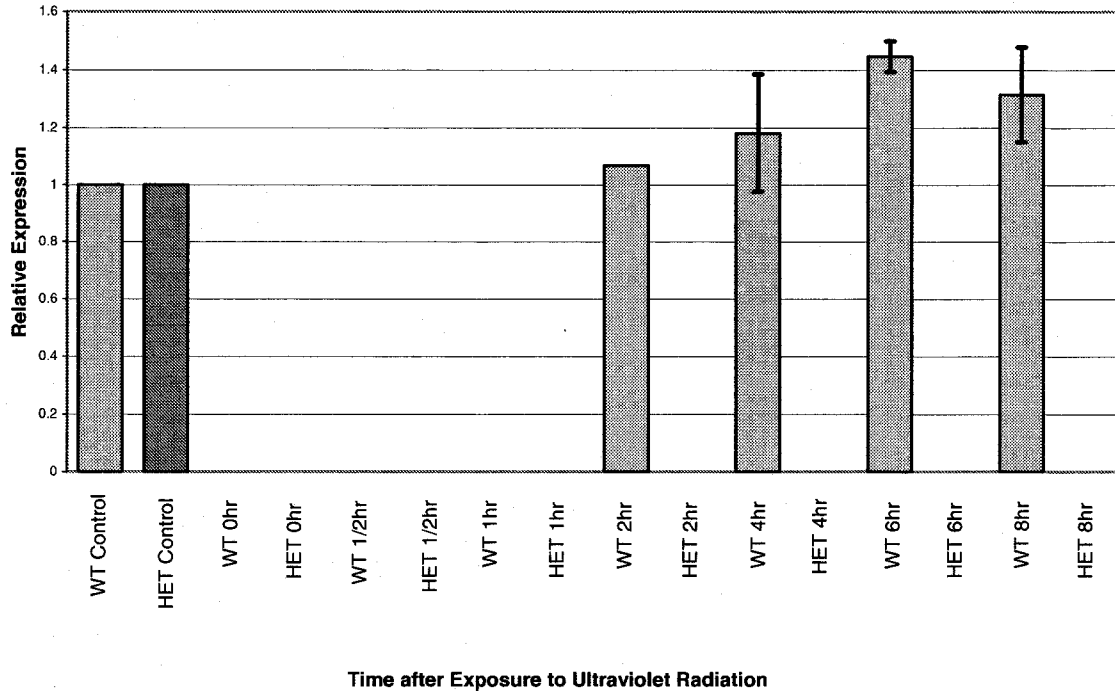
D

Comparison Between Wild Type and Heterozygous PLK4 MEFS exposed to 40mJ/cm2 Ultraviolet Radiation: Second Time Point

Time after Exposure to Ultraviolet Radiation
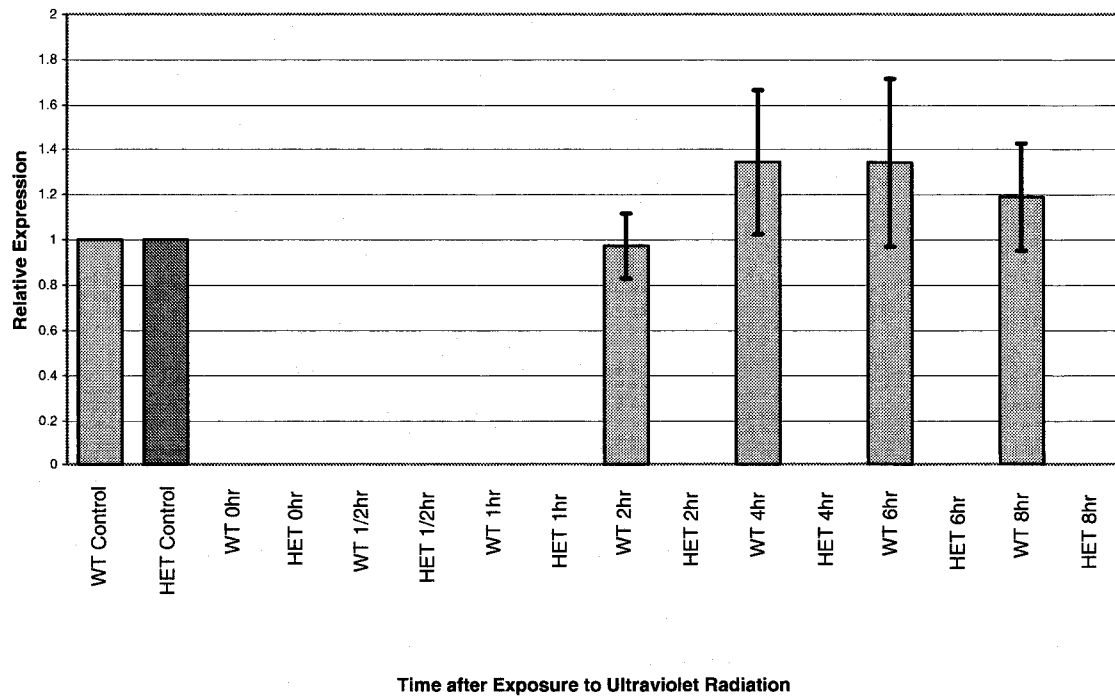
E

Comparison Between Wild Type and Heterozygous PLK4 MEFs exposed to 40mJ/cm2
Ultraviolet Radiation: Third Time Point

Time after Exposure to Ultraviolet Radiation
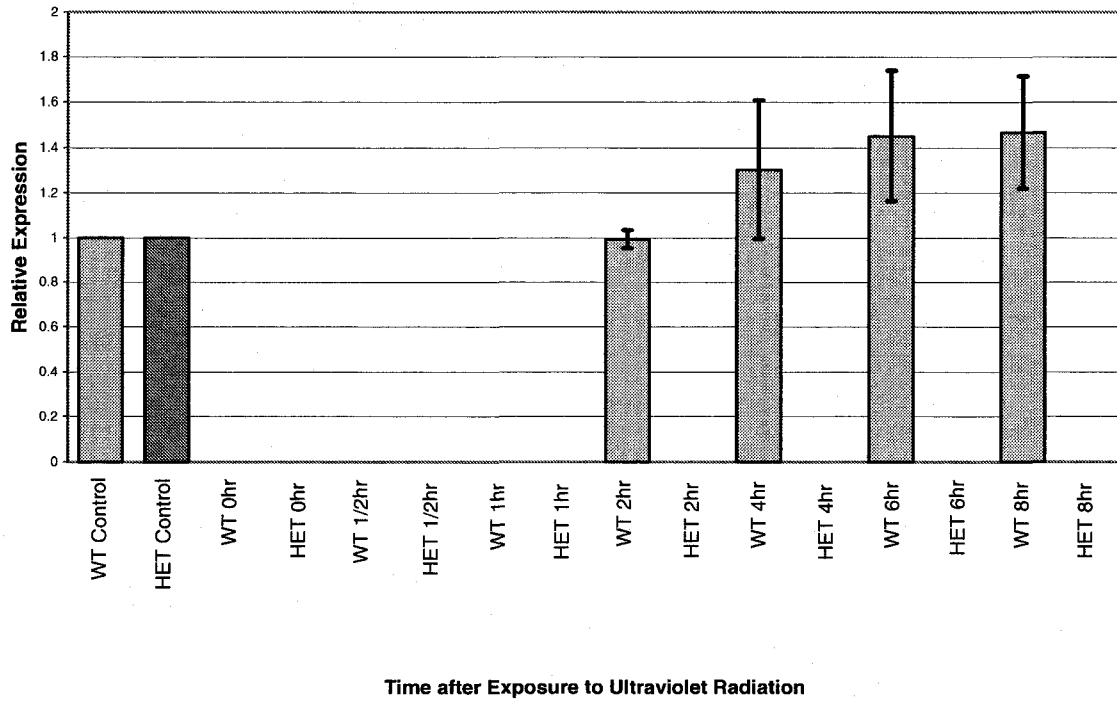
is a difference in response to both ionizing and ultraviolet radiation. Wild type and heterozygous Plk4 MEFs were exposed to 25 Gy IR and 40mJ/cm^2 UV, lysed 6hr post exposure, and the cell extracts were subjected to Western Blot analysis. For both wild type and heterozygous MEFs, levels of protein expression do not change when the MEFs were exposed to either IR or UV; 6 hours post exposure (Figure 11). GAPDH was used as a loading control to ensure equal protein loading. Though, it is apparent that protein levels in heterozygous MEFs are half the level present in wild type MEFs. This finding supports previous evidence presented by Swallow *et al*, 2005.

The Effect of Plk4 Gene Dosage on Protein Levels of DNA Damage Proteins

Plk4 is able to interact with a number of DNA damage and DNA repair proteins including Cdc25c, Chk1, Chk2, Cyclin B1, p53 and Gadd45α, and in the case of Cdc25c (Bonni *et al.*, 2008), Chk2 (Hudson, unpublished data) and p53 (Swallow *et al.*, 2005) is able to phosphorylate these proteins. It was interesting to determine whether there is a difference in protein levels in wild type and heterozygous Plk4 MEFs in response to DNA damage. Wild type and heterozygous Plk4 MEFs were exposed to 25 Gy IR or 40mJ/cm^2 UV, lysed 6hr post exposure, and the cell extracts were subjected to Western Blot analysis. Results displayed are the representative data from three experiments. Cdc25c is the phosphatase responsible for removing the inhibitory phosphates from the cyclin B1/Cdk1 complex, promoting its activation and initiating the G$_2$/M transition. When protein levels of Cdc25c were observed in wild type and heterozygous Plk4 MEFs, in general there is no difference in levels of Cdc25c (Figure 12a). Interestingly, the levels of Cdc25c do not change in response to IR or UV relative to the control. Also, there is no
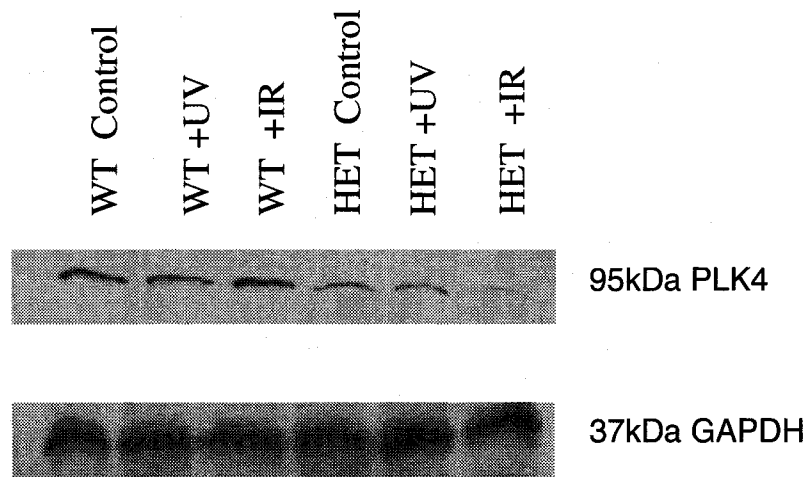
Figure 11: Plk4 Protein Levels do not Change in Response to IR or UV

Wild type and heterozygous Plk4 MEFs were exposed to either 25 Gy ionizing radiation

(IR) or 40mJ/cm^2 ultraviolet radiation (UV) and lysed 6 hr post exposure to obtain whole

cell lysates. The lysates were run on SDS Page gel and then subjected to Western blot.

The blots were probed with an anti-Plk4 antibody and with an anti-GAPDH antibody, as

a control to ensure equal protein loading. No difference in Plk4 protein levels were

observed for either wild type or heterozygous MEFs in response to IR or UV. Plk4

protein levels in heterozygous MEFs were approximately half the observable level than in

wild type MEFs. (NB WT: Wild Type; HET: Heterozygous)

observable change in Cdc25c levels in response to DNA damage between wild type and heterozygous MEFs. GAPDH was used as a loading control to ensure equal protein loading and it is used in all subsequently experiments with additional proteins.

Chk1 is a signal transducer protein activated in response to DNA damage (Abraham, 2001). When Chk1 levels were examined, there is no detectable difference between wild type and heterozygous Chk1 protein levels (Figure 12b). Strikingly, there was no increase in protein level in either the wild type or heterozygous MEFs in response to IR. Similarly, there was no change in protein level in cells exposed to UV.

Chk2 is another signal transducer protein activated in response to DNA damage (Matsuoka et al., 2000). In general, Chk2 levels in heterozygous MEFs appear to be greater than in the wild type (Figure 12c). While in response to UV, levels of Chk2 are elevated in both the wild type and heterozygous MEFs. Interestingly, levels of Chk2 are also elevated in response to IR, indicating that there is some degree of cross talk between the IR and UV DNA damage pathways.

Activation of the cyclin B1/Cdk1 complex is necessary for the G_2/M transition to occur (Bassermann et al., 2005). In general, cyclin B1 levels in heterozygous MEFs are significantly lower than those observed in the wild types (Figure 12d). While in response to UV, both wild type and heterozygous levels of cyclin B1 are decreased proportionately to the levels observed in the controls. In contrast, levels observed with IR exposure are similar to levels of cyclin B1 seen with their respective controls.

The tumor suppressor protein, p53 is considered the "guardian of the genome for the numerous cellular functions it performs (Efeyan and Serrano, 2007). p53 plays a crucial role in the cells response to genotoxic stress by initiating DNA damage pathways. In

Figure 12: Differences in Protein Levels of DNA Damage Proteins in Plk4 MEFs

Wild type and heterozygous Plk4 MEFs were exposed to either 25 Gy ionizing radiation

(IR) or 40mJ/cm^2 ultraviolet radiation (UV) and lysed 6 hr post exposure to obtain whole

cell lysates. The lysates were run on SDS Page gel and then subjected to Western blot

analysis. GAPDH was used to ensure equal protein loading. a) No change in Cdc25c

levels were observed in response to IR or UV. b) In response to IR or UV, no observable

differences in Chk1 protein levels were observed. c) Chk2 levels are elevated in

heterozygous MEFs in comparison to the wild types, while in response to both IR and

UV in both type of MEFs Chk2 levels increase. d) In general, cyclin B1 levels are lower

in heterozygous MEFs than wild types. In addition, for both wild type and heterozygous

MEFs, cyclin B1 levels decrease in response to UV. e) Levels of p53 are increased in

heterozygous MEFs in general and in response to UV, while levels are constant in both

wild type and heterozygous MEFs in response to IR. f) Gadd45α levels are increased in

heterozygous MEFs and in response to IR, while no induction of Gadd45α is observed in

wild type MEFs. (NB: WT: Wild Type; HET: Heterozygous)

A

W T Control
W T +U V
W T +IR
H E T Control
H E T +U V
H E T +IR

55kDa Cdc25c

37kDa GAPDH

B

W T Control
W T +U V
W T +IR
H E T Control
H E T +U V
H E T +IR

54 kDa Chk1

37kDA GAPDH

C

W T Control
W T +U V
W T +IR
H E T Control
H E T +U V
H E T +IR

61 kDa Chk2

37 kDa GAPDH

D

W T Control
W T +U V
W T +IR
H E T Control
H E T +U V
H E T +IR

62kDa Cyclin B1

37kDa GAPDH
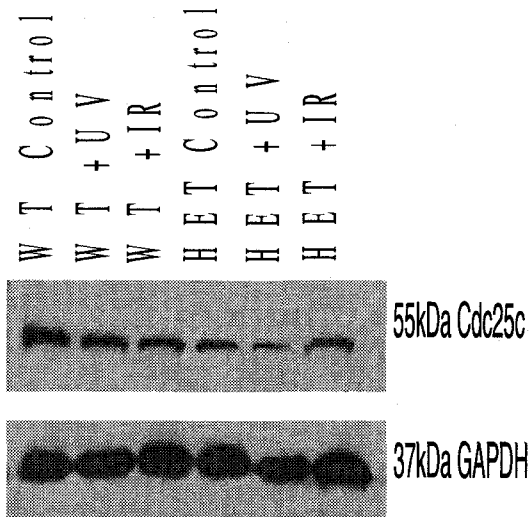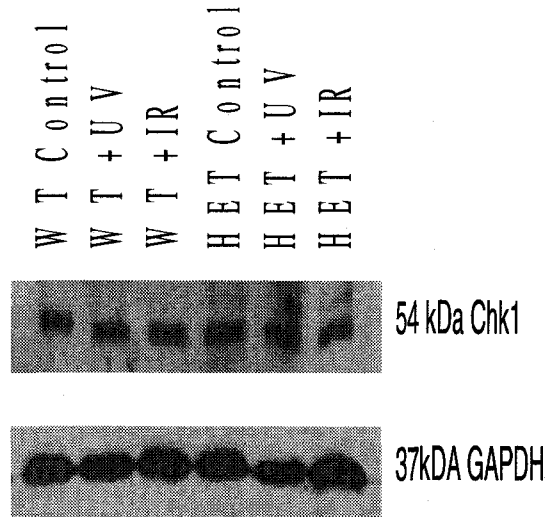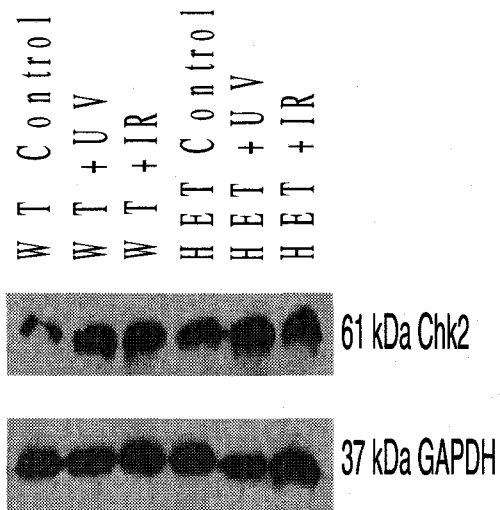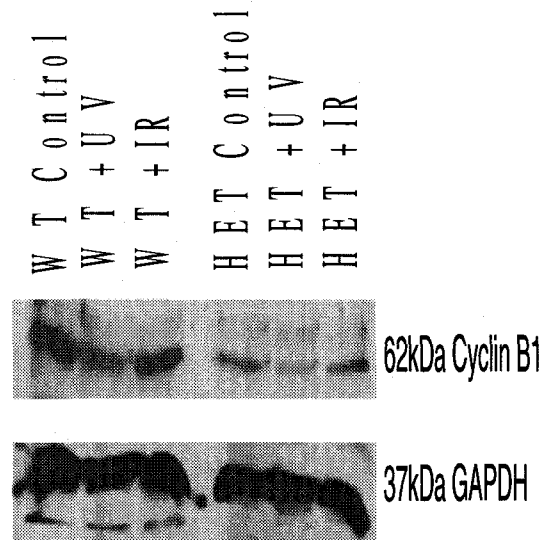
E
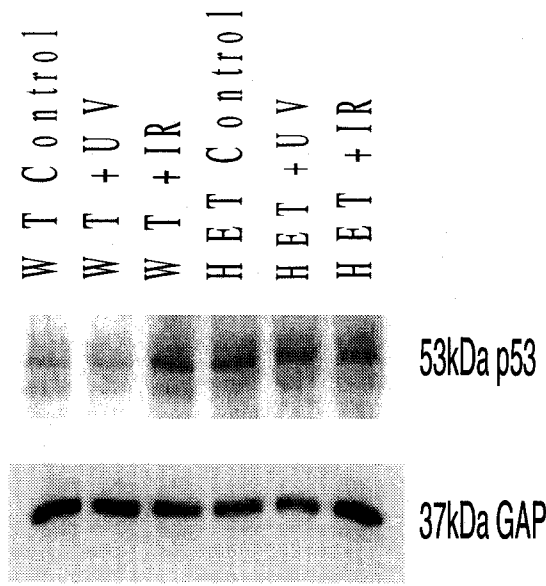
F

response to DNA damage, p53 expression is crucial to blocking cell cycle progression until the DNA is repaired or apoptotic pathways are initiated (Bunz *et al.*, 1999). In Plk4 MEFs, there is a sharp contrast between wild type and heterozygous MEFs, with levels of p53 protein expression substantially higher in the heterozygotes. A similar finding is observed in response to UV. In contrast, levels of p53 are similar for both wild type and heterozygous samples when exposed to IR (Figure 12e).

The growth arrest and DNA damage-inducible gene (Gadd45α) expression is induced by DNA damage and growth arrest signals (Zhan, 2005). In Plk4 MEFs, Gadd45α expression is significantly higher in heterozygous than wild type MEFs. No Gadd45α induction is observed in wild type MEFs in response to either IR or UV. Levels of Gadd45α are similar to the wild type control. Interestingly, Gadd45α expression is elevated in heterozygous control and IR exposed MEFs. In comparison to the heterozygous control MEFs, no increase in Gadd45α expression levels occurred in the UV exposed MEFs (Figure 12f).

Apoptotic Rate for Plk4 MEFs in Response to UV

In response to 40 mJ/cm^2 of ultraviolet radiation, a significantly high percentage of both wild type and heterozygous MEFs undergo apoptosis before 24 hours. Therefore, to determine whether there was a difference between susceptibility, a TdT-mediated dUTP Nick-End Labeling (TUNEL) assay was performed. Wild type and heterozygous MEFs were grown on glass cover slips, exposed to 40 mJ/cm^2 of UV and a TUNEL assay performed 0, 1, 2, 4, 6, 8 hours post exposure. DNase I treatment was used as a positive control as the enzyme induces fragmentation of DNA similar to what is observed in

apoptotic cells. The cells were stained red with propidium iodide (PI) to locate the nuclei, while staining green with fluorescein-12-dUTP was indicative of apoptotic cells (Figure 13a) 200 cells were counted per slide and the percentage of apoptotic cells per slide was determined. Three trials at each time point were performed and the average percentage of apoptotic cells and the standard error of the mean was determined (Figure 13b) (Appendix I).

In response to UV, there was a no significant difference in susceptibility to apoptosis between wild type and heterozygous MEFs. At 0 and 1 hour post exposure, no apoptotic cells were observed; similar to what was seen in MEFs exposed to no UV. At 2 hours post exposure, between 5 to 10% of the cells were apoptotic, though there was no statistical difference between wild type and heterozygous MEFs. The percentage of apoptotic cells at 4 hours increased to 20%, again with no statistical difference. At 6 hours post exposure, there appears to be a difference in susceptibility with 28% of wild type MEFs with 37% of heterozygotes apoptotic. At 8 hours, 65% of both wild type and heterozygous cells were apoptotic. The only statistical difference in apoptotic rate between the wild type and heterozygous MEFs was observed at 6 hours.

Figure 13: No Difference in Apoptotic Susceptibility between Wild Type and Heterozygous MEFs

Wild type and heterozygous MEFs were exposed to 40mJ/cm^2 of ultraviolet radiation (UV) and a TUNEL assay was performed at various time points post exposure a) Cells were stained red with propidium iodide (PI) to identify the nucleus, while green staining with TUNEL was indicative of apoptotic cells. DNase I treatment was used as a positive indicator of apoptotic cells. b) As time post exposure increased, there was a greater percentage of both wild type and heterozygous MEFs susceptible to apoptosis. Though, no statistical differences between susceptibility rates of apoptosis were observed.

A

Wild Type Positive Control

PI Stained   TUNEL Stained

Heterozygous Positive Control

PI Stained   TUNEL Stained

Wild Type Negative Control

Heterozygous Negative Control

Wild Type 1hr post UV

Heterozygous 1hr post UV

Wild Type 8hr post UV

Heterozygous 8 hr post UV

B

Examining Susceptability to Apoptosis between Wild Type and Heterozygous Mouse Embryonic Fibroblasts after Exposure to 40 mJ/cm2 Ultraviolet Radiation

Percent of Apoptotic Mouse Embryonic Fibroblasts

Time After Exposure to Ultraviolet Radiation

Comparison between Transcript Profiles in Wild Type and Heterozygous Plk4 MEFs in Response to UV using Microarray.

In response to ultraviolet radiation (UV), the transcript profiles for Plk4 differ significantly between wild type and heterozygous. After exposure to UV, transcript profiles in heterozygous MEFs decline significantly in comparison to control levels. In contrast, in wild type MEFs after an initial decline in Plk4 transcript levels, levels increase after 2 hours exposure and continue to increase. Therefore, it was of interest to investigate transcript profiles of other genes in response to UV.

Both wild type and heterozygous MEFs were exposed to 40mJ/cm^2 and RNA was isolated 4 hours post exposure to UV. The RNA was sent to the UHN Microarray Centre where three microarray replicates were performed using an indirect labeling methodology. A face to face hybridization using a Mouse 7.4k and Mouse 15k microarray chips was performed. A QuantArray microarray gene list was obtaining from the University Health Network (UHN) Microarray Centre website indicating the identification of each spot on the Mouse 7.4K and Mouse 15k array (http://www.microarrays.ca/products/glists.html). Quantification and analysis of the microarray chips was done in a similar method as previously stated. To obtain differences in transcript profiles between the wild type and heterozygous MEFs, the analysis of the Mouse 7.4k and Mouse 15k array were performed separately. Similarly to the previous microarray, genes were identified with a log ratio equal or greater than 1, corresponding to genes within the heterozygous MEFs that have at least a 2 fold or greater rate of transcript expression than in the wild type MEFs. These genes were up-regulated in the heterozygous MEFs. Genes identified with a log ratio equal of less than -1, corresponded

to genes having at least a 2 fold or greater rate of transcript expression or were down-regulated in the heterozygous MEFs.

From the microarray data, 27 genes were identified as having at least a two fold increase in transcript profile or were down-regulated in the heterozygous MEFs 4 hours post exposure to UV (Table 3) (Appendix L), while 84 genes were identified as having at least a two fold increase in transcript profile in the heterozygous MEFs 4 hours post exposure to UV, or were up-regulated in the heterozygous MEFs (Table 4) (Appendix J). Cellular function for each gene was identified using either Pubmed database or the Online Mendelian Inheritance in Man (OMIM) database.

Table 3: Down-regulated Genes in the Heterozygous MEFs 4 hours Post UV Exposure

Cell Cycle
CLIP-associating protein CLASP2 isoform a (Clasp2)
Centromere protein P (CENPP)
Tousled-like kinase 1

DNA Damage/DNA Repair
Rad51-like 3 (RAD51)
Essential meiotic endonuclease (Eme2)
Excision repair cross-complementing rodent repair deficiency, complementation group 6 (Ercc6)

Transcription/Translation
General transcription factor II A, 1 isoform 1 (Gtf2a1)
Polypyrimidine tract binding protein 2 (Ptbp2)
MIF4G domain containing (Mif4gd)

Cell Signaling
Phosphatidylinositol-4-phosphate 5-kinase, type II, alpha (Pip5k2a)
Lymphocyte protein tyrosine kinase (Lck)

Cellular Transport
Complement component 3a receptor 1 (C3ar1)
Membrane-spanning 4-domains, subfamily A, member 4B (Ms4a4b)
Glutamate receptor, ionotropic, AMPA4 (alpha 4) (Gria4)

Developmental
Developing brain homeobox 1 (Dbx1)

DNA Binding
Thymocyte selection-associated HMG box (TOX)

Epigenetics
Ring finger protein 20

Metabolism
Neuraminidase 1 (NEU1)
Atpase, class VI, type 11C isoform a (Atp11c)
Phosphodiesterase 3B, cGMP-inhibited (Pde3b)
DnaJ (Hsp40) homolog, subfamily C, member 1 (Dnajc1)

Unknown Function
Testis-specific LRR protein (Leucine rich repeat containing 18 (Lrrc18))
Hypothetical protein LOC236312
C21orf19-like protein
Hypothetical protein LOC66132
Zinc finger protein 655 isoform a (Zfp655)

Table 4: Up-regulated Genes in the Heterozygous MEFs 4 hours Post UV Exposure

Cell Cycle
Cell division cell 25B; Cdc25B
SCY1-like 1
Protein phosphatase 2, regulatory subunit B'', alpha; (PPP2R2A)
Transcription factor ELYS; AT hook containing transcription factor 1 (Ahctf1)

Apoptosis
WW domain-containing oxidoreductase (Wwox) (Wox1)
CASP2 and RIPK1 domain containing adaptor with death domain (Cradd) (RAIDD)
Transducin-like enhancer of split 1; Groucho-Related Gene 1
Tumor necrosis factor, alpha-induced protein 3 (A20)
Notch gene homolog 2 (Notch2)
bromodomain PHD finger transcription factor (Bptf); FETAL ALZHEIMER ANTIGEN
Forehead box O3a (Foxo3a)

DNA Damage
Mitogen activated protein kinase kinase 5 (MAP2K5)
Fanconi anemia, complementation group M (Fancm)

Tumorigenesis
Deleted in bladder cancer chromosome region candidate 1 (DBC1)
Cadherin 6
Rho-related BTB domain containing 1 (Rhobtb1)

Metabolism
Gamma-aminobutyric acid (GABA-A) receptor, subunit gamma 2 isoform 1
Glutathione reductase 1 (Gsr)
Leucyl/cystinyl aminopeptidase (Lnpep) (IRAP)
Fatty acid desaturase 3 (Fads)
Mannosidase alpha class 2B member 2 (Man2b2)
Phosphatidylinositol glycan, class A (Piga)
ADP-ribosylation factor related protein 2 (Arl15)
SH3-domain GRB2-like (endophilin) interacting protein 1 (SGIP1)
Dipeptidylpeptidase 8 (Dpp8)
Dual specificity phosphatase 27 (Dusp27)
Xylosyltransferase I (Xylt1)

Cellular Transport
Protein phosphatase 1F (PP2C domain containing) (Ppm1f)
Frequenin homolog (Freq)
Myotubularin related protein 10 (Mtmr10)
Oxysterol binding protein (Osbp)
Ring finger protein 17 (Rnf17)

Epigenetics
Sal-like protein 3
TOX high mobility group box family member 3 (Tox3)
Cat eye syndrome critical region protein 2 isoform 9 (Cecr2)
Synovial sarcoma translocation, Chromosome 18 (Ss18)

Table 4: Up-regulated Genes in the Heterozygous MEFs 4 hours Post UV Exposure Cont.

Transcriptional/Translational Regulation
WW domain-containing protein 2
Avian musculoaponeurotic fibrosarcoma (v-maf) AS42 oncogene homolog
Phenylalanine-tRNA synthetase 2 (mitochondrial) (Fars2)
WW domain-containing protein 4 (Wbp4)
GLIS family zinc finger 3 (Glis3)
cAMP responsive element binding protein 3 like-2 (Creb3l2)

Cellular Signaling
Estrogen related receptor, beta (Esrrb)
Eukaryotic translation initiation factor 4 gamma, 3 (Eif4g3)
Rap guanine nucleotide exchange factor (GEF) 6 (Rapgef6)
Unc93 homolog B (Unc93b1)
Transmembrane protein 32 (Tmem32)
Bassoon protein (BSN); zinc finger protein 231 (ZNF231)
RUN and FYVE domain-containing 2 (Rufy2)
Nuclear receptor co-repressor 1 (Ncor1)
Neurexophilin 2 (Nxph2)
RNA-binding region containing protein 2 (Rnpc2) (Caper)
Pleckstrin (Plek)
Nuclear receptor subfamily 2, group F, member 2 isoform 2
Activin receptor IIA (Acvr2a)

Developmental
Thrombospondin 2
Frizzled 5 precursor (FZD5)
T-cell factor 4 (Tcf4)
Stathmin-like 2
Odd Oz/ten-m homolog 3 (Odz3)
Chemokine-like factor super family 3 (CKLFSF3);
Transducin-like enhancer protein 3 isoform 1 (Tle3)
ADAMTS-like 3 (Adamtsl3)
Angiopoietin-like 2
SWI/SNF-related, matrix associated actin dependent regulator of chromatin, subfamily a, containing DEAD/H box 1 (Smarcad1)

Miscellaneous Function
CDC42 effector protein (Rho GTPase binding) 4 (CDC42EP4) (binder of Rho GTPases)
Pleckstrin homology domain containing, family F (with FYVE domain) member 1 (Plekhf1)
Similar to high-mobility group box 3
CD96 antigen (CD96)
FERM, RhoGEF and pleckstrin domain protein 2 (FGD2)
Ubiquitin specific protease 31 (Usp31)
Kalirin, RhoGEF kinase (Kalm)
DCN1, defective in cullin neddylation 1, domain containing 2 isoform a (Dcun1d2)
Villin 1 (Vil)

Comparison between Transcript Profile in Wild Type vs. Wild Type UV Exposure

and Heterozygous vs. Heterozygous UV Exposure Using Microarray

The data from the two microarray experiments was analyzed to determine

differences in transcript profile, firstly in the wild type vs. wild type MEFs 4 hours post

UV exposure; and secondly for the heterozygous vs. heterozygous MEFs 4 hours post

UV exposure. Since a substantial percentage of the MEFs exposed to UV were destined

for apoptosis, the analysis would provide a general survey of differences in cellular

mechanics between normal and apoptotic MEFs.

Since the two different microarray experiments were performed using chips with

different formats, similar analysis to the previous two microarray experiments couldn't be

performed. Instead, data for each cyanine labeled sample was quantified individually,

unlike the previous two experiments where a composite of the Cy3 and Cy5 image were

quantified together. Quantification was performed using LOWESS normalization within

the ScanArray Express Software. From this normalization, data was removed from

analysis if the raw intensity was not at least two standard deviations above the

background. Secondly, data was removed if the minimum signal to noise ratio was not

greater than 200. The parameter of signal to noise ratio uses the ratio of the spot intensity

to the standard deviation of the local background of all spots on the microarray. The data

was transferred to MEV where a low intensity cutoff of 100 000 was used to further

streamline the data. In order to determine differences in transcript profile, the raw

intensity values for the three non UV exposure chips were compared to the raw intensity

values of the UV exposure chips. To eliminate possible error in selecting candidate genes

due to variance between raw intensity values between the three chips of one treatment, genes with at least a three fold increase in raw intensity were selected.

For the comparison of normal wild type MEFs versus wild type MEFs exposed to UV, 171 genes were identified with at least a three fold greater raw intensity, or being up-regulated in the normal wild type MEFs (Table 5). Conversely, 83 genes were identified as having at least a three fold greater expression in the wild type MEFs 4 hours post UV exposure, or being down-regulated in the normal wild type MEFs (Table 6). Comparing the normal heterozygous MEFs to heterozygous MEFs 4 hours post UV exposure, 151 genes were observed with at least a three fold increase in raw intensity, or being up-regulated in the normal heterozygous MEFs (Table 7). While 24 genes were identified as having at least a three fold increase in expression in the heterozygous MEFs 4 hours post UV exposure, or being down-regulated in the normal heterozygous MEFs (Table 8). Cellular function for each gene was identified using either Pubmed database or the Online Mendelian Inheritance in Man (OMIM) database.

The analysis from this microarray experiment was compared to the other two microarray experiments (wild type vs. heterozygous MEFs; UV wild type vs. UV heterozygous MEFs) and there was no overlap between the genes that were up- or down-regulated in the experiments. Though, from the comparisons in this experiment (wild type MEFs vs. UV wild type MEFs; heterozygous MEFs vs. UV heterozygous MEFs), there were 56 genes that were up-regulated in both the wild type and heterozygous MEFs, while 115 genes in just the wild type MEFs and 95 genes in just the heterozygous MEFs were up-regulated. Similarly, 19 genes were up-regulated in both the wild and

heterozygous MEFs exposed to UV, while 64 genes were up-regulated in just the UV

wild type MEFs and 5 genes were up-regulated in just the UV heterozygous MEFs.

Table 5: Up-regulated Genes in Normal Wild Type MEFs Cont.

Cell Signaling
Growth factor receptor bound protein 7
Sequestosome 1
Protease (prosome, macropain) 26S subunit, ATPase 5
Calmodulin 2
Ral-interacting protein 1
Protein O-fucosyltransferase 1 isoform 1
Tnf receptor-associated factor 7
NTF2-related export protein 1
Ly6/neurotoxin 1
Rho GDP dissociation inhibitor (GDI) alpha
transglutaminase 2, C polypeptide
GRIP1 associated protein 1
Rab11-family interacting protein 2
Neurexophilin 1
Guanine nucleotide-binding protein, beta-5 subunit isoform 1

Cellular Transport
Sorting nexin 3
Annexin A11
Golgi transport 1 homolog B
ATP-binding cassette, sub-family F (GCN20), member 1
UPF3 regulator of nonsense transcripts homolog B
DnaJ (Hsp40) homolog, subfamily B, member 6 isoform a
Golgi apparatus protein 1
Transient receptor potential cation channel, subfamily C,
member 2
Sorting nexin 4

Solute carrier family 22 member 5
Solute carrier family 6 (neurotransmitter transporter, taurine),
member 6
Endoplasmic reticulum chaperone SIL1 homolog
Receptor-activity modifying protein 1
Solute carrier family 25 (mitochondrial carrier oxoglutarate
carrier), member 11
Transmembrane protein 38a
ADP-ribosylation factor-like 4

NB: An additional 54 genes with miscellaneous or unknown
function were upregulated in the normal wild type MEFs

Table 6: Down-regulated Genes in Normal Wild Type MEFs

Cell Cycle
Apoptosis antagonizing transcription factor
Large tumor supressor, homolog 1
Budding uninhibited by benzimidazoles 1 homolog, beta
Protein phosphatase 2a, catalytic subunit, beta isoform
Nuclear mitotic apparatus protein 1
Tousled-like kinase 2 isoform A
Dual specificity phosphatase 12
SMC6 protein
Retinoblastoma binding protein 6 isoform 1
Nuclease sensitive element binding protein 1
Enabled homolog isoform 1
Presenilin 1
Interleukin-1 receptor-associated kinase 1

Developmental
Glutamate receptor, ionotropic, N-methyl D-aspartate-like 1A
Ganglioside-induced differentiation-associated-protein 1
Armadillo repeat gene deleted in velo-cardio-facial syndrome

Metabolism
Lactotransferrin
Solute carrier family 25 (mitochondrial carrier, glutamate), member 22
UDP-GlcNAc:betaGal beta-1,3-N-acetylglucosaminyltransferase 7
Uridine monophosphate synthetase

Epigenetics
Sarcosine dehydrogenase

Cellular Stress
AKT1 substrate 1 (proline-rich)
Docking protein 4
IK cytokine
Oxidative stress responsive 1
Thymosin beta-4
NudC domain containing 2
TAP binding protein-like
Interferon (alpha and beta) receptor 1
Fanconi anemia, complementation group E
Thrombospondin type 1 motif

Cell Signaling
Catenin, delta 1 isoform 1
IQ motif containing GTPase activating protein 1
Epidermal growth factor receptor pathway substrate 8-like protein 2
SH3-domain GRB2-like (endophilin) interacting protein 1
Guanine nucleotide-binding protein, beta-5 subunit isoform 1
Hematopoietic SH2 domain containing
Alsin

DNA/RNA Synthesis
Zinc finger protein 9
Sng-6 homolog, nonsense mediated mRNA decay factor
Small nuclear ribonucleoprotein N

Table 6: Down-regulated Genes in Normal Wild Type MEFs Cont.

Cellular Transport
Solute carrier family 25 member 10
SAR1a gene homolog
ADP-ribosylation factor 6
Ferritin light chain 1
Ankyrin repeat and FYVE domain containing 1
Clathrin, light polypeptide (Lcb)
Solute carrier family 39 member 1
DnaJ (Hsp40) homolog, subfamily A, member 1
Transmembrane protein 16F
Solute carrier family 39 (metal ion transporter), member 6
Phospholipase A2, group IVA
Intraflagellar transport 140

Transcriptional/Translational Regulation
Heterogeneous nuclear ribonucleoprotein F
Guanine nucleotide binding protein (G protein), beta polypeptide 2 like 1
Ets family transcription factor ELF2A2
Nuclear factor of activated T-cells, cytoplasmic, calcineurin-dependent 2
Zinc finger protein of the cerebellum 5
Selenoprotein O
Bromodomain PHD finger transcription factor
RRN3 RNA polymerase I transcription factor homolog

Miscellaneous
Peptidylprolyl isomerase H isoform 2
DEAD (Asp-Glu-Ala-Asp) box polypeptide 52
Down syndrome critical region protein 3
Zinc finger protein 507
Kelch repeat and BTB domain-containing protein 9
EBNA1 binding protein 2
Short coiled-coil protein
Tetratricopeptide repeat domain 3
DEAH (Asp-Glu-Ala-His) box polypeptide 37
Transmembrane gamma-carboxyglutamic acid protein 4 precursor isoform 1
Ubiquitin-Conjugating Enzyme E2D 2
LAS1-like isoform 1
Acidic nuclear phosphoprotein 32 family, member B
Polycomb group ring finger 3
Single-stranded DNA-binding protein isoform a
Zinc and ring finger 2
Kelch-like 26
Schwannomin interacting protein 1 isoform a
Pleckstrin and Sec7 domain containing 2
Dual-specificity tyrosine-(Y)-phosphorylation regulated kinase 3
Solute carrier family 34 (sodium phosphate), member 1
Ubiquitin specific protease 13 (isopeptidase T-3)
Leucine rich repeat and coiled-coil domain containing 1
Kelch-like 24

Table 7: Up-regulated Genes in Normal Heterozygous MEFs

Cell Cycle
MOB1, Mps One Binder kinase activator-like 2A
Tubulin, beta 5
Sirtuin 2 (silent mating type information regulation 2, homolog) 2
Cell division cycle 37 homolog
Catenin (cadherin associated protein), alpha 1
SET translocation
Serine/threonine kinase 11
Transformed mouse 3T3 cell double minute 4
Cyclin B1
Actin, gamma, cytoplasmic
Kinesin-like 1
Tuberous sclerosis 1
H1 histone family, member 0
Src homology 2 domain-containing transforming protein C1
Protein regulator of cytokinesis 1-like
Perlecan (heparan sulfate proteoglycan 2)
Transformation related protein 53 inducible nuclear protein 1
DNA polymerase delta interacting protein 3
Tumor endothelial marker 7 related precursor
Tubulin, alpha 3
Vaccinia related kinase 1

Epigenetics
Chromobox homolog 3
Interferon-related developmental regulator 1

Developmental
Actin, beta, cytoplasmic
Semaphorin 3E
Parathyroid hormone-like peptide precursor
Hbs1-like isoform 1
Arkadia
Ankyrin repeat domain 6
Neural regeneration protein
Delta-like 1 homolog
RAB23, member RAS oncogene family
Semaphorin
Developmental pluripotency associated 4
Alport syndrome, mental retardation, midface hypoplasia and elliptocytosis chromosomal region gene 1 homolog
Growth differentiation factor 10
Skeletrophin

Cellular Stress
RAD50 homolog
RAD1 homolog
Polymerase (DNA directed), beta
neural-salient serine/arginine-rich
Eukaryotic translation initiation factor 2 alpha kinase 1

Table 7: Up-regulated Genes in Normal Heterozygous MEFs Cont.

Transcriptional/Translational Regulation
Splicing factor 3a, subunit 2
Heterogeneous nuclear ribonucleoprotein C
Kruppel-like factor 6
Thyroid hormone receptor interactor 13
Myeloid differentiation primary response gene 116
Eukaryotic translation initiation factor 2B
Polymerase (RNA) II (DNA directed) polypeptide E
Myeloblastosis oncogene-like 1
Aryl hydrocarbon receptor nuclear translocator isoform a
Cytoplasmic nuclear factor of activated T-cells 3
Nuclear transcription factor, X-box binding 1
Chromobox homolog 4
U2 small nuclear ribonucleoprotein auxiliary factor

Metabolism
Lysophosphatidic acid acyltransferase zeta
Alpha 1,4-galactosyltransferase
ADP-ribosylarginine hydrolase
Solute carrier family 27 (fatty acid transporter), member 4
Methylcrotonoyl-Coenzyme A carboxylase 2 (beta)
Solute carrier family 33 (acetyl-CoA transporter), member 1
Procollagen lysine, 2-oxoglutarate 5-dioxygenase 2

Cell Signaling
Ribosomal protein S6 kinase, polypeptide 2
Paternally expressed 10 isoform RF1
Growth factor receptor bound protein 7
Syndecan 1

Metadherin
Nuclear receptor binding protein
Ral-interacting protein 1
RAB11a, member RAS oncogene family
Ly6/neurotoxin 1
GRIP associated protein 1
NADH dehydrogenase (ubiquinone) Fe-S protein 3
Intersectin (SH3 domain protein 1A)
Intercellular adhesion molecule 2
Tumor protein D52
Neurexophilin 1

DNA/RNA Synthesis
Ribosomal protein L41
Ribosomal protein S8
SH2 domain binding protein 1 (tetratricopeptide repeat containing)
Ribosomal protein S20
Ribosomal protein L27a
Ribosomal protein L36a-like
Polymerase (RNA) III (DNA directed) polypeptide F
Ribosomal protein L23
Ribosomal protein S15a
High mobility group box 3
Eukaryotic translation elongation factor 1 alpha 1
Tripartite motif protein 27

Table 7: Up-regulated Genes in Normal Heterozygous MEFs Cont.

Cellular Transport

ATPase, Ca++ transporting, cardiac muscle, slow twitch 2 isoform a

Solute carrier family 35, member E1

Na+/K+ -ATPase beta 1 subunit

Target of myb1-like 1

UBX domain containing 1

ATP-binding cassette, sub-family B (MDR/TAP), member 7

Sorting nexin 9

Albumin 1

Solute carrier family 22 (organic cation transporter), member 5

RAB2, member RAS oncogene family-like

Calumenin

Phospholipid transfer protein

ADP-ribosylation factor-like 4

Solute carrier family 2 (facilitated glucose transporter), member 2

NB: An additional 46 genes with miscellaneous or unknown function were upregulated in the normal heterozygous MEFs

Table 8: Down-regulated Genes in Normal Heterozygous MEFs

Cell Cycle
Apoptosis antagonizing transcription factor
Budding uninhibited by benzimidazoles 1 homolog, beta

Cellular Stress
Docking protein 4
Interleukin-1 receptor-associated kinase 1
Oxidative stress responsive 1
NudC domain containing 2

Cellular Transport
Solute carrier family 25 (mitochondrial carrier, dicarboxylate transporter), member 10
ADP-ribosylation factor 6
Ferritin light chain 1
Ankyrin repeat and FYVE domain containing 1

Transcriptional/Translational Regulation
Zinc finger protein of the cerebellum 5

Developmental
Neurofascin

Cell Signaling
SH3-domain GRB2-like (endophilin) interacting protein 1

DNA/RNA Synthesis
Uridine monophosphate synthetase

Miscellaneous
ring finger protein 2
DEAD (Asp-Glu-Ala-Asp) box polypeptide 52
short coiled-coil protein
DEAH (Asp-Glu-Ala-His) box polypeptide 37
proline rich Gla (G-carboxyglutamic acid) 4 (transmembrane)
ubiquitin specific protease 3
dual-specificity tyrosine-(Y)-phosphorylation regulated kinase 3
ubiquitin specific protease 13 (isopeptidase T-3)
peptidylprolyl isomerase-like 2
leucine rich repeat and coiled-coil domain containing 1

Chapter 5

Discussion

Transcript Analysis in Wild Type and Heterozygous Plk4 MEFs

Wild type and heterozygous Plk4 MEFs exhibit a number of phenotypic

differences including a slower proliferation rate and increased centrosomal number

leading to chromosomal misalignment and improper segregation in heterozygotes (Ko *et*

al., 2005). It can be hypothesized that these cell cycle abnormalities lead to the increased

incidence of tumor formation observed in the heterozygous mice. In this study, murine

embryonic fibroblasts (MEFs) derived from approximately 12.5 day old embryos were

used as a model to examine the effect of lower Plk4 levels on the expression pattern of

other genes. Both wild-type and heterozygous Plk4 MEFs were used as they are both

viable. Since Plk4 nulls spontaneously abort at E7.5, the use of MEFs from this genotype

was not an option. In order to examine the nature of these global differences a microarray

based approach was utilized. MEFs were used to do the microarray and subsequent

confirmation *via* RT-PCR because they are easier to manipulate and provide a strong

reference point to compare differences between the wild type and heterozygous Plk4

phenotype. Analysis done within the MEFs would provide clues to possible differences

that may exist within adult cells.

It was determined that 9 genes contained at least a two fold decrease in

transcriptional expression in the heterozygous MEFs (Table 1), while 146 genes were

identified that had at least a two fold increase in transcriptional expression in the

heterozygous MEFs (Table 2). Three candidate genes were picked for further analysis

that may potentially contribute to the malignant phenotype seen in adults. This is

discussed in more detail below. Specifically, a RT-PCR densitometry based approach was used to re-examine that the relative expressions of Wisp1 (Figure 6), SAP30 Binding Protein (Figure 7), and Prohibitin (Figure 8) were greater in heterozygous than wild type MEFs. The results obtained through RT-PCR analysis parallel the microarray data observed.

i) Wisp1 Expression in Heterozygous MEFs

Wnt1-inducible signaling pathway protein 1 (Wisp1) is a member of the connective tissue growth factor family (CCN). It was first identified as being upregulated in Wnt1-transformed mouse mammary epithelial cells and elevated levels were present in colon cancer (Pennica et al., 1998). Additionaly, aberrant Wnt signaling has been implicated in the development of hepatocellular carcinomas (HCC) (Lee et al., 2006), and Wisp1 (Cervello et al., 2004) over expression has been characterized in HCC. It is plausible to believe that aberrant Wnt regulation and Wisp1 over expression could contribute to the increased incidence of HCC observed in heterozygous mice. Wisp1 activity is transcriptionally regulated by both Wnt1 and β-catenin. In addition, Wnt1 and β-catenin regulated over expression of Wisp1 contributes to increased morphological transformation and accelerated cell growth. Also, over expression of Wisp1 in nude mice contributed to tumor formation, therefore promoting Wisp1 as an oncogene (Xu et al., 2000). Wisp1 over expression has been implicated in additional malignancies including scirrhous gastric carcinoma (Tanaka et al., 2001), breast cancer (Xie et al., 2001), and cholangiocarcinoma (Tanaka et al., 2003). Interestingly, Wisp1

also attenuates p53-mediated apoptosis through the Akt/PKB signaling pathway (Su *et al.*, 2002).

Members of the CCN family contain four conserved modules present in other unrelated extracellular proteins. One of the modules is a thrombospondin domain (Lau and Lam, 1999). Interestingly, thrombospondin was one of the genes that also contained increased transcript expression in heterozygous MEFs. Thrombospondin is a potent inhibitor of angiogenesis, which is crucial for the growth and metastasis of tumors. Thrombospondin expression is positively regulated by p53 (Dameron *et al.*, 1994). Loss of wild type p53 leads to a loss of thrombospondin expression and the development of an angiogenic phenotype (Volpert *et al.*, 1997). Though no direct interaction has been shown between Wisp1 and thrombospondin, it could be interesting to speculate that Wisp1 could bind to thrombospondin, inhibiting its function, promoting angiogenesis and tumor formation.

In addition, in response to DNA damage, data shows that Wisp1 can attenuate p53 mediated apoptosis through the activation of the Akt pathway (Su *et al.*, 2002). Wisp1 activation of Akt allows Akt to block the release of cytochrome c from the mitochondria (Kennedy *et al.*, 1999), preventing cytochrome c activation of the caspases which would lead to apoptosis (Gottlob *et al.*, 2001). Also, expression of Wisp1 upregulates Bcl-X$_L$ activity. Bcl-X$_L$ has been shown to interact with caspase-9 (Pan *et al.*, 1998) and Apaf-1 (Hu *et al.*, 1998) resulting in inhibition of caspase activity. In addition, Bcl-X$_L$ also can block cytochrome c release from the mitochondria, preventing apoptosis (Kharbanda *et al.*, 1997).

Interestingly, in the microarray data, phosphatidylinositol 3-kinase (PI3K) was also over expressed in the heterozygous MEFs. PI3K has shown to be an upstream regulator of Akt (Nicholson and Anderson, 2002). Wisp1 activation of Akt and Bcl-X$_L$ pathways along with PI3K activation of Akt provides a mechanism within the heterozygous MEFs to overcome apoptotic pathways in response to DNA damage. Therefore, it is likely that genetic instability becomes prevalent leading to possible tumorigenesis and the increased incidence of tumors observed in heterozygous mice.

Wisp1 was first identified as a Wnt1 and β-catenin induced oncogene (Xu *et al.*, 2000). Though the exact method of Wisp1 activation has yet to be elucidated, it is known that activation of Wnt target genes occurs through β-catenin. β-catenin forms a complex with the T-cell factor/lymphocyte enhancing factor (TCF/LEF) family of transcription factors to activate the expression of target genes (Polakis, 1999). Interestingly, TCF4 also came up as being over expressed in heterozygous MEFs. Though the transcription factor responsible for the activation of Wisp1 is yet to be known, it is interesting to speculate that TCF4 may be responsible as both were observed as being over expressed in heterozygous MEFs.

Along with Wisp1 (Cervello *et al.*, 2004), TCF4 (Zhao *et al.*, 2004) over expression has also been implicated in the development of HCC. It is plausible to believe that aberrant Wnt regulation could contribute to the increased incidence of HCC observed in heterozygous mice. It has been established that Wisp1 expression blocks p53 mediated apoptosis (Su *et al.*, 2002). Heterozygous Plk4 MEFs present a number of abnormal phenotypes including abnormal centrosome number leading to improper chromosome segregation (Ko *et al.*, 2005). Therefore, it seems plausible that heterozygous MEFs may

be unable to undergo p53 mediated apoptosis due to over-expression of Wisp1. It is possible that a similar phenotype as seen in the heterozygous MEFs may occur in adult cells. Without apoptosis occurring, these cells continue to go through the cell cycle leading to a greater number of cells with abnormalities and greater genomic instability which eventually will contribute to tumor formation.

ii) SAP30 Binding Protein Expression in Heterozygous MEFs

Epigenetic modification to genes has been well documented as a method to promote oncogenesis within the cell. Since heterozygous mice develop cancer at a rate significantly higher than there wild type littermates, it has been hypothesized that epigenetic silencing of Plk4 could be a possible mechanism for the increased incidence of tumorigenesis observed. Plk2 has been implicated in mediating apoptosis as a target gene of p53, though epigenetic silencing of Plk2 transcriptional expression *via* methylation is a common occurrence in B cell lymphomas (Smith *et al.*, 2006). While epigenetic silencing of Plk1 or Plk3 has not been characterized, preliminary evidence suggests that Plk4 in heterozygous mice livers undergoes methylation in the CpG island region of its promoter at a significantly higher rate than wild types. Methylation of Plk4 has also been observed in the liver tumors of heterozygous mice. Methylation of the Plk4 promoter increases with age and is more frequent in male mice. Additionally, chronic alcohol exposure has been implicated to promote methylation (Kim and Shukla, 2006). Heterozygous MEFs become methylated upon exposure to a lower concentration of ethanol than wild types (Ward, Hudson unpublished data).

Though little is known about the function of SAP30 binding protein (SAP30BP), it has been determined that SAP30BP binds to SAP30, a component of the Sin3 histone deactylase complex (Sin3-HDAC) (Li *et al.*, 2004). The Sin3-HDAC complex is primarily responsible for deacetylating nucleosomes in Sin3 regulated promoters, resulting in repressed chromatin structure and transcriptional silencing (Kuzmichev *et al.*, 2002). In addition, through the enzymatic function of Sin3, the Sin3-HDAC complex can also participate in DNA methylation, N-acetylglucoseamine transferase activity, and histone methylation. The Sin3-HDAC lacks DNA-binding capacity, so therefore it must be targeted to gene promoters by DNA-binding proteins (Silverstein and Ekwall, 2005). In yeast, SAP30 has the ability to recruit the complex to the gene promoters, but as yet this function hasn't been established in mammals (Zhang *et al.*, 1998). Therefore, though the structure of SAP30BP has yet to be elucidated, it is interesting to speculate that SAP30BP could contain a DNA-binding domain to target the Sin3-HDAC complex to the promoter region.

In addition, p53 is able interact with TATA box binding-protein (TBP) to facilitate the recruitment of Sin3-HDAC complex to the gene promoter for transcriptional repression (Farmer *et al.*, 1996). Li *et al*, 2005 found that in response to DNA damaging agents, p53-mediated transcriptional repression of Plk4 occurs through the activity of HDAC. p53 regulates not only DNA damage pathways but also the mitotic spindle checkpoint. Previous work showed that in heterozygous Plk4 hepatocytes there was a significant increase in multipolar spindle complexes with aberrant mitosis (Ko *et al.*, 2005). The mitotic spindle checkpoint is necessary to ensure proper mitotic spindle formation, so that inaccurate chromosomal segregation does not occur (Xie *et al.*, 2005).

Therefore, it could be hypothesized that methylation of Plk4 occurs in a p53-mediated manner and consequently could inhibit oncogenesis.

Methylation and other epigenetic modifications are responsible for altering chromatin structure. Preliminary evidence shows that Plk4 is methylated, though the functional cascade responsible for this methylation is unknown. Li *et al.*, 2005 showed that Plk4 undergoes repression in a p53-mediated manner through HDAC. Plk4 is able to interact and phosphorylate p53 on Ser-293 (Swallow *et al.*, 2005), though the functional significance of this interaction is unknown. Observed results within the heterozygous MEFs show that p53 levels are significantly greater than in the wild types (Figure 13e). Therefore, it can be hypothesized that with lower levels of Plk4 in heterozygous MEFs, Plk4 is unable to phosphorylate p53 to the extent that wild type Plk4 can; thus p53 function is not inhibited in the heterozygous MEFs. This could explain the increase in methylation observed in heterozygous mice livers, as p53 which is not inhibited by Plk4 is able to inhibit Plk4 function through methylation.

iii) Prohibitin Expression in Heterozygous MEFs

Cellular senescence occurs when normal cells lose their ability to divide and is indicative of cells with a flattened morphology and an increased granularity phenotype (Campisi, 2001). These phenotypes are observed at a greater frequency and at an earlier passage in heterozygous Plk4 MEFs than in wild types.

The cellular senescent phenotype is observed when shortening of the telomeres is recognized by the cell as a DNA double strand break, and DNA damage pathways are initiated. ATM/ATR mediate the activation of cell-cycle checkpoints associated with

cellular senescence, mainly via p53, CHK1 and CHK2, with the participation of p21, p16 and retinoblastoma protein (RB) (Schmitt *et al.*, 2007). RB function has been deemed necessary for inducing senescence (Lowe and Sheer, 2003). RB has been shown to interact with various transcriptional co repressors including heterochromatin protein 1 (HP1) (Narita *et al.*, 2003), histone deacetyase 1 (HDAC1) (Brehm *et al.*, 1998), DNA methyltransferase (Vandel et *al.*, 2001), Polycomb proteins (Ross *et al.*, 1999), and chromatin-remodeling complexes Brg and Brm (Strober *et al.*, 1996) to repress E2F transcription factor (E2F) transcriptional activity. E2F activity is essential for cell proliferation and its reduction immediately provokes cellular senescence (Maehara *et al.*, 2005).

Prohibitin has been implicated to play a crucial role in cellular senescence though the mechanism has yet to be elucidated (Dell'Orco *et al.*, 1996). It is believed that prohibitin's role in senescence acts through its ability to repress E2F transcription factor 1 (E2F1) mediated transcriptional activity (Wang *et al.*, 1999). In response to senescence-inducing DNA damage agents, prohibitin localizes to specific heterochromatic foci, where it binds with members of the heterochromatin protein 1 (HP1) family of proteins. Prohibitin and HP1 bind to the E2F1-responsive proliferative promoter, leading to repression of E2F1 transcriptional activity (Rastogi *et al.*, 2006). Prohibitin is able to bind p53 to enhance its transcriptional abilities (Fusaro *et al.*, 2003), though it is not clear whether p53 functions in a positive feedback loop to activate prohibitin or an upstream protein is responsible. Also, p53 levels are elevated within heterozygous MEFs (Figure 12e), indicative of senescence occurring at an earlier passage in the heterozygous MEFs.

Additionally, with both prohibitin and RB binding HP1 to inactivate E2F1, this suggests redundancy within the signaling cascade.

Testing for the senescent phenotype in Plk4 MEFs was attempted through a β-galactosidase staining assay. Though efforts to get the assay to work failed, as no blue colour indicate of senescence was observed, even though characteristics such as flattened morphology and increased granularity were observed in the heterozygous MEFs at an earlier passage than wild types.

It is plausible that heterozygous Plk4 MEFs are senescent at an earlier passage than wild types, as a mechanism to prevent oncogenesis. Though no DNA replicative differences have been characterized between wild type and heterozygous MEFs, aberrant DNA replication may cause the telomeres in heterozygous MEFs to shorten at an accelerated rate. Therefore, the shortening of the telomeres could give cause to genetic instability which would lead to oncogenesis.

Plk4 Expression in MEFs: Response to DNA Damaging Agents

Other members of the Plk family are implicated to play crucial roles in response to DNA damage. In response to both ionizing radiation (IR) and ultraviolet radiation (UV), Plk1 activity is repressed by the DNA damage sensor protein ATM and ATR, respectively, to inhibit Plk1 from pushing cells through the cell cycle (van Vugt *et al.*, 2001). In contrast, Plk3 is activated by ATM in response to IR to prevent cell cycle progression (Xie *et al.*, 2001), while Plk2 is activated by p53 (Shimizu-Yoshida *et al.*, 2001). Subsequently, Plk4 has been hypothesized to play a role in the DNA damage pathways, therefore Plk4 MEFs were examined in response to IR or UV.

i) Plk4 Transcript Abundance in Response in Ionizing Radiation

In response to IR, for both wild type and heterozygous MEFs, the levels of Plk4 decreased to 60 to 80% relative to the control, with no difference between the two (Figure 9). Both wild type and heterozygous MEFs were resistant to this dose of IR, as 24 hours post exposure, the cells were viable. As Plk4's prominent identified role within the cell is centrosome duplication and dynamics (Habendanck *et al.*, 2005), it is likely that cell cycle checkpoints were enabled to ensure that any damage to the genome was repaired before cell growth and division ensued, coinciding with a decrease in Plk4 levels. At 8 and 24 hours post exposure, Plk4 levels in both wild type and heterozygous MEFs started to increase to levels relative to the control, indicating that any DNA damage was repaired and the normal cellular dynamics were resuming.

ii) Plk4 Transcript Abundance in Response to Ultraviolet Radiation

In response to UV exposure, there was a sharp contrast observed between Plk4 levels in the wild type and heterozygous MEFs. After UV exposure, both wild type and heterozygous levels decrease immediately, until 2 hours when wild type levels increased and continued to increase to levels greater relative to the control, 8 hours post exposure. In contrast, no detectable levels of Plk4 were observed in the heterozygous MEFs (Figure 10). p53 transcriptionally represses Plk4 function (Li *et al*, 2005), so it is possible that with lower levels of Plk4 as observed in the heterozygous MEFs, the repression of Plk4 by p53 is stronger. Furthermore, p53 protein levels are also increased in heterozygous MEFs in comparison to wild types in response to UV (Figure 12e).

Twenty-four hours post exposure to UV, both wild type and heterozygous MEFs were not viable, as greater than 95% of the cells were floating. It can be assumed that the heterozygous MEFs undergo apoptosis through a p53-mediated pathway, but for wild type MEFs it is difficult to make this assumption. Over-expression of Plk4 attenuates p53-mediated apoptosis (Li *et al.*, 2005) and p53 protein levels were not elevated in wild type MEFs in response to UV (Figure 12e), so it can be hypothesized that wild type MEFs undergo apoptosis through another pathway.

iii) Plk4 Protein Levels in Response to DNA Damage

As differences were observed in mRNA levels, it was of interest to see whether changes in protein levels actually corresponding to the mRNA levels. In response to both IR and UV, no changes were observed in Plk4 protein levels for both wild type and heterozygous MEFs, 6 hours post exposure. Consistent with previous studies Plk4 protein levels in the heterozygous MEFs were half the level observed in the wild type MEFs (Figure 11) (Swallow *et al.*, 2005).

iv) DNA Damage Protein Levels

Proteins with known roles in the DNA damage pathways were examined in the MEFs to see if a difference in Plk4 gene dose would have an effect on their response to either IR or UV. Cdc25c is the phosphatase responsible for removing the inhibitory phosphates from the cyclin B1/Cdk1 complex, promoting its activation and initiating the G_2/M transition. In response to ionizing radiation and ultraviolet radiation, Cdc25c activity is inhibited by Chk2 (Matsuoka *et al.*, 1998) and Chk1 (Lam and Rosen, 2004),

respectively. Levels of Cdc25c did not change in either wild type or heterozygous MEFs in response to either IR or UV (Figure 12a).

Activation of the cyclin B1/Cdk1 complex is necessary for the G_2/M transition to occur (Bassermann *et al.*, 2005). In response to DNA damage, a cell cycle block occurs at the G_2/M transition and either the damage to the genome is repaired or the cell enters programmed cell death. In response to UV, levels are minimal in comparison to the control, indicative of a cell cycle block that would occur as the cells prepare to undergo apoptosis. In contrast, levels of cyclin B1 in IR exposed cells were identical to control levels, indicating that any DNA damage done was repaired and the cells are normally going through the cell cycle. Though, control and IR levels of cyclin B1 in heterozygous MEFs were about half of what was observed in the wild types (Figure 12d). Since no flow cytometry was performed to assure a normal cell cycle profile amongst the MEFs, it is impossible to state that there was an equal percentage of wild type and heterozygous MEFs at the G_2/M transition. Though, the observed data is supported by previous findings, which showed that heterozygous MEFs have a slower growth rate which would be consistent with a delay entry into mitosis (Ko *et al.*, 2005). Additionally, when examining hepatocytes, the appearance of cyclin B1 protein levels was delayed and persisted longer in heterozygous Plk4 hepatocytes than in wild types (Ko *et al.*, 2005).

The checkpoint kinase members Chk1 and Chk2 protein levels were examined to observe the response elicited by DNA damage. Chk1 is a signal transducer protein activated in response to DNA damage. In response to ultraviolet radiation, Chk1 is activated by ATR (Abraham, 2001), allowing it to phosphorylate members of the Cdc25 phosphatase family inhibiting there ability to promote cellular progression (Lam and

Rosen, 2004). Interestingly, no differences in Chk1 protein levels were observed in response to either IR or UV (Figure 12b). Assuming a normal cell cycle profile, the majority of MEFs would have been present within either G_1 or S phases of the cell cycle. Cann and Hicks, 2006 found that in response to IR, primary MEFs lack an immediate G_1/S checkpoint and that any response to DNA damage occurs at the level of individual replication origins, instead of inducing a complete shutdown of S-phase entry. This rationale explains why no Chk1 response was elicited in the MEFs.

Chk2 is another signal transducer protein activated in response to DNA damage. In response to ionizing radiation, Chk2 is activated by ATM (Matsuoka *et al.*, 2000). Chk2 phosphorylates members of the Cdc25 phosphatase family inhibiting there function and delaying the cell cycle (Lam and Rosen, 2004). In addition, Chk2 is able to activate p53, allowing p53 to initiate a halt to cell cycle progression (Hirao *et al.*, 1998). Chk2 protein levels increased for both wild type and heterozygous MEFs in response to both IR and UV (Figure 12c). Elevated levels in response to UV suggest that there may be some cross talk in the DNA damage pathways. Previous work confirms the notion of cross talk between the DNA damage pathways. Cisplatin, an anticancer drug functions by inducing DNA cross linking in base pairs which is a similar phenotype observed in response to UV. Interestingly, in response to cisplatin treatment ATR and not ATM was activated (Pabla *et al.*, 2007). Downstream, both Chk1 and Chk2 are phosphorylated in an ATR-dependent manner, though Chk1 degradation occurs by the proteosome shortly after phosphorylation. Chk2 activation of p53 leads to a p53-dependent cell cycle checkpoint activation. In terms of the MEFs, the induction of Chk2 in response to IR probably

activated cell cycle checkpoints while DNA damage was repaired, while in response to UV, Chk2 activated p53-dependent apoptotic pathways.

p53 is widely considered the guardian of the genome, and its expression is activated in response to genotoxic stresses (Efeyan and Serrano, 2007) .). p53 plays a crucial role in the cells response to genotoxic stress by initiating DNA damage pathways. In response to DNA damage, p53 expression is crucial to blocking cell cycle progression until the DNA is repaired or apoptotic pathways are initiated (Bunz *et al.*, 1999). In heterozygous Plk4 MEFs, protein levels of p53 are substantially higher than in wild types, with a similar scenario observed in response to UV. In response to IR, an induction of p53 expression is observed in wild type MEFs, while levels of p53 are constant with control levels for the heterozygotes (Figure 12e). There are a multitude of possible reasons to explain these variances. Firstly, Plk4 has been shown to phosphorylate p53 on serine 293 (Swallow *et al.*, 2005). Though the significance of this interaction has yet to be characterized, it could be possible that the phosphorylation of p53 on this residue is inhibitory or that it may affect p53 stability. Based on the fact that there is only one dose of Plk4 present in the heterozygous MEFs, there may not be enough Plk4 present to inhibit p53 transcriptional activity, explaining the higher degree of p53 expression observed in the heterozygotes. It is also possible that the interaction between Plk4 and p53 maybe part of a negative feedback mechanism as p53 inhibits Plk4 through HDAC (Li *et al.*, 2005) and Plk4 inhibits p53 through direct phosphorylation. The second reason for increased p53 levels in heterozygous MEFs may be due to the fact that aberrant mitotic spindle formation and chromosome mis-segregation is exhibited in heterozygous MEFs (Ko *et al.*, 2005). In response to these defects, p53 is activated by the mitotic

spindle checkpoint causing a delay in mitotic progression (Xie *et al.*, 2005). In addition, the lack of p53 induction in wild type MEFs in response to UV, suggests that apoptosis occurs in these cells in a p53-independent manner, while in response to IR, cell cycle checkpoints are established in a p53-dependent manner.

The growth arrest and DNA damage-inducible gene (Gadd45α) expression is induced by DNA damage and growth arrest signals (Zhan, 2005). In response to ionizing radiation, Gadd45α is transcriptionally activated by p53 (Zhan *et al.*, 1994), while disruption of p53 transcriptional ability inhibits Gadd45α induction (Zhan *et al.*, 1996). In contrast, the induction of Gadd45α via UV is p53 independent. The induction is dependent on transcription factors Oct-1 and NF-YA (Jin *et al.*, 2001). In response to genotoxic stress, Gadd45α is able to initiate a G_2/M block on the cell cycle but is not necessary for the block to occur (Wang *et al.*, 1999). Induction of Gadd45α was only observed in the control heterozygous MEFs and the heterozygous MEFs exposed to IR. In the heterozygous MEFs where p53 expression was induced, this corresponded to an increase in Gadd45α, except in the MEFs exposed to UV (Figure 12f). As these cells would eventually undergo apoptosis, as would the wild type MEFs, it is unclear whether Gadd45α expression is necessary. Gadd45α has been implicated to play a role in apoptosis (Takekawa and Saito, 1998), though it is unclear whether Gadd45α activates apoptosis or whether Gadd45α up-regulation occurs as a consequence of apoptotic response to genotoxic stress (Zhan, 2005). No induction of Gadd45α expression was observed in the control wild type or IR exposed wild type MEFs. As p53 expression was observed in the wild type MEFs exposed to IR and no Gadd45α induction was observed,

it is possible that p53 mechanism of inducing cell cycle checkpoints and DNA repair was independent of Gadd45α expression.

Apoptotic Susceptibility in MEFs

Wild type and heterozygous Plk4 MEFs were exposed to 40 mJ/cm^2 UV and subjected to a TUNEL assay to determine if there was a difference in susceptibility to undergo apoptosis. At each of the time points examined, there was no statistical difference between the percentages of MEFs that stained positive for DNA fragmentation characteristic of apoptotic cells (Figure 13). As this experiment was performed using 40 mJ/cm^2 UV, it is unknown whether there would be a difference in percentages at a lower exposure rate. Subsequently, it is not known the dose of UV where the majority of MEFs start undergoing apoptosis. At a lower dose it could be hypothesized that there would be statistical differences observed with a higher percentage of heterozygous cells escaping apoptosis and promoting oncogenesis. This assumption is made as a microarray experiment comparing wild type and heterozygous MEFs exposed to 40 mJ/cm^2 UV, 4 hours post exposure showed Cdc25b as being over expressed in the heterozygous MEFs. Cdc25b is essential for mitotic entry when cells recover from a DNA damage checkpoint-induced arrest (van Vugt *et al.*, 2004). Cdc25b's requirement for mitotic entry after DNA damage and its involvement in tumorigenesis will be explained in further detail in the next section.

Transcript Differences in Plk4 MEFs: Response to Ultraviolet Radiation

Transcriptional differences were observed in Plk4 mRNA transcript profiles between wild type and heterozygous MEFs upon exposure to UV. Therefore, it was of interest to gain a further understanding of differences in the transcript profiles of additional genes within the Plk4 MEFs. Microarray analysis was performed comparing wild type and heterozygous MEFs 4 hours post UV exposure. It was discovered that 27 genes presented at least a two fold decrease in transcript profile in the heterozygous MEFs (Table 3), while 84 genes had a least a two fold increase in transcript profile in the heterozygous MEFs (Table 4). As stated above, by far the most unique finding from the microarray data was Cdc25b being over expressed in the heterozygous MEFs.

Cell division cycle 25b (Cdc25b) is a member of the Cdc25 phosphatase family that plays a major role in the cell cycle control by dephosphorylating and activating cyclin-dependent kinases at stages during the cell cycle (Burgler *et al.*, 2006). Cdc25b plays a role in mitotic entry though its function is dispensible (van Vugt *et al.*, 2004). Ferguson *et al.*, 2005 showed that mice lacking Cdc25b were normal for development, cell cycle and DNA damage response and that Cdc25a or additional phosphatases could compensate for its loss. In contrast, Cdc25b function is essential for resuming the cell cycle after DNA-damage cell cycle arrest (van Vugt *et al.*, 2004). Re-entry of the cell cycle is also reliant on Plk1-dependent degradation of Wee1 (Watanabe *et al.*, 2004), which phosphorylates and inhibits the CDKs. Removal of Wee1 allows Cdc25b to more efficiently dephosphorylate and activate cyclin B1/CDK1 (van Vugt *et al.*, 2004). Additionally, over expression of Cdc25b can lead to the accelerated exit of cells from the G_2/M transition after the checkpoint has been activated. Though, this acceleration can be

reversed by inhibiting the catalytic activity of Cdc25b using pharmalogical inhibitors against Cdc25 (Bugler *et al.*, 2006).

Cdc25b has been identified as being over expressed in a number of human cancers including head and neck cancer (Gasparotto *et al.*, 1997), non-small cell lung cancer (Wu *et al.*, 1998) gastic cancer (Kudo *et al.*, 1997), non-Hodgkins lymphoma (Hernandez *et al.*, 1998), colon cancer (Takemasa *et al.*, 2000), esophagus cancer (Nishioka *et al.*, 2000), breast cancer (Cangi *et al.*, 2000), and ovarian cancer (Broggini *et al.*, 2000). In these types of cancers, over expression of Cdc25b correlated with a higher degree of malignancy and a poorer prognosis for the patient (Kristjansdottir and Rudolph, 2004).

In addition, in an examination of hepatocellular carcinomas (HCC), Cdc25b was one of the most significantly over expressed genes in comparison to non-tumor liver tissue (Chen *et al.*, 2002); while silencing of Cdc25b expression in HCC cell lines has been shown to prevent cell proliferation, migration and invasion and delay xenograft growth (Yan *et al.*, 2008).

It can be hypothesized that over expression of Cdc25b in heterozygous Plk4 mice could contribute to the increased tumorigenesis observed. In response to DNA damage, cell cycle checkpoints are employed to repair any damage to the genome. Loss of an upstream tumor suppressor which targets Cdc25b and Plk1 for repression would contribute to Cdc25b and Plk1 initiating re-entry to the cell cycle without errors in the genome being repaired. Combined with the heterozygous Plk4 MEFs and hepatocytes displaying aberrant spindle formation and abnormal chromosome segregation during mitosis (Ko *et al.*, 2005), it is plausible that these factors could contribute to cellular

transformation leading to an oncogenic state. It will be interesting to examine Cdc25b mRNA and protein levels within heterozygous liver tumors in comparison to normal tissue within both wild type and heterozygous liver samples to see if there is an observable difference in Cdc25b levels. If Cdc25b levels are elevated within heterozygous liver tumors, it provides a possible explanation for increased liver tumor incidence within heterozygous Plk4 mice.

In comparison of the microarray data between normal wild type and heterozygous MEFs and Plk4 MEFs exposed to UV, six genes were over expressed in heterozygous MEFs within both data sets. This indicates that these genes are over expressed in heterozygous MEFs in normal pathways and in response to DNA damage. These genes include T-cell factor 4, villin 1, fetal alzheimer antigen, thromospondin, transducin-like enhancer of split 1 and sal-like 3.

The T-cell factor/ lymphocyte enhancing factor (TCF/LEF) are a family of transcription factors involved in the Wnt signaling pathway (Polakis, 1999). B-catenin binds TCF4 to activate its transcriptional activity in Wnt signaling and TCF4 has been implicated in neural and limb development (Cho and Dressler, 1998). TCF4 has been shown to transcriptionally activate cell cycle regulating genes such as cyclin D1 and c-myc. As stated above, TCF4 over expression has been implicated in the development of hepatocellular carcinoma (Zhao *et al.*, 2004). As numerous Wnt genes and their targets over expression has been characterized in hepatocellular carcinoma, it is possible that aberrant Wnt regulation could be a contributing factor in the development of liver tumors in heterozygous mice.

Villin 1 has been characterized as an actin-binding protein associated with the striated border of simple columnar epithelium in the body. Villin is believed to function in the bundling, nucleation, capping, and severing of actin filaments, though its exact function is unknown (Friederich *et al.*, 1999). Since the exact cellular function of villin has yet to be fully characterized, it is difficult to speculate as to the exact implications over expression of villin may have in heterozygous MEFs.

Fetal alzheimer antigen (FAC1) was first characterized as being developmentally regulated in the cortex of the brain (Bowser *et al.*, 1995). Subsequent results show FAC1 as a DNA binding protein capable of functioning as a transcription factor (Jordan-Sciutto *et al.*, 1999), and capable of inducing apoptosis by activating caspase 3 (Strachan *et al.*, 2005). Over expression of FAC1 in heterozygous MEFs exposed to UV is rational as these MEFs undergo apoptosis due to UV exposure. Given FAC1's role to activate caspase 3 and initiate apoptotic pathway in normal heterozygous MEFs, it possible to speculate that there is genomic instability within these cells that would mediate the initiation of these pathways. Since the heterozygous MEFs continue to divide, it is also possible that some downstream effector inhibits these apoptotic pathways, continuing the presence of genomic instability leading to cellular transformation.

Thrombospondin is a crucial inhibitor of angiogenesis (Volpert *et al.*, 1997) whose expression is positively regulated by p53 (Dameron *et al.*, 1994). p53 mutations have been extensively characterized in hepatocellular carcinomas (Aguilar *et al.*, 1994). Therefore it is possible that loss of or a mutation in p53 would inhibit thrombospondin from prevent angiogenesis and allowing tumor formation to occur. It would be interesting

to examine levels of both p53 and thrombospondin in hepatocellular carcinomas in heterozygous mice to see if this hypothesis is true.

Transducin-like enhancer of split 1 (TLE1) or Groucho-related gene 1 (GRE1) is a member of the Notch signaling pathway that is a transcriptional repressors of Wnt signaling and other cell fate determination signals (Liu *et al.*, 1996). In a study examining dedifferentiation from a well-differentiated tumor to a moderately-differentiated tumor in hepatocellular carcinomas (HCC), TLE1 was discovered as being over expressed (Midorikawa *et al.*, 2002). TLE1 over expression in HCC may provide for an additional mechanism for tumor formation within heterozygous Plk4 mice. In addition, Allen *et al.*, 2006 used a mouse model to examine TLE1 over expression. TLE1 over expression induced lung adenocarcinoma formation with reduced levels of p53 and increased levels of the receptor tyrosines kinases ErbB1 and ErbB2. Interestingly, in Plk4 heterozygous mice, the second most common site of tumor formation was the lung, with the tumors characterized as adenocarcinomas (Ko *et al.*, 2005). TLE1 over expression and p53 down regulation may provide a mechanism for lung tumor formation in heterozygous Plk4 mice.

Sal-like 3 (SALL3) is a homologue of the *Drosophila* splat gene which is required for development of the head and tail segments in an organism (Kohlhase *et al.*, 1999). Loss of SALL3 expression leads to embryonic lethality from failure of cranial nerve formation from the hindbrain (Parrish *et al.*, 2004). Beyond this information, little is known about SALL3 and its functional role within the cell. Therefore it is difficult to make an assumption to the exact role that SALL3 over expression plays within heterozygous MEFs.

Transcriptional Difference between Normal & UV Wild Type and Normal & UV Heterozygous MEFs

To gain an understanding of the transcriptional differences between normal and UV exposed MEFs, the two previous microarray data sets were compared. It was discovered that 171 genes were up-regulated in normal wild type MEFs (Table 5), while 83 genes were down-regulated in the normal wild type MEFs (Table 6). 151 genes were observed to be up-regulated in normal heterozygous MEFs (Table 7), while 24 genes were down-regulated in the normal heterozygous MEFs (Table 8). In addition, there were a number of common genes that were up-regulated in both the normal wild type and normal heterozygous MEFs. Similarly, there were common genes within the UV wild type MEFs and the UV heterozygous MEFs. The differences in the genes that were up-regulated in both the wild type and heterozygous MEFs provide additional clues to possible mechanistic differences, explaining the phenotypic differences observed between wild type and heterozygous MEFs. Likewise, differences observed between the UV wild type MEFs and UV heterozygous MEFs could provide mechanistic pathways to explain possible differences in the MEFs response to ultraviolet radiation.

While this analysis may provide a general survey of the differences between normal and UV exposed MEFs, without secondary validation using northern analysis, RT-PCR or real-time PCR, the validity of the results remains debatable. Proper statistical microarray analysis was unable to be performed due to software limitations with the TIGR software suite. The microarray analysis was performed manually using comparing raw intensity, so it is possible that errors could have been made.

Future Directions

It is necessary to determine the function significance of the interaction between Plk4 and p53. Plk4 is able to phosphorylate p53 on Ser-293 (Swallow *et al.*, 2005). Ser-293 is within the DNA-binding domain of p53 (Bell *et al.*, 2002). It is hypothesized that Plk4 and p53 interact through a feedback mechanism and p53 is able to repress Plk4 function through HDAC. It is assumed that over-expressing Plk4 causing phosphorylation of Ser-293 will inhibit p53's ability to bind the TATA box binding protein to facilitate the recruitment of HDAC to repress Plk4. Additionally, it is of interest to determine how the phosphorylation of Ser-293 affects the conformational structure of p53 and how this affects its function. Furthermore, it is of interest to investigate how the phosphorylation of Ser-293 affect protein levels of known downstream p53 targets and that this phosphorylation could affect p53 function in multiple signaling cascades. Elucidating the functional interaction between p53 and Plk4 will provide a more thorough incite to the observed phenotypic differences between wild type and heterozygous MEFs. This interaction may provide a clue as to why heterozygous Plk4 mice develop cancer at a rate twenty times greater than wild types.

Appendix A

Antibodies used for Western Blotting

Primary Antibody	Species of Origin	Company
Anti-Plk4	Rabbit	Cell Signaling
Anti-Chk1	Mouse	Sigma
Anti-Chk2	Mouse	Sigma
Anti-Cdc25c	Rabbit	Santa Cruz
Anti-Cyclin B1	Rabbit	Sigma
Anti-Gadd45α	Mouse	Santa Cruz
Anti-p53	Mouse	Sigma
Anti-GAPDH	Rabbit	Santa Cruz

Appendix B: Densitometry Values Measuring the Difference between Wisp1 in Wild Type and Heterozygous Plk4 MEFs

background	Raw vol. 26364.0996	Raw vol. - background	Wisp1: GAPDH ratio	GAPDH: Wisp1 ratio	Relative Expression
Wild type GAPDH 28 cycles	919925.125	893561.0254	0.420814145	2.376345974	1
Wild type Wisp1 36 cycles	402387.219	376023.1191			
Wild type GAPDH 30 cylces	1541912.75	1515548.65	0.551950213	1.811757612	1
Wild type Wisp1 38 cycles	862871.5	836507.4004			
Wild type GAPDH 32 cycles	2336858.5	2310494.4	0.62828486	1.591634725	1
Wild type Wisp1 40 cycles	1478012.75	1451648.65			
Het GAPDH 28 cycles	820753.938	794389.8379	0.597460705		1.419773342
Het Wisp1 36 cycles	500980.813	474616.7129			
Het GAPDH 30 cycles	1360938.5	1334574.4	1.071343812		1.941015307
Het Wisp1 38 cycles	1456152.13	1429788.025			
Het GAPDH 32 cycles	2260383.5	2234019.4	1.091606635		1.737439026
Het Wisp1 40 cycles	2465034.5	2438670.4			

background	Raw vol. 11052.71	Raw vol.- background	Wisp1: GAPDH ratio	GAPDH: Wisp1 ratio	Relative Expression
Wild type GAPDH 28 cycles	670245.8	659193.0996	0.473523909	2.111825783	1
Wild type Wisp1 36 cycles	323196.4	312143.6934			
Wild type GAPDH 30 cylces	1284027	1272974.412	0.541718155	1.845978377	1
Wild type Wisp1 38 cycles	700646.1	689593.3496			
Wild type GAPDH 32 cycles	1935105	1924052.037	0.6045299992	1.654177648	1
Wild type Wisp1 40 cycles	1174200	1163147.162			
Het GAPDH 28 cycles	665106.8	654054.0996	0.594620642		1.255735202
Het Wisp1 36 cycles	399966.8	388914.0684			
Het GAPDH 30 cycles	1540087	1529034.662	0.643154918		1.187250071
Het Wisp1 38 cycles	994458.9	983406.1621			
Het GAPDH 32 cycles	2092982	2081929.287	0.844774207		1.397406611
Het Wisp1 40 cycles	1769813	1758760.162			

Appendix B: Densitometry Values Measuring the Difference between Wisp1 in Wild Type and Heterozygous Plk4 MEFs

	Raw vol. background 29219.66	Raw vol. - background	Wisp1: GAPDH ratio	GAPDH: Wisp1 ratio	Relative Expression
Wild type GAPDH 28 cycles Wild type Wisp1 36 cycles	790256.4 439129.4	761036.7188 409909.7813	0.538620242	1.856595655	1
Wild type GAPDH 30 cylces Wild type Wisp1 38 cycles	1751340 1167629	1722120.469 1138409.344	0.661050934	1.512742739	1
Wild type GAPDH 32 cycles Wild type Wisp1 40 cycles	2641537 1682409	2612316.844 1653188.844	0.632843925	1.580168445	1
Het GAPDH 28 cycles Het Wisp1 36 cycles	1418071 1096446	1388851.094 1067226.219	0.768423788		1.426652266
Het GAPDH 30 cycles Het Wisp1 38 cycles	2425696 1849739	2396475.844 1820519.344	0.759665218		1.149178042
Het GAPDH 32 cycles Het Wisp1 40 cycles	3010125 2512858	2980905.344 2483638.344	0.833182559		1.316568789

	Mean of Relative Expression	Standard Error of the Mean
Wild type GAPDH 28 cycles Wild type Wisp1 36 cycles	1	6.40988E-17
Wild type GAPDH 30 cylces Wild type Wisp1 38 cycles	1	4.53247E-17
Wild type GAPDH 32 cycles Wild type Wisp1 40 cycles	1	0
Het GAPDH 28 cycles Het Wisp1 36 cycles	1.3673886937	0.055861174
Het GAPDH 30 cycles Het Wisp1 38 cycles	1.425814473	0.257834762
Het GAPDH 32 cycles Het Wisp1 40 cycles	1.483804809	0.128946275

Appendix C: Densitometry Values Measuring the Difference between SAP30BP in Wild Type and Heterozygous Plk4 MEFs

background	Raw vol. 18514.45508	Raw vol. - background	SAP30:GAPDH ratio	GAPDH:SAP30 ratio	Relative Expression
wild type GAPDH 28 cycles	2446141.25	2427626.795	0.193433375	5.169738668	1
wild type SAP30 36 cycles	488098.5	469584.0449			
wild type GAPDH 30 cycles	3041062.75	3022548.295	0.252182627	3.965380213	1
wild type SAP30 38 cycles	780748.625	762234.1699			
wild type GAPDH 32 cycles	3544022	3525507.545	0.347919102	2.874231376	1
wild type SAP30 40 cycles	1245105.875	1226591.42			
het GAPDH 28 cycles	1474111.875	1455597.42	0.39897513		2.062597157
het SAP30 36 cycles	599261.625	580747.1699			
het GAPDH 30 cycles	2555974.25	2537459.795	0.403064754		1.598304999
het SAP30 38 cycles	1041275.063	1022760.607			
het GAPDH 32 cycles	3615165.75	3596651.295	0.428416093		1.231366976
het SAP30 40 cycles	1559377.75	1540863.295			

background	Raw vol. 63960.99	Raw vol. - background	SAP30:GAPDH ratio	GAPDH:SAP30 ratio	Relative Expression
wild type GAPDH 28 cycles	1160815	1096853.887	0.463718452	2.156480932	1
wild type SAP30 36 cycles	572592.4	508631.3867			
wild type GAPDH 30 cycles	1705416	1641454.762	0.702618594	1.423247276	1
wild type SAP30 38 cycles	1217278	1153316.637			
wild type GAPDH 32 cycles	2901811	2837850.262	0.755072789	1.324375629	1
wild type SAP30 40 cycles	2206745	2142783.512			
het GAPDH 28 cycles	1150743	1086781.762	0.916715455		1.976879398
het SAP30 36 cycles	1060231	996269.6367			
het GAPDH 30 cycles	1952738	1888776.887	1.170751838		1.666269364
het SAP30 38 cycles	2275250	2211289.012			
het GAPDH 32 cycles	2713188	2649227.012	1.169204073		1.54846538
het SAP30 40 cycles	3161448	3097487.012			

Appendix C: Densitometry Values Measuring the Difference between SAP30BP in Wild Type and Heterozygous Plk4 MEFs

background	Raw vol. 37715.93	Raw vol. - background	SAP30:GAPDH ratio	GAPDH:SAP30 ratio	Relative Expression
wild type GAPDH 28 cycles	1892347	1854631.441	0.776019987	1.288626604	1
wild type SAP30 36 cycles	1476947	1439231.066			
wild type GAPDH 30 cycles	2442998	2405281.816	0.831769401	1.202256297	1
wild type SAP30 38 cycles	2038356	2000639.816			
wild type GAPDH 32 cycles	3206160	3168444.066	0.704065787	1.420321819	1
wild type SAP30 40 cycles	2268509	2230793.066			
het GAPDH 28 cycles	1898739	1861023.191	1.095554424		1.411760577
het SAP30 36 cycles	2076568	2038852.191			
het GAPDH 30 cycles	2568537	2530821.066	1.05762211		1.271532841
het SAP30 38 cycles	2714368	2676652.316			
het GAPDH 32 cycles	3262060	3224344.066	0.929154505		1.319698418
het SAP30 40 cycles	3033630	2995913.816			

	Mean of Relative Expression	Standard Error of Mean
wild type GAPDH 28 cycles	1	0
wild type SAP30 36 cycles		
wild type GAPDH 30 cycles	1	0
wild type SAP30 38 cycles		
wild type GAPDH 32 cycles	1	0
wild type SAP30 40 cycles		
het GAPDH 28 cycles	1.817079044	0.204164295
het SAP30 36 cycles		
het GAPDH 30 cycles	1.512035735	0.121841455
het SAP30 38 cycles		
het GAPDH 32 cycles	1.366510258	0.094483439
het SAP30 40 cycles		

Appendix D: Densitometry Values Measuring the Difference between Prohibitin in Wild Type and Heterozygous Plk4 MEFs

background

	Raw vol. 7580.438	Raw vol. -background	Prohibitin:GAPDH ratio	GAPDH:Prohibitin ratio	Relative Expression
Wild Type GAPDH 28 cycles	1099192	1091611.063	0.093499176	10.69528147	1
Wild Type Prohibitin 32 cycles	109645.2	102064.7344			
Wild Type GAPDH 30 cycles	2557978	2550397.313	0.117779731	8.490425234	1
Wild Type Prohibitin 34 cycles	307965.5	300385.1094			
Wild Type GAPDH 32 cycles	3357395	3349814.813	0.129183177	7.740946041	1
Wild Type Prohibitin 36 cycles	440320.2	432739.7188			
Heterozygous GAPDH 28 cycles	1780317	1772736.563	0.25336474		2.709807205
Heterozygous Prohibitin 32 cycles	456729.4	449148.9375			
Heterozygous GAPDH 30 cycles	2768097	2760516.813	0.257723458		2.188181747
Heterozygous Prohibitin 34 cycles	719030.4	711449.9375			
Heterozygous GAPDH 32 cycles	3167132	3159551.563	0.272387883		2.108539907
Heterozygous Prohibitin 36 cycles	868204	860623.5625			

background

	Raw vol. 323.7324219	Raw vol. -background	Prohibitin:GAPDH ratio	GAPDH:Prohibitin ratio	Relative Expression
Wild Type GAPDH 28 cycles	1132657.125	1132333.393	0.268635479	3.722516482	1
Wild Type Prohibitin 30 cycles	304508.6563	304184.9238			
Wild Type GAPDH 30 cycles	2297342.75	2297019.018	0.265195271	3.77080631	1
Wild Type Prohibitin 32 cycles	609482.3125	609158.5801			
Wild Type GAPDH 32 cycles	3159474.25	3159150.518	0.270344872	3.698978983	1
Wild Type Prohibitin 34 cycles	854383.875	854060.1426			
Heterozygous GAPDH 28 cycles	1219420	1219096.268	0.592161105		2.204329472
Heterozygous Prohibitin 30 cycles	722225.125	721901.3926			
Heterozygous GAPDH 30 cycles	2469992	2469668.268	0.490350846		1.849018063
Heterozygous Prohibitin 32 cycles	1211327.656	1211003.924			
Heterozygous GAPDH 32 cycles	3301639.5	3301315.768	0.467749339		1.730194974
Heterozygous Prohibitin 34 cycles	1544512	1544188.268			

Appendix D: Densitometry Values Measuring the Difference between Prohibitin in Wild Type and Heterozygous Plk4 MEFs

	Raw vol.	Raw vol. -background	Prohibitin:GAPDH ratio	GAPDH:Prohibitin ratio	Relative Expression
background	1508.041016				
Wild Type GAPDH 28 cycles	599444.6875	597936.6465	0.529391405	1.888961532	1
Wild Type Prohibitin 30 cycles	318050.5625	316542.5215			
Wild Type GAPDH 30 cycles	1044770.375	1043262.334	0.574597289	1.740349317	1
Wild Type Prohibitin 32 cycles	600963.75	599455.709			
Wild Type GAPDH 32 cycles	1630274.25	1628766.209	0.464413964	2.153251361	1
Wild Type Prohibitin 34 cycles	757929.8125	756421.7715			
Heterozygous GAPDH 28 cycles	555335.0625	553827.0215	1.17326326		2.216249165
Heterozygous Prohibitin 30 cycles	651292.9375	649784.8965			
Heterozygous GAPDH 30 cycles	1005245.563	1003737.521	1.249696006		2.174907591
Heterozygous Prohibitin 32 cycles	1255874.813	1254366.771			
Heterozygous GAPDH 32 cycles	2106043.5	2104535.459	0.769611984		1.657168051
Heterozygous Prohibitin 34 cycles	1621183.75	1619675.709			

	Mean of Relative Expression	Standard Error of Mean
Wild Type GAPDH 28 cycles	1	4.53247E-17
Wild Type Prohibitin 30 cycles		
Wild Type GAPDH 30 cycles	1	0
Wild Type Prohibitin 32 cycles		
Wild Type GAPDH 32 cycles	1	0
Wild Type Prohibitin 34 cycles		
Heterozygous GAPDH 28 cycles	2.376795281	0.166541512
Heterozygous Prohibitin 30 cycles		
Heterozygous GAPDH 30 cycles	2.070702467	0.110908419
Heterozygous Prohibitin 32 cycles		
Heterozygous GAPDH 32 cycles	1.831967644	0.139883756
Heterozygous Prohibitin 34 cycles		

Appendix E: Densitometry Values for Wild Type MEFs Exposed to Ionizing Radiation

background	Raw vol.	Raw vol. - background	Sak:GAPDH ratio	GAPDH:Sak ratio	Relative Expression
	8481.902				
GAPDH control 28 cycles	702238.4	693756.4727	1.136308999	0.880042314	1
Sak control 38 cycles	796803.6	788321.7227	0.749084222	1.334963373	1
GAPDH control 30 cycles	1296124	1287642.223	0.493576757	2.026027333	1
Sak control 40 cycles	973034.4	964552.4727			
GAPDH control 32 cycles	1800180	1791698.223			
Sak control 42 cycles	892822.5	884340.5977			
GAPDH 0hr 28 cycles	989309.4	980827.4727	1.017872919		0.895771239
Sak 0hr 38 cycles	1006840	998357.7227			
GAPDH 0hr 30 cycles	1977185	1968703.098	0.611115243		0.815816467
Sak 0hr 40 cycles	1211586	1203104.473			
GAPDH 0hr 32 cycles	2223148	2214665.848	0.562372863		1.139382791
Sak 0hr 42 cycles	1253950	1245467.973			
GAPDH 1/2hr 28 cycles	834707.9	826226.0352	1.236792571		1.088429796
Sak 1/2hr 38 cycles	1030352	1021870.223	0.574401676		0.76629135
GAPDH 1/2hr 30 cycles	1720896	1712414.348			
Sak 1/2hr 40 cycles	991436.4	982954.5352			
GAPDH 1/2hr 32 cycles	1955446	1946964.348	0.366356271		0.742247818
Sak 1/2hr 42 cycles	721764.5	713282.5977			
GAPDH 1hr 28 cycles	729699.1	721217.2227	1.165653802		1.025824669
Sak 1hr 38 cycles	849171.5	840689.5977	0.636301933		0.849439775
GAPDH 1hr 30 cycles	1574422	1565939.723			
Sak 1hr 40 cycles	1004892	996410.4727			
GAPDH 1hr 32 cycles	1926760	1918277.973	0.318230553		0.644743799
Sak 1hr 42 cycles	618936.6	610454.6602			
GAPDH 2hr 28 cycles	770014.1	761532.2227	0.783986652		0.689941427
Sak 2hr 38 cycles	605513	597031.0977	0.509528159		0.680020143
GAPDH 2hr 30 cycles	1374963	1366481.098			
Sak 2hr 40 cycles	704742.5	696260.5977			
GAPDH 2hr 32 cycles	1643080	1634597.598	0.457810365		0.927536313
Sak 2hr 42 cycles	756817.6	748335.7227			
GAPDH 4hr 28 cycles	2185418	2176936.098	0.888869843		0.782243073
Sak 4hr 38 cycles	1943495	1935012.848	0.635879818		0.848876266
GAPDH 4hr 30 cycles	3282291	3273808.848			
Sak 4hr 40 cycles	2090231	2081748.973			
GAPDH 4hr 32 cycles	4525526	4517043.598	0.3783031		0.766452422
Sak 4hr 42 cycles	1717294	1708811.598			
GAPDH 6hr 28 cycles	2023361	2014878.723	0.946284608		0.832770496
Sak 6hr 38 cycles	1915131	1906648.723	0.459519581		0.61344181
GAPDH 6hr 30 cycles	4137496	4129013.598			
Sak 6hr 40 cycles	1905845	1897362.598			
GAPDH 6hr 32 cycles	4548805	4540322.598	0.42571465		0.862509518
Sak 6hr 42 cycles	1941364	1932881.848			
GAPDH 8hr 28 cycles	2440065	2431583.098	0.819181997		0.72091482
Sak 8hr 38 cycles	2000391	1991909.098	0.491641671		0.656323624
GAPDH 8hr 30 cycles	3765103	3756621.348			
Sak 8hr 40 cycles	1855394	1846911.598			
GAPDH 8hr 32 cycles	4207909	4199427.098	0.40025968		0.810937053
Sak 8hr 42 cycles	1689343	1680861.348			
GAPDH 24hr 28 cycles	2126415	2117933.348	0.875723721		0.770673393
Sak 24hr 38 cycles	1863206	1854724.473	0.545454948		0.728162378
GAPDH 24hr 30 cycles	2912037	2903554.598			
Sak 24hr 40 cycles	1592240	1583758.223			
GAPDH 24hr 32 cycles	3535848	3527366.098	0.342492511		0.693899189
Sak 24hr 40 cycles	1216578	1208096.473			

Appendix E: Densitometry Values for Wild Type MEFs Exposed to Ionizing Radiation Cont.

background: 1956.2637

background	Raw vol.	Raw vol. - background	Sak:GAPDH ratio	GAPDH:Sak ratio	Relative Expression
GAPDH control 28 cycles	1059922.1	1057965.861	1.381142142	0.724038438	1
Sak control 38 cycles	1463157.5	1461201.236	0.83937601	1.191361188	1
GAPDH control 30 cycles	2085045.6	2083089.361			
Sak control 40 cycles	1750451.5	1748495.236	0.546554943	1.829642221	1
GAPDH control 32 cycles	2655020.3	2653063.986			
Sak control 42 cycles	1452001.5	1450045.236			
GAPDH 0hr 28 cycles	883568.63	881612.3613	1.052105596		0.761764893
Sak 0hr 38 cycles	929505.56	927549.2988			
GAPDH 0hr 30 cycles	2510125.5	2508169.236	0.861032802		1.025801062
Sak 0hr 40 cycles	2161572.3	2159615.986			
GAPDH 0hr 32 cycles	2826076.3	2824119.986	0.351807131		0.64368118
Sak 0hr 42 cycles	995501.81	993545.5488			
GAPDH 1/2hr 28 cycles	1350329.5	1348373.236	0.985296634		0.713392636
Sak 1/2hr 38 cycles	1330503.9	1328547.611			
GAPDH 1/2hr 30 cycles	2569185.3	2567228.986	0.58140898		0.692668093
Sak 1/2hr 40 cycles	1494566.3	1492609.986			
GAPDH 1/2hr 32 cycles	2974576	2972619.736	0.498918502		0.912842356
Sak 1/2hr 42 cycles	1485051.3	1483094.986			
GAPDH 1hr 28 cycles	1205650.6	1203694.361	1.038238528		0.751724602
Sak 1hr 38 cycles	1251678.1	1249721.861			
GAPDH 1hr 30 cycles	2077074.5	2075118.236	0.628164621		0.748370949
Sak 1hr 40 cycles	1305472.1	1303515.861			
GAPDH 1hr 32 cycles	2464406.5	2462450.236	0.383843107		0.702295554
Sak 1hr 42 cycles	947150.81	945194.5488			
GAPDH 2hr 28 cycles	897976.44	896020.1738	1.105149348		0.800170608
Sak 2hr 38 cycles	992192.38	990236.1113			
GAPDH 2hr 30 cycles	1876667.4	1874711.111	0.615821208		0.733665486
Sak 2hr 40 cycles	1156443.1	1154486.861			
GAPDH 2hr 32 cycles	2413922.8	2411966.486	0.436933563		0.799432095
Sak 2hr 42 cycles	1055825.4	1053869.111			
GAPDH 4hr 28 cycles	2546391.3	2544434.986	1.2083199923		0.87487007
Sak 4hr 38 cycles	3076447.8	3074491.486			
GAPDH 4hr 30 cycles	3632823	3630866.736	0.889535742		1.059758358
Sak 4hr 40 cycles	3231742	3229785.736			
GAPDH 4hr 32 cycles	5578102	5576145.736	0.393274018		0.719550747
Sak 4hr 42 cycles	2194909.5	2192953.236			
GAPDH 6hr 28 cycles	3140174.3	3138217.986	0.829493043		0.600584847
Sak 6hr 38 cycles	2605086.3	2603129.986			
GAPDH 6hr 30 cycles	5744787.5	5742831.236	0.671963197		0.800550872
Sak 6hr 40 cycles	3860927.5	3858971.236			
GAPDH 6hr 32 cycles	6275831.5	6273875.236	0.336912619		0.616429552
Sak 6hr 42 cycles	2115704	2113747.736			
GAPDH 8hr 28 cycles	2041274.4	2039318.111	0.713634365		0.516698712
Sak 8hr 38 cycles	1457283.8	1455327.486			
GAPDH 8hr 30 cycles	4053269.3	4051312.986	0.808203846		0.962862694
Sak 8hr 40 cycles	3276243	3274286.736			
GAPDH 8hr 32 cycles	4371520	4369563.736	0.402341851		0.73614638
Sak 8hr 42 cycles	1760014.6	1758058.361			
GAPDH 24hr 28 cycles	2284749.8	2282793.486	1.279250074		0.926226226
Sak 24hr 38 cycles	2922220	2920263.736			
GAPDH 24hr 30 cycles	3086777.3	3084820.986	1.072770349		1.278056957
Sak 24hr 40 cycles	3311260.8	3309304.486			
GAPDH 24hr 32 cycles	3626775.8	3624819.486	0.427216822		0.781653935
Sak 24hr 40 cycles	1550540.1	1548583.861			

Appendix E: Densitometry Values for Wild Type MEFs Exposed to Ionizing Radiation Cont.

background	Raw vol. 900.0781	Raw vol. - background	Sak:GAPDH ratio	GAPDH:Sak ratio	Relative Expression
GAPDH control 28 cycles	691122.6	690222.5469	1.164413819	0.858801213	1
Sak control 38 cycles	804604.8	803704.6719			
GAPDH control 30 cycles	1295595	1294695.172	0.75022972	1.332925066	1
Sak control 40 cycles	972218.9	971318.7969			
GAPDH control 32 cycles	1794171	1793271.297	0.505510996	1.978196336	1
Sak control 42 cycles	907418.4	906518.3594			
GAPDH 0hr 28 cycles	988478.8	987578.6719	1.070719809		0.919553547
Sak 0hr 38 cycles	1058320	1057420.047			
GAPDH 0hr 30 cycles	1966436	1965536.047	0.619449742		0.825680088
Sak 0hr 40 cycles	1218451	1217550.797			
GAPDH 0hr 32 cycles	2233251	2232350.922	0.577691957		1.142788112
Sak 0hr 42 cycles	1290511	1289611.172			
GAPDH 1/2hr 28 cycles	918507.3	917607.1719	1.13108067		0.971373451
Sak 1/2hr 38 cycles	1038788	1037887.734			
GAPDH 1/2hr 30 cycles	1733738	1732838.172	0.608784443		0.811464045
Sak 1/2hr 40 cycles	1055825	1054924.922			
GAPDH 1/2hr 32 cycles	2047224	2046323.422	0.511664468		1.012172775
Sak 1/2hr 42 cycles	1047931	1047030.984			
GAPDH 1hr 28 cycles	753076.4	752176.3594	1.171453391		1.006045593
Sak 1hr 38 cycles	882039.6	881139.5469			
GAPDH 1hr 30 cycles	1594260	1593359.797	0.653836934		0.871515639
Sak 1hr 40 cycles	1042698	1041797.484			
GAPDH 1hr 32 cycles	1960351	1959450.922	0.381513216		0.754708045
Sak 1hr 42 cycles	748456.5	747556.4219			
GAPDH 2hr 28 cycles	734772.4	733872.2969	0.844831995		0.725542742
Sak 2hr 38 cycles	620898.9	619998.7969			
GAPDH 2hr 30 cycles	1392800	1391900.172	0.585243109		0.78008521
Sak 2hr 40 cycles	815500.1	814599.9844			
GAPDH 2hr 32 cycles	1651074	1650173.922	0.453030306		0.896182891
Sak 2hr 42 cycles	748478.9	747578.7969			
GAPDH 4hr 28 cycles	1342800	1341900.172	0.605928818		0.520372403
Sak 4hr 38 cycles	813996.1	813095.9844			
GAPDH 4hr 30 cycles	2670197	2669296.672	0.43470226		0.579425539
Sak 4hr 40 cycles	1161249	1160349.297			
GAPDH 4hr 32 cycles	3069432	3068531.922	0.384085233		0.759796
Sak 4hr 42 cycles	1179478	1178577.797			
GAPDH 6hr 28 cycles	1726413	1725512.922	0.562959988		0.483470721
Sak 6hr 38 cycles	972294.8	971394.7344			
GAPDH 6hr 30 cycles	3216178	3215277.422	0.357580084		0.476627458
Sak 6hr 40 cycles	1150619	1149719.172			
GAPDH 6hr 32 cycles	4133191	4132290.422	0.341880871		0.676307485
Sak 6hr 42 cycles	1413651	1412751.047			
GAPDH 8hr 28 cycles	1995970	1995070.047	0.511499295		0.439276215
Sak 8hr 38 cycles	1021377	1020476.922			
GAPDH 8hr 30 cycles	2679478	2678577.672	0.423410691		0.564374723
Sak 8hr 40 cycles	1135039	1134138.422			
GAPDH 8hr 32 cycles	3281407	3280506.922	0.312920326		0.619017843
Sak 8hr 42 cycles	1026537	1026537.297			
GAPDH 24hr 28 cycles	1528991	1528090.672	0.6185718		0.531230212
Sak 24hr 38 cycles	946133.9	945233.7969			
GAPDH 24hr 30 cycles	2437934	2437033.672	0.415457605		0.553773855
Sak 24hr 40 cycles	1013384	1012484.172			
GAPDH 24hr 32 cycles	2423779	2422878.422	0.289621676		0.572928538
Sak 24hr 40 cycles	702618.2	701718.1094			

Appendix E: Densitometry Values for Wild Type MEFs Exposed to Ionizing Radiation Cont.

	Mean of Relative Expression	Standard error of Mean
GAPDH control 28 cycles	1	9.06493E-17
Sak control 38 cycles		
GAPDH control 30 cycles	1	4.53247E-17
Sak control 40 cycles		
GAPDH control 32 cycles	1	0
Sak control 42 cycles		
GAPDH 0hr 28 cycles	0.8590023867	0.049110982
Sak 0hr 38 cycles	0.8890099206	0.068410211
GAPDH 0hr 30 cycles	0.975284028	0.165804338
Sak 0hr 40 cycles		
GAPDH 0hr 32 cycles		
Sak 0hr 42 cycles		
GAPDH 1/2hr 28 cycles	0.9243988628	0.1110782359
Sak 1/2hr 38 cycles	0.756807829	0.034619707
GAPDH 1/2hr 30 cycles	0.889908765	0.0788820651
Sak 1/2hr 40 cycles		
GAPDH 1/2hr 32 cycles		
Sak 1/2hr 42 cycles		
GAPDH 1hr 28 cycles	0.927864955	0.088255067
Sak 1hr 38 cycles	0.823108788	0.0379084 17
GAPDH 1hr 30 cycles	0.700582466	0.031755498
Sak 1hr 40 cycles		
GAPDH 1hr 32 cycles		
Sak 1hr 42 cycles		
GAPDH 2hr 28 cycles	0.738551593	0.032478407
Sak 2hr 38 cycles	0.731317375	0.028857856
GAPDH 2hr 30 cycles	0.874383766	0.0385553314
Sak 2hr 40 cycles		
GAPDH 2hr 32 cycles		
Sak 2hr 42 cycles		
GAPDH 4hr 28 cycles	0.725828516	0.106150994
Sak 4hr 38 cycles	0.829353388	0.139003311
GAPDH 4hr 30 cycles	0.748599723	0.014651044
Sak 4hr 40 cycles		
GAPDH 4hr 32 cycles		
Sak 4hr 42 cycles		
GAPDH 6hr 28 cycles	0.6389942021	0.102641833
Sak 6hr 38 cycles	0.6302006713	0.09388836
GAPDH 6hr 30 cycles	0.718415519	0.074091502
Sak 6hr 40 cycles		
GAPDH 6hr 32 cycles		
Sak 6hr 42 cycles		
GAPDH 8hr 28 cycles	0.5589963249	0.08400356
Sak 8hr 38 cycles	0.72785368	0.120465178
GAPDH 8hr 30 cycles	0.722032178	0.055849659
Sak 8hr 40 cycles		
GAPDH 8hr 32 cycles		
Sak 8hr 42 cycles		
GAPDH 24hr 28 cycles	0.742710122	0.114879565
Sak 24hr 38 cycles	0.853331063	0.218248255
GAPDH 24hr 30 cycles	0.682827221	0.060507614
Sak 24hr 40 cycles		
GAPDH 24hr 32 cycles		
Sak 24hr 40 cycles		

Appendix F: Densitometry Values for Heterozygous MEFs Exposed to Ionizing Radiation

background: 2018.098

	Raw vol.	Raw vol. - background	Sak:GAPDH ratio	GAPDH:Sak ratio	Relative Expression	Normalized to Wild Type
GAPDH control 28 cycles	690090	688071.9023	0.642759355	1.555792213	1	1.007555423
Sak control 38 cycles	444282.8	442264.6523				
GAPDH control 30 cycles	1210246	1208227.527	0.430865061	2.320912254	1	1.007555423
Sak control 40 cycles	522601.1	520583.0273				
GAPDH control 32 cycles	1936247	1934228.652	0.29271119	3.416336762	1	1.007555423
Sak control 42 cycles	568188.5	566170.3711				
GAPDH 0hr 28 cycles	1308765	1306747.152	0.688258886		1.070787816	1.078878071
Sak 0hr 38 cycles	901398.4	899380.3398				
GAPDH 0hr 30 cycles	1849793	1847775.152	0.423298271		0.982438144	0.985231361
Sak 0hr 40 cycles	784178.1	782160.0273				
GAPDH 0hr 32 cycles	2441155	2439136.652	0.350198769		1.196396928	1.198666386
Sak 0hr 42 cycles	856200.8	854182.6523				
GAPDH 1/2hr 28 cycles	1127984	1125965.652	0.717632927		1.116487721	1.124923258
Sak 1/2hr 38 cycles	810048.1	808030.0273				
GAPDH 1/2hr 30 cycles	1726937	1724918.777	0.363818197		0.844390112	0.846790838
Sak 1/2hr 40 cycles	629574.9	627556.8398				
GAPDH 1/2hr 32 cycles	2165768	2163749.902	0.313056122		1.069505136	1.071533893
Sak 1/2hr 42 cycles	679393.3	677375.1523				
GAPDH 1hr 28 cycles	869814.6	867796.5273	0.822697493		1.279946353	1.289616889
Sak 1hr 38 cycles	715952.1	713934.0273				
GAPDH 1hr 30 cycles	1476930	1474912.027	0.528313986		1.226170404	1.229656588
Sak 1hr 40 cycles	781234.8	779216.6523				
GAPDH 1hr 32 cycles	1783100	1781082.277	0.296088597		1.011538358	1.013457157
Sak 1hr 42 cycles	529376.3	527358.1523				
GAPDH 2hr 28 cycles	975225.1	973206.9648	0.243731795		0.379196029	0.382061015
Sak 2hr 38 cycles	239219.6	237201.4805				
GAPDH 2hr 30 cycles	1299305	1297287.152	0.50552717		1.173284203	1.176620023
Sak 2hr 40 cycles	657832	655813.9023				
GAPDH 2hr 32 cycles	1905785	1903766.652	0.364368003		1.244803802	1.247165084
Sak 2hr 42 cycles	695689.8	693671.6523				
GAPDH 4hr 28 cycles	1156448	1154429.527	0.515538232		0.795847199	0.801860161
Sak 4hr 38 cycles	592552.9	590534.8398				
GAPDH 4hr 30 cycles	1745490	1743471.652	0.393473792		0.913218146	0.915814559
Sak 4hr 40 cycles	688028.5	686010.4023				
GAPDH 4hr 32 cycles	2335954	2333936.152	0.281989731		0.963371884	0.965199315
Sak 4hr 42 cycles	660164.1	658146.0273				
GAPDH 6hr 28 cycles	1008075	1006056.402	0.405525968		0.630914143	0.635680966
Sak 6hr 38 cycles	410000.1	407981.9961				
GAPDH 6hr 30 cycles	1817829	1815811.152	0.411566148		0.955208917	0.957924717
Sak 6hr 40 cycles	749344.5	747326.4023				
GAPDH 6hr 32 cycles	2309807	2307789.152	0.342406049		1.169774372	1.17199333
Sak 6hr 42 cycles	792219.1	790200.9648				
GAPDH 8hr 28 cycles	1242701	1240683.027	0.517973175		0.805858633	0.811947236
Sak 8hr 38 cycles	644658.6	642640.5273				
GAPDH 8hr 30 cycles	1614866	1612847.402	0.37819284		0.877752397	0.880247977
Sak 8hr 40 cycles	611985.4	609967.3398				
GAPDH 8hr 32 cycles	2099068	2097049.902	0.262461131		0.896655612	0.898356488
Sak 8hr 42 cycles	552412.2	550394.0898				
GAPDH 24hr 28 cycles	898806.5	896788.4023	0.452788035		0.704444099	0.709766472
Sak 24hr 38 cycles	408073.2	406055.0586				
GAPDH 24hr 30 cycles	1670976	1668957.527	0.394584279		0.915795488	0.91839923
Sak 24hr 40 cycles	660562.5	658544.4023				
GAPDH 24hr 32 cycles	1744869	1744850.527	0.239903606		0.819591509	0.821146201
Sak 24hr 40 cycles	420614	418595.9336				

Appendix F: Densitometry Values for Heterozygous MEFs Exposed to Ionizing Radiation Cont.

background	Raw vol. 2762.744	Raw vol.- background	Sak:GAPDH ratio	GAPDH:Sak ratio	Relative Expression	Normalized to Wild Type
GAPDH control 28 cycles	388117.8	385355.0684	3.281547616	0.304734265	1	1.007555423
Sak control 38 cycles	1267324	1264561.006	1.352031819	0.739627564	1	1.007555423
GAPDH control 30 cycles	584931	582168.2559			1	1.007555423
Sak control 40 cycles	789872.8	787110.0059				
GAPDH control 32 cycles	1281879	1279116.506	1.015329819	0.984901636		
Sak control 42 cycles	1301488	1298725.131				
GAPDH 0hr 28 cycles	802584.3	799821.5684	2.139690368		0.652036971	0.656963386
Sak 0hr 38 cycles	1714133	1711370.506	1.304485316		0.964833296	0.972123019
GAPDH 0hr 30 cycles	1593659	1590896.506			0.713711367	0.719103758
Sak 0hr 40 cycles	2078064	2075301.131				
GAPDH 0hr 32 cycles	2099443	2096680.506	0.724652434			
Sak 0hr 42 cycles	1522127	1519364.631				
GAPDH 1/2hr 28 cycles	789836.7	787073.9434	2.121156176		0.646388968	0.65127271
Sak 1/2hr 38 cycles	1672270	1669506.756	1.298206295		0.960189159	0.967443794
GAPDH 1/2hr 30 cycles	1581702	1578939.256			0.929795179	0.936820175
Sak 1/2hr 40 cycles	2052552	2049788.881				
GAPDH 1/2hr 32 cycles	2192000	2189237.006	0.944048771			
Sak 1/2hr 42 cycles	2069509	2066746.506				
GAPDH 1hr 28 cycles	606799.6	604036.8184	2.4978523		0.761181184	0.76693223
Sak 1hr 38 cycles	1511558	1508794.756	1.426457627		1.055047379	1.063018708
GAPDH 1hr 30 cycles	1326141	1323378.256			0.877929856	0.884562988
Sak 1hr 40 cycles	1890506	1887743.006				
GAPDH 1hr 32 cycles	1895845	1893082.131	0.891388363			
Sak 1hr 42 cycles	1690234	1687471.381				
GAPDH 2hr 28 cycles	720569.1	717806.3184	1.915267177		0.583647535	0.588057239
Sak 2hr 38 cycles	1377554	1374790.881	0.940954181		0.695955648	0.701213888
GAPDH 2hr 30 cycles	1602326	1599562.881			0.536742077	0.54079739
Sak 2hr 40 cycles	1507878	1505115.381				
GAPDH 2hr 32 cycles	2380766	2378003.506	0.544970236			
Sak 2hr 42 cycles	1298704	1295941.131				
GAPDH 4hr 28 cycles	975247	972484.2559	1.185799666		0.361353789	0.36408397
Sak 4hr 38 cycles	1559934	1153171.506	0.904699099		0.66914039	0.674196029
GAPDH 4hr 30 cycles	1754758	1751995.506			0.69648554	0.701747783
Sak 4hr 40 cycles	1587792	1585028.756				
GAPDH 4hr 32 cycles	2281446	2278683.006	0.707162537			
Sak 4hr 42 cycles	1614162	1611399.256				
GAPDH 6hr 28 cycles	1229665	1226902.381	1.107768048		0.337574882	0.340125403
Sak 6hr 38 cycles	1361886	1359123.256	0.854032147		0.631665716	0.636438217
GAPDH 6hr 30 cycles	2164143	2161380.006			0.733323796	0.738864368
Sak 6hr 40 cycles	1848651	1845888.006				
GAPDH 6hr 32 cycles	2550314	2547551.506	0.744565518			
Sak 6hr 42 cycles	1899582	1896819.006				
GAPDH 8hr 28 cycles	1295924	1293161.506	1.810663521		0.359910524	0.3626298
Sak 8hr 38 cycles	1530606	1527305.881	0.9121148532		0.67465097	0.679747464
GAPDH 8hr 30 cycles	1720037	1717573.756			0.616677585	0.621336845
Sak 8hr 40 cycles	1569445	1566682.381				
GAPDH 8hr 32 cycles	2394625	2391861.756	0.626131141			
Sak 8hr 42 cycles	1500382	1497619.131				
GAPDH 24hr 28 cycles	1251852	1249088.756	1.087730755		0.331468832	0.339373219
Sak 24hr 38 cycles	1361435	1358672.256	0.852103764		0.630239431	0.635001157
GAPDH 24hr 30 cycles	1693462	1690698.881			0.352572114	0.352235945
Sak 24hr 40 cycles	1443414	1440650.881				
GAPDH 24hr 32 cycles	2731595	2728832.256	0.35797698			
Sak 24hr 40 cycles	656829.9	654067.1621				

Appendix F: Densitometry for Values Heterozygous MEFs Exposed to Ionizing Radiation Cont.

background	Raw vol.	Raw vol.- background	Sak:GAPDH ratio	GAPDH:Sak ratio	Relative Expression	Normalized to Wild Type
	2561.938					
GAPDH control 28 cycles	402594.8	400032.8438	1.095350999	0.912949366	1	1.007555423
Sak control 38 cycles	440738.3	438176.375	0.783753688	1.275911061	1	1.007555423
GAPDH control 30 cycles	621421.6	618859.6875	0.439750406	2.274017229	1	1.007555423
Sak control 40 cycles	487595.5	485033.5625				
GAPDH control 32 cycles	1188975	1186412.563				
Sak control 42 cycles	524287.3	521725.4063				
GAPDH 0hr 28 cycles	649169.8	646607.8125	0.631955276		0.576943169	0.581302218
Sak 0hr 38 cycles	411189.2	408627.2188	0.71580416		0.913302445	0.920202831
GAPDH 0hr 30 cycles	1400020	1397458.438	0.240616072		0.547165094	0.551299157
Sak 0hr 40 cycles	1002869	1000306.563				
GAPDH 0hr 32 cycles	1815814	1813251.563				
Sak 0hr 42 cycles	438859.4	436297.4688				
GAPDH 1/2hr 28 cycles	629375.4	626813.5	0.660233068		0.602759361	0.607313463
Sak 1/2hr 38 cycles	416404.9	413843	0.626803572		0.79974561	0.805788027
GAPDH 1/2hr 30 cycles	1478873	1476311.188	0.488018086		1.109761534	1.118146252
Sak 1/2hr 40 cycles	927919.1	925357.125				
GAPDH 1/2hr 32 cycles	1798005	1795442.938				
Sak 1/2hr 42 cycles	878770.6	876208.625				
GAPDH 1hr 28 cycles	691157.4	688595.5	1.056593185		0.964616078	0.971904161
Sak 1hr 38 cycles	730127.3	727565.3125	0.819149984		1.045162525	1.05305917
GAPDH 1hr 30 cycles	108211	1079548.563	0.482781217		1.097852805	1.106147547
Sak 1hr 40 cycles	886874.1	884312.1875				
GAPDH 1hr 32 cycles	1345091	1342529.188				
Sak 1hr 42 cycles	650709.8	648147.875				
GAPDH 2hr 28 cycles	666158.9	663596.9375	0.826237048		0.75431259	0.76001174
Sak 2hr 38 cycles	550850.3	548288.375	0.537662255		0.686009218	0.691192308
GAPDH 2hr 30 cycles	1326903	1324340.688	0.314858069		0.715992673	0.7214023
Sak 2hr 40 cycles	714609.9	712048				
GAPDH 2hr 32 cycles	1651636	1649073.688				
Sak 2hr 42 cycles	521786.1	519224.1563				
GAPDH 4hr 28 cycles	438493	435931.0625	0.908033051		0.828988198	0.835251554
Sak 4hr 38 cycles	398401.8	395839.8125	0.761321782		0.971378883	0.978718062
GAPDH 4hr 30 cycles	931436.5	928874.5625	0.507076881		1.153101563	1.161813733
Sak 4hr 40 cycles	709734.4	707172.4375				
GAPDH 4hr 32 cycles	1625465	1622903.438				
Sak 4hr 42 cycles	825498.8	822936.8125				
GAPDH 6hr 28 cycles	655852	653290.0625	1.156414058		1.055747481	1.0637241
Sak 6hr 38 cycles	758035.8	755473.8125	0.684371025		0.87319656	0.87979393
GAPDH 6hr 30 cycles	1292747	1290184.938	0.496498814		1.129046858	1.137577284
Sak 6hr 40 cycles	885527.1	882965.1875				
GAPDH 6hr 32 cycles	1846161	1843598.688				
Sak 6hr 42 cycles	917906.5	915344.5625				
GAPDH 8hr 28 cycles	534187.7	531625.75	0.932730109		0.851535362	0.857969071
Sak 8hr 38 cycles	498425.3	495863.3438	0.698114706		0.890732275	0.897462135
GAPDH 8hr 30 cycles	939067.1	936505.125	0.45654734		1.038196517	1.046040531
Sak 8hr 40 cycles	656349.9	653788				
GAPDH 8hr 32 cycles	1435782	1433219.938				
Sak 8hr 42 cycles	656894.7	654332.75				
GAPDH 24hr 28 cycles	706207	703645.0625	1.170250164		1.068379146	1.076451202
Sak 24hr 38 cycles	826002.7	823440.75	0.798128727		1.018341272	1.026035271
GAPDH 24hr 30 cycles	958241.8	955679.875	0.5880765		1.337296094	1.347399932
Sak 24hr 40 cycles	765317.5	762755.5625				
GAPDH 24hr 32 cycles	1663671	1661108.938				
Sak 24hr 40 cycles	979621.9	976859.1309				

Appendix F: Densitometry for Values Heterozygous MEFs Exposed to Ionizing Radiation Cont.

	Mean of Normalized to Wild Type	Standard Error of Mean
GAPDH control 28 cycles	1.0075555423	9.06493E-17
Sak control 38 cycles		
GAPDH control 30 cycles	1.0075555423	0
Sak control 40 cycles		
GAPDH control 32 cycles	1.0075555423	0
Sak control 42 cycles		
GAPDH 0hr 28 cycles	0.7772381225	0.125890957
Sak 0hr 38 cycles	0.9591857737	0.007518778
GAPDH 0hr 30 cycles	0.823023101	0.145657021
Sak 0hr 40 cycles		
GAPDH 0hr 32 cycles		
Sak 0hr 42 cycles		
GAPDH 1/2hr 28 cycles	0.7945003143	0.140245271
Sak 1/2hr 38 cycles	0.8733408886	0.036604036
GAPDH 1/2hr 30 cycles	1.042166773	0.040898329
Sak 1/2hr 40 cycles		
GAPDH 1/2hr 32 cycles		
Sak 1/2hr 42 cycles		
GAPDH 1hr 28 cycles	1.009484427	0.151016007
Sak 1hr 38 cycles	1.115244822	0.049208063
GAPDH 1hr 30 cycles	1.001389231	0.041101306
Sak 1hr 40 cycles		
GAPDH 1hr 32 cycles		
Sak 1hr 42 cycles		
GAPDH 2hr 28 cycles	0.576709998	0.066854498
Sak 2hr 38 cycles	0.8563342073	0.139970972
GAPDH 2hr 30 cycles	0.8364454925	0.204810418
Sak 2hr 40 cycles		
GAPDH 2hr 32 cycles		
Sak 2hr 42 cycles		
GAPDH 4hr 28 cycles	0.6670665228	0.129446538
Sak 4hr 38 cycles	0.856242883	0.07267483
GAPDH 4hr 30 cycles	0.942920277	0.08434955
Sak 4hr 40 cycles		
GAPDH 4hr 32 cycles		
Sak 4hr 42 cycles		
GAPDH 6hr 28 cycles	0.679843349	0.106643695
Sak 6hr 38 cycles	0.8247188955	0.093258
GAPDH 6hr 30 cycles	1.0161144994	0.126660953
Sak 6hr 40 cycles		
GAPDH 6hr 32 cycles		
Sak 6hr 42 cycles		
GAPDH 8hr 28 cycles	0.6775515369	0.1331147998
Sak 8hr 38 cycles	0.8191152525	0.0593332809
GAPDH 8hr 30 cycles	0.8552444621	0.086059205
Sak 8hr 40 cycles		
GAPDH 8hr 32 cycles		
Sak 8hr 42 cycles		
GAPDH 24hr 28 cycles	0.7067300298	0.124761467
Sak 24hr 38 cycles	0.8598811886	0.086373481
GAPDH 24hr 30 cycles	0.841260693	0.158762054
Sak 24hr 40 cycles		
GAPDH 24hr 32 cycles		
Sak 24hr 40 cycles		

Appendix G: Densitometry Values for Wild Type MEFs Exposed to Ultraviolet Radiation

background	Raw vol. 1687.57	Raw vol. - background	Sak:GAPDH ratio	GAPDH:Sak ratio	Relative Expression
GAPDH control 28 cycles	437738.5	436050.8984	0.587836139	1.701154341	1
Sak control 38 cycles	258014	256326.4766			
GAPDH control 30 cycles	1182325	1180637.055	0.38529013	2.595446707	1
Sak control 40 cycles	456575.4	454887.8047			
GAPDH control 32 cycles	1921768	1920080.305	0.319020458	3.13459521	1
Sak control 42 cycles	614232.5	612544.8984			
GAPDH 0hr 28 cycles	413432.5	411744.9297			
Sak 0hr 38 cycles	0	0			
GAPDH 0hr 30 cycles	951685.8	949998.1797			
Sak 0hr 40 cycles	0	0			
GAPDH 0hr 32 cycles	1955311	1953623.805			
Sak 0hr 42 cycles	0	0			
GAPDH 1/2hr 28 cycles	590606.6	588919.0547			
Sak 1/2 38 cycles	0	0			
GADPH 1/2hr 30 cycles	1089748	1088059.93			
Sak 1/2hr 40 cycles	0	0			
GAPDH 1/2hr 32 cycles	1572133	1570445.305			
Sak 1/2hr 42 cycles	0	0			
GAPDH 1hr 28 cycles	364703.3	363015.7734			
Sak 1hr 38 cycles	0	0			
GAPDH 1hr 30 cycles	898024.3	896336.7422			
Sak 1hr 40 cycles	0	0			
GAPDH 1hr 32 cycles	1766910	1765222.305			
Sak 1hr 42 cycles	0	0			
GAPDH 2hr 28 cycles	483397.5	481709.9609			
Sak 2hr 38 cycles	0	0			
GAPDH 2hr 30 cycles	973693.2	972005.6172	0.430358166	1.116971685	
Sak 2hr 40 cycles	419998.1	418310.5547			
GAPDH 2hr 32 cycles	1443704	1442016.836	0.32934989	1.032378587	
Sak 2hr 42 cycles	476615.7	474928.0859			
GAPDH 4hr 28 cycles	519915.7	518228.1484	0.864743634	1.471062387	
Sak 4hr 38 cycles	449822.1	448134.4922			
GAPDH 4hr 30 cycles	909660.8	907973.2734	0.752250451	1.952425957	
Sak 4hr 40 cycles	684710.9	683023.3047			
GAPDH 4hr 32 cycles	1472138	1470450.18	0.600583204	1.882585233	
Sak 4hr 42 cycles	884815.3	883127.6797			
GAPDH 6hr 28 cycles	522515.3	520827.7656	0.789577706	1.343193542	
Sak 6hr 38 cycles	412921.6	411233.9922			
GAPDH 6hr 30 cycles	902189.4	900501.8672	0.766291851	1.98886966	
Sak 6hr 40 cycles	691734.8	690047.2422			
GAPDH 6hr 32 cycles	1387049	1385361.18	0.618406551	1.938454214	
Sak 6hr 42 cycles	858404	856716.4297			
GAPDH 8hr 28 cycles	577882.9	576195.3047	0.753456968	1.281746592	
Sak 8hr 38 cycles	435825.9	434138.3672			
GAPDH 8hr 30 cycles	950614.2	948926.6484	0.639376532	1.659467715	
Sak 8hr 40 cycles	608409	606721.4297			
GAPDH 8hr 32 cycles	1547949	1546261.305	0.606801622	1.920077457	
Sak 8hr 42 cycles	939961.4	938273.8672			

Appendix G: Densitometry Values for Wild Type MEFs Exposed to Ultraviolet Radiation Cont.

background	Raw vol. 523.457	Raw vol. - background	Sak:GAPDH ratio	GAPDH:Sak ratio	Relative Expression
GAPDH control 28 cycles	540731.9	540208.4492	0.334300085	2.991324397	1
Sak control 38 cycles	181115.2	180591.7305	0.355796175	2.81059795	1
GAPDH control 30 cycles	1089224	1088700.168			
Sak control 40 cycles	387878.8	387355.3555			
GAPDH control 32 cycles	2345458	2344934.793	0.208044316	4.806668206	1
Sak control 42 cycles	488373.8	487850.3555			
GAPDH 0hr 28 cycles	179113.1	178589.6523			
Sak 0hr 38 cycles	0	0			
GAPDH 0hr 30 cycles	702877.1	702353.6055			
Sak 0hr 40 cycles	0	0			
GAPDH 0hr 32 cycles	1266252	1265728.918			
Sak 0hr 42 cycles	0	0			
GAPDH 1/2hr 28 cycles	305634.9	305111.418			
Sak 1/2 38 cycles	0	0			
GADPH 1/2hr 30 cycles	981367.6	980844.168			
Sak 1/2hr 40 cycles	0	0			
GAPDH 1/2hr 32 cycles	2162811	2162287.793			
Sak 1/2hr 42 cycles	0	0			
GAPDH 1hr 28 cycles	647551.9	647028.4805			
Sak 1hr 38 cycles	0	0			
GAPDH 1hr 30 cycles	1858039	1857515.043			
Sak 1hr 40 cycles	0	0			
GAPDH 1hr 32 cycles	2424097	2423573.543			
Sak 1hr 42 cycles	0	0			
GAPDH 2hr 28 cycles	736435.4	735911.918			
Sak 2hr 38 cycles	0	0			
GAPDH 2hr 30 cycles	1354064	1353540.543			
Sak 2hr 40 cycles	0	0			
GAPDH 2hr 32 cycles	2706790	2706266.043			
Sak 2hr 42 cycles	0	0			
GAPDH 4hr 28 cycles	972809.4	972285.918	0.262911085		0.786452344
Sak 4hr 38 cycles	256148.2	255624.7461			
GAPDH 4hr 30 cycles	2680852	2680328.293	0.307049017		0.862991338
Sak 4hr 40 cycles	823515.6	822992.168			
GAPDH 4hr 32 cycles	4827451	4826927.043	0.175267108		0.842450835
Sak 4hr 42 cycles	846525	846001.543			
GAPDH 6hr 28 cycles	1281142	1280618.418	0.493297396		1.475612535
Sak 6hr 38 cycles	632249.2	631725.7305			
GAPDH 6hr 30 cycles	3290406	3289882.293	0.247885553		0.696706628
Sak 6hr 40 cycles	816037.8	815514.293			
GAPDH 6hr 32 cycles	4002461	4001937.293	0.196156945		0.94286135
Sak 6hr 42 cycles	785531.3	785007.793			
GAPDH 8hr 28 cycles	1270481	1269957.168	0.350826949		1.049437213
Sak 8hr 38 cycles	446058.7	445535.1992			
GAPDH 8hr 30 cycles	2504709	2504185.793	0.323331383		0.908754522
Sak 8hr 40 cycles	810205.3	809681.8555			
GAPDH 8hr 32 cycles	3010530	3010006.543	0.302264681		1.452886033
Sak 8hr 42 cycles	910342.1	909818.668			

Appendix G: Densitometry Values for Wild Type MEFs Exposed to Ultraviolet Radiation Cont.

background	Raw vol. 6928.547	Raw vol. - background	Sak:GAPDH ratio	GAPDH:Sak ratio	Relative Expression
GAPDH control 28 cycles	809263	802334.4219	0.259718248	3.850326292	1
Sak control 38 cycles	215309.4	208380.8906			
GAPDH control 30 cycles	987128.6	980200.0156	0.27540044	3.631076261	1
Sak control 40 cycles	276876.1	269947.5156			
GAPDH control 32 cycles	1567487	1560558.828	0.244863997	4.083899688	1
Sak control 42 cycles	389053.2	382124.6719			
GAPDH 0hr 28 cycles	255405.5	248476.9375			
Sak 0hr 38 cycles	0	0			
GAPDH 0hr 30 cycles	1436830	1429901.578			
Sak 0hr 40 cycles	0	0			
GAPDH 0hr 32 cycles	1884558	1877629.578			
Sak 0hr 42 cycles	0	0			
GAPDH 1/2hr 28 cycles	546146.4	539217.8906			
Sak 1/2 38 cycles	0	0			
GADPH 1/2hr 30 cycles	1501213	1494284.703			
Sak 1/2hr 40 cycles	0	0			
GAPDH 1/2hr 32 cycles	2114262	2107333.453			
Sak 1/2hr 42 cycles	0	0			
GAPDH 1hr 28 cycles	1605900	1598971.578			
Sak 1hr 38 cycles	0	0			
GAPDH 1hr 30 cycles	2375434	2368505.703			
Sak 1hr 40 cycles	0	0			
GAPDH 1hr 32 cycles	2489072	2482143.203			
Sak 1hr 42 cycles	0	0			
GAPDH 2hr 28 cycles	1089703	1082774.328	0.274450372		1.068274464
Sak 2hr 38 cycles	307344.7	300416.1406			
GAPDH 2hr 30 cycles	2327681	2320752.703	0.228804951		0.82806516
Sak 2hr 40 cycles	536175.1	529246.5156			
GAPDH 2hr 32 cycles	2780612	2773683.578	0.232873158		0.951030616
Sak 2hr 42 cycles	652845	645916.4531			
GAPDH 4hr 28 cycles	917943.1	911014.5156	0.333448738		1.283886443
Sak 4hr 38 cycles	310705.2	303776.6406			
GAPDH 4hr 30 cycles	1029543	1022614.703	0.335856013		1.219518795
Sak 4hr 40 cycles	350379.8	343451.2969			
GAPDH 4hr 32 cycles	1635007	1628078.703	0.288379611		1.177713403
Sak 4hr 42 cycles	476433.3	469504.7031			
GAPDH 6hr 28 cycles	528957.4	522028.8906	0.394329918		1.518298849
Sak 6hr 38 cycles	212780.2	205851.6094			
GAPDH 6hr 30 cycles	1707375	1700446.328	0.368868863		1.339390971
Sak 6hr 40 cycles	634170.3	627241.7031			
GAPDH 6hr 32 cycles	2360298	2353369.203	0.360178272		1.470931933
Sak 6hr 42 cycles	854561	847632.4531			
GAPDH 8hr 28 cycles	815348.9	808420.3281	0.419091372		1.613638528
Sak 8hr 38 cycles	345730.5	338801.9844			
GAPDH 8hr 30 cycles	1651241	1644311.953	0.274434249		0.996491686
Sak 8hr 40 cycles	458184.1	451255.5156			
GAPDH 8hr 32 cycles	2250523	2243594.453	0.256160133		1.046132286
Sak 8hr 42 cycles	581648	574719.4531			

Appendix G: Densitometry Values for Wild Type MEFs Exposed to Ultraviolet Radiation Cont.

	Mean Relative Expression	Standard Error of Mean
GAPDH control 28 cycles	1	6.40988E-17
Sak control 38 cycles		
GAPDH control 30 cycles	1	0
Sak control 40 cycles		
GAPDH control 32 cycles	1	9.06493E-17
Sak control 42 cycles		
GAPDH 0hr 28 cycles	0	0
Sak 0hr 38 cycles		
GAPDH 0hr 30 cycles	0	0
Sak 0hr 40 cycles		
GAPDH 0hr 32 cycles	0	0
Sak 0hr 42 cycles		
GAPDH 1/2hr 28 cycles	0	0
Sak 1/2 38 cycles		
GADPH 1/2hr 30 cycles	0	0
Sak 1/2hr 40 cycles		
GAPDH 1/2hr 32 cycles	0	0
Sak 1/2hr 42 cycles		
GAPDH 1hr 28 cycles	0	0
Sak 1hr 38 cycles		
GAPDH 1hr 30 cycles	0	0
Sak 1hr 40 cycles		
GAPDH 1hr 32 cycles	0	0
Sak 1hr 42 cycles		
GAPDH 2hr 28 cycles	1.068274464	0
Sak 2hr 38 cycles		
GAPDH 2hr 30 cycles	0.9725184422	0.144453262
Sak 2hr 40 cycles		
GAPDH 2hr 32 cycles	0.991704601	0.040673986
Sak 2hr 42 cycles		
GAPDH 4hr 28 cycles	1.180467058	0.204282814
Sak 4hr 38 cycles		
GAPDH 4hr 30 cycles	1.344978697	0.320687848
Sak 4hr 40 cycles		
GAPDH 4hr 32 cycles	1.300916491	0.306514895
Sak 4hr 42 cycles		
GAPDH 6hr 28 cycles	1.445701642	0.052714525
Sak 6hr 38 cycles		
GAPDH 6hr 30 cycles	1.341655753	0.373017056
Sak 6hr 40 cycles		
GAPDH 6hr 32 cycles	1.450749166	0.287580015
Sak 6hr 42 cycles		
GAPDH 8hr 28 cycles	1.314940778	0.163714356
Sak 8hr 38 cycles		
GAPDH 8hr 30 cycles	1.182237974	0.236972258
Sak 8hr 40 cycles		
GAPDH 8hr 32 cycles	1.467031925	0.247191298
Sak 8hr 42 cycles		

Appendix H: Densitometry Values for Heterozygous MEFs Exposed to Ultraviolet Radiation

background	Raw vol. 8935.063	Raw vol.- background	Sak:GAPDH ratio	GAPDH:Sak ratio	Relative Expression
GAPDH control 28 cycles	667782.5	658847.4365	0.691714717	1.445682701	1
Sak 38 control cycles	464669.5	455734.4678			
GAPDH control 30 cycles	810614.6	801679.499	0.656255788	1.523796084	1
Sak control 40 cycles	535041.9	526106.8115			
GAPDH control 32 cycles	1004538	995603.0615	0.701750757	1.425007369	1
Sak control 42 cycles	707600.3	698665.2021			
GAPDH 0hr 28 cycles	357890.3	348955.249			
Sak 0hr 38 cycles	0	0			
GAPDH 0hr 30 cycles	614615.8	605680.749			
Sak 0hr 40 cycles	0	0			
GAPDH 0hr 32 cycles	1341820	1332885.312			
Sak 0hr 42 cycles	0	0			
GAPDH 1/2hr 28 cycles	1123085.4	1114150.3115			
Sak 1/2hr 38 cycles	0	0			
GAPDH 1/2hr 30 cycles	654589.8	645654.6865			
Sak 1/2hr 40 cycles	0	0			
GAPDH 1/2hr 32 cycles	1055439	1046503.937			
Sak 1/2 42 cycles	0	0			
GAPDH 1hr 28 cycles	1034122	1025186.874			
Sak 1hr 38 cycles	0	0			
GAPDH 1hr 30 cycles	1151510	1142575.312			
Sak 1hr 40 cycles	0	0			
GAPDH 1hr 32 cycles	1401482	1392547.312			
Sak 1hr 42 cycles	0	0			
GAPDH 2hr 28 cycles	700286.6	691351.5615			
Sak 2hr 38 cycles	0	0			
GAPDH 2hr 30 cycles	1231939	1223003.937			
Sak 2hr 40 cycles	0	0			
GAPDH 2hr 32 cycles	1444603	1435668.312			
Sak 2hr 42 cycles	0	0			
GAPDH 4hr 28 cycles	983222.6	974287.5615			
Sak 4hr 38 cycles	0	0			
GAPDH 4hr 30 cycles	1256032	1247096.812			
Sak 4hr 40 cycles	0	0			
GAPDH 4hr 32 cycles	1381248	1372312.437			
Sak 4hr 42 cycles	0	0			
GAPDH 6hr 28 cycles	840651.3	831716.1865			
Sak 6hr 38 cycles	0	0			
GAPDH 6hr 30 cycles	1110815	1101879.562			
Sak 6hr 40 cycles	0	0			
GAPDH 6hr 32cycles	1342411	1333475.937			
Sak 6hr 42 cycles	0	0			
GAPDH 8hr 28 cycles	894366.5	885431.4365			
Sak 8hr 38 cycles	0	0			
GAPDH 8hr 30 cycles	1412738	1403802.437			
Sak 8hr 40 cycles	0	0			
GAPDH 8hr 32 cycles	1455394	1446458.687			
Sak 8hr 42 cycles	0	0			

Appendix H: Densitometry Values for Heterozygous MEFs Exposed to Ultraviolet Radiation Cont.

background	Raw vol. 5339.945	Raw vol.- background	Sak:GAPDH ratio	GAPDH:Sak ratio	Relative Expression
GAPDH control 28 cycles	471356	466016.0547	0.587019191	1.70352182	1
Sak 38 control cycles	278900.3	273560.3672			
GAPDH control 30 cycles	886325.8	880985.8047	0.424980732	2.353047855	1
Sak control 40 cycles	379741.9	374401.9922			
GAPDH control 32 cycles	1267690	1262349.555	0.385077911	2.596877076	1
Sak control 42 cycles	491442.9	486102.9297			
GAPDH 0hr 28 cycles	395971	390631.0234			
Sak 0hr 38 cycles	0	0			
GAPDH 0hr 30 cycles	607076.7	601736.7422			
Sak 0hr 40 cycles	0	0			
GAPDH 0hr 32 cycles	977942.4	972602.4297			
Sak 0hr 42 cycles	0	0			
GAPDH 1/2hr 28 cycles	484627.6	479287.6797			
Sak 1/2hr 38 cycles	0	0			
GAPDH 1/2hr 30 cycles	873180.4	867840.4922			
Sak 1/2hr 40 cycles	0	0			
GAPDH 1/2hr 32 cycles	1411158	1405817.555			
Sak 1/2 42 cycles	0	0			
GAPDH 1hr 28 cycles	658438.1	653098.1797			
Sak 1hr 38 cycles	0	0			
GAPDH 1hr 30 cycles	1105072	1099732.18			
Sak 1hr 40 cycles	0	0			
GAPDH 1hr 32 cycles	1520348	1515008.055			
Sak 1hr 42 cycles	0	0			
GAPDH 2hr 28 cycles	583304.6	577964.6797			
Sak 2hr 38 cycles	0	0			
GAPDH 2hr 30 cycles	827645.9	822305.9297			
Sak 2hr 40 cycles	0	0			
GAPDH 2hr 32 cycles	1112043	1106702.555			
Sak 2hr 42 cycles	0	0			
GAPDH 4hrs 28 cycles	94147.57	88807.625			
Sak 4hr 38 cycles	0	0			
GAPDH 4hrs 30 cycles	233369.7	228029.7422			
Sak 4hr 40 cycles	0	0			
GAPDH 4hrs 32 cycles	655216.4	649876.4922			
Sak 4hr 42 cycles	0	0			
GAPDH 6hrs 28 cycles	77240.42	71900.47656			
Sak 6hr 38 cycles	0	0			
GAPDH 6hrs 30 cycles	285871.3	280531.3672			
Sak 6hr 40 cycles	0	0			
GAPDH 6hrs 32cycles	632169.5	626829.5547			
Sak 6hr 42 cycles	0	0			
GAPDH 8hrs 28 cycles	122619.5	117279.5703			
Sak 8hr 38 cycles	0	0			
GAPDH 8hrs 30 cycles	239956.8	234616.8828			
Sak 8hr 40 cycles	0	0			
GAPDH 8hrs 32 cycles	564296.4	558956.4297			
Sak 8hr 42 cycles	0	0			

Appendix H: Densitometry Values for Heterozygous MEFs Exposed to Ultraviolet Radiation Cont.

background	Raw vol. 9821.264	Raw vol.- background	Sak:GAPDH ratio	GAPDH:Sak ratio	Relative Expression
GAPDH control 28 cycles	477466.8	467645.4863	0.142538868	7.015630296	1
Sak 38 control cycles	76478.92	66657.6582	0.178140694	5.613540504	1
GAPDH control 30 cycles	940679.9	930858.6113	0.160177941	6.243056902	1
Sak control 40 cycles	175645.1	165823.7988			
GAPDH control 32 cycles	1495702	1485881.111			
Sak control 42 cycles	247826.6	238005.377			
GAPDH 0hr 28 cycles	363923.9	354102.6738			
Sak 0hr 38 cycles	0	0			
GAPDH 0hr 30 cycles	726161	716339.7363			
Sak 0hr 40 cycles	0	0			
GAPDH 0hr 32 cycles	1050719	1040897.486			
Sak 0hr 42 cycles	0	0			
GAPDH 1/2hr 28 cycles	758847.9	749026.6738			
Sak 1/2hr 38 cycles	0	0			
GAPDH 1/2hr 30 cycles	1422505	1412683.736			
Sak 1/2hr 40 cycles	0	0			
GAPDH 1/2hr 32 cycles	1705247	1695425.361			
Sak 1/2 42 cycles	0	0			
GAPDH 1hr 28 cycles	865052.7	855231.4238			
Sak 1hr 38 cycles	0	0			
GAPDH 1hr 30 cycles	1385855	1376033.236			
Sak 1hr 40 cycles	0	0			
GAPDH 1hr 32 cycles	1677178	1667356.361			
Sak 1hr 42 cycles	0	0			
GAPDH 2hr 28 cycles	614887.5	605066.2363			
Sak 2hr 38 cycles	0	0			
GAPDH 2hr 30 cycles	1057177	1047355.736			
Sak 2hr 40 cycles	0	0			
GAPDH 2hr 32 cycles	1533491	1523669.986			
Sak 2hr 42 cycles	0	0			
GAPDH 4hrs 28 cycles	691883.3	682062.0488			
Sak 4hr 38 cycles	0	0			
GAPDH 4hrs 30 cycles	725901.1	716079.7988			
Sak 4hr 40 cycles	0	0			
GAPDH 4hrs 32 cycles	1068194	1058373.111			
Sak 4hr 42 cycles	0	0			
GAPDH 6hrs 28 cycles	492708.2	482886.9238			
Sak 6hr 38 cycles	0	0			
GAPDH 6hrs 30 cycles	835678.1	825856.7988			
Sak 6hr 40 cycles	0	0			
GAPDH 6hrs 32cycles	1069042	1059220.861			
Sak 6hr 42 cycles	0	0			
GAPDH 8hrs 28 cycles	501955.1	492133.7988			
Sak 8hr 38 cycles	0	0			
GAPDH 8hrs 30 cycles	723000.5	713179.2363			
Sak 8hr 40 cycles	0	0			
GAPDH 8hrs 32 cycles	891402.1	881580.7988			
Sak 8hr 42 cycles	0	0			

Appendix H: Densitometry Values for Heterozygous MEFs Exposed to Ultraviolet Radiation Cont.

	Mean Relative Expression	Standard Error of Mean
GAPDH control 28 cycles	1	0
Sak control 38 cycles		
GAPDH control 30 cycles	1	0
Sak control 40 cycles		
GAPDH control 32 cycles	1	0
Sak control 42 cycles		
GAPDH 0hr 28 cycles	0	0
Sak 0hr 38 cycles		
GAPDH 0hr 30 cycles	0	0
Sak 0hr 40 cycles		
GAPDH 0hr 32 cycles	0	0
Sak 0hr 42 cycles		
GAPDH 1/2hr 28 cycles	0	0
Sak 1/2 38 cycles		
GADPH 1/2hr 30 cycles	0	0
Sak 1/2hr 40 cycles		
GAPDH 1/2hr 32 cycles	0	0
Sak 1/2hr 42 cycles		
GAPDH 1hr 28 cycles	0	0
Sak 1hr 38 cycles		
GAPDH 1hr 30 cycles	0	0
Sak 1hr 40 cycles		
GAPDH 1hr 32 cycles	0	0
Sak 1hr 42 cycles		
GAPDH 2hr 28 cycles	0	0
Sak 2hr 38 cycles		
GAPDH 2hr 30 cycles	0	0
Sak 2hr 40 cycles		
GAPDH 2hr 32 cycles	0	0
Sak 2hr 42 cycles		
GAPDH 4hr 28 cycles	0	0
Sak 4hr 38 cycles		
GAPDH 4hr 30 cycles	0	0
Sak 4hr 40 cycles		
GAPDH 4hr 32 cycles	0	0
Sak 4hr 42 cycles		
GAPDH 6hr 28 cycles	0	0
Sak 6hr 38 cycles		
GAPDH 6hr 30 cycles	0	0
Sak 6hr 40 cycles		
GAPDH 6hr 32 cycles	0	0
Sak 6hr 42 cycles		
GAPDH 8hr 28 cycles	0	0
Sak 8hr 38 cycles		
GAPDH 8hr 30 cycles	0	0
Sak 8hr 40 cycles		
GAPDH 8hr 32 cycles	0	0
Sak 8hr 42 cycles		

Appendix I: Apoptosis Values for TUNEL Assay

Time Point	Slide	# of apoptotic cells	# of cells counted	% of cells apoptotic	average % of apoptotic cells	Standard Error of Average
Positive Control Wild Type	Wild type #1	200	200	100	100	0
	Wild type #2	200	200	100		
	Wild type #	200	200	100		
Positive Control Heterozygous	Het #1	200	200	100	100	0
	Het #2	200	200	100		
	Het #3	200	200	100		
Negative Control Wild Type	Wild type #1	0	200	0	0	0
	Wild type #2	0	200	0		
	Wild type #3	0	200	0		
Negative Control Heterozygous	Het #1	0	200	0	0	0
	Het #2	0	200	0		
	Het #3	0	200	0		
0hr post UV Wild Type	Wild type #1	0	200	0	0	0
	Wild type #2	0	200	0		
	Wild type #3	0	200	0		
0hr post UV Heterozygous	Het #1	0	200	0	0	0
	Het #2	0	200	0		
	Het #3	0	200	0		
1hr post UV Wild Type	Wild type #1	0	200	0	0	0
	Wild type #2	0	200	0		
	Wild type #3	0	200	0		
1hr post UV Heterozygous	Het #1	0	200	0	0	0
	Het #2	0	200	0		
	Het #3	0	200	0		
2hr post UV Wild Type	Wild type #1	27	200	13.5	9	2.254624876
	Wild type #2	13	200	6.5		
	Wild type #3	14	200	7		
2hr post UV Heterozygous	Het #1	12	200	6	6.166666667	1.589898669
	Het #2	7	200	3.5		
	Het #3	18	200	9		
4hr post UV Wild Type	Wild type #1	38	200	19	18.5	1.322875656
	Wild type #2	41	200	20.5		
	Wild type #3	32	200	16		
4hr post UV Heterozygous	Het #1	30	200	15	18.33333333	1.763834207
	Het #2	38	200	19		
	Het #3	42	200	21		
6hr post UV Wild Type	Wild type #1	52	200	26	27.5	2.843120352
	Wild type #2	47	200	23.5		
	Wild type #3	66	200	33		
6hr post UV Heterozygous	Het #1	63	200	31.5	36.5	3.818813079
	Het #2	68	200	34		
	Het #3	88	200	44		
8hr post UV Wild Type	Wild type #1	123	200	61.5	64	1.322875656
	Wild type #2	129	200	64.5		
	Wild type #3	132	200	66		
8hr post UV Heterozygous	Het #1	145	200	72.5	64.66666667	4.044887033
	Het #2	118	200	59		
	Het #3	125	200	62.5		

Appendix J: Expression Levels of Down-Regulated Genes in Heterozygous MEFs

Change in Expression

Developmental

Procollagen, type III, alpha 1   -4.6364

Procollagen, type V, alpha 2   -4.1420

Oral-facial-digital syndrome 1 gene homolog   -3.0782

Procollagen, type I, alpha 2   -2.9648

Metabolism

Stearoyl-Coenzyme A desaturase 2   -2.4729

Unknown Function

Mus musculus mVL30-1 retroelement mRNA sequence   -2.5566

Transmembrane protein 34   -2.5241

Mus musculus 0 day neonate cerebellum cDNA   -2.3000

Hypothetical protein LOC639390   -2.2121

Appendix K: Expression Levels of Up-Regulated Genes in Heterozygous MEFs

	Change in Expression		Change in Expression
Cell Cycle		**Metabolism**	
Casein kinase II	5.8040	N-acylsphingosine amidohydrolase (acid ceramidase) like	6.0539
Protein phosphatase 1F (PP2C domain containing)	4.8644	Leucyl/cystinyl aminopeptidase	4.8539
Squamous cell carcinoma antigen recognized by T-cells	4.6888	Galactose-4-epimerase	4.7700
Origin recognition complex, subunit 4-like	4.5661	L-2-hydroxyglutarate dehydrogenase	4.6257
Inhibitor of DNA binding 2	4.4323	Fatty acid desaturase 3	4.2976
Protein phosphatase 5	4.0765	Carbohydrate sulfotransferase 2	4.2926
Prohibitin	3.0459	Stearoyl-Coenzyme A desaturase 1	3.9806
Cyclin dependent kinase 8	3.0094	CCR4 carbon catabolite repression like 4	3.7939
Phosphatidylinositol 3-kinase	2.1636	protein kinase, cAMP dependent regulatory, type I beta	3.3199
Pituitary tumor-transforming 1	1.9518		
Heterogeneous nuclear ribonucleoprotein C	2.5962	**DNA Repair**	
heme binding protein 2	3.8955	Thymine DNA glycosylase	2.0156
TVMSFG fibroblast growth factor receptor 1 precursor	2.2643	Uracil-DNA glycosylase	4.1846
Neuropilin	3.0956	MutS homolog 6	2.1811
Developmental		**Transcriptional/Translational Regulation**	
Sal-like 3	7.9335	Transcription factor A	2.0680
Transducin-like enhancer of split 1	6.7010	Zinc finger protein 689	3.0464
T-cell factor 4	4.7804	Transmembrane and tetratricopeptide repeat containing	2.2096
Inositol 1,4,5-triphosphate receptor 5	3.6909	GLIS family zinc finger 3	2.6233
Procollagen, type VI, alpha 3	3.5828	Phenylalanine-tRNA synthetase 2	3.0678
Fetal Alzheimer antigen	3.3594	Glutamyl-prolyl-tRNA synthetase	3.3065
WNT1 inducible signaling pathway protein 1	3.2886	Highly similar to CBP_MOUSE CREB-binding protein	3.7483
T-box transcription factor Tbx15	2.9248	Tetratricopeptide repeat domain 1	4.0003
Nuclear factor I/X	2.8883	Cysteinyl -tRNA synthetase	4.8072
Thrombospondin 2	2.5437	Negative elongation factor B	4.2456
Osteopontin	2.4717		
Fukuyama type congenital muscular dystrophy homolog	2.2362		
Nuclear receptor co-repressor 1	4.4658		

Appendix K: Expression Levels of Up-Regulated Genes in Heterozygous MEFs Cont.

	Change in Expression
DNA Methylation	
SET domain ERG-associated histone methyltransferase	2.0889
SAP30 binding protein	2.9834
Miscellaneous Cellular Functions	
Thyroid hormone receptor interactor 11	5.8691
Smg-6 homolog	5.3375
Talin 2	5.2780
Tomoregulin1	5.1116
Syntaxin 18	5.0970
Channel-interacting PDZ domain protein	4.9504
Inositol hexaphosphate kinase 1	4.8086
Multiple PDZ domain protein	4.0596
Myosin heavy chain 10	3.8880
CDC42 effector protein (Rho GTPase binding) 2	3.5581
Zinc finger protein 507	3.4688
Zinc finger protein 689	3.4636
Ring finger protein 11	3.1199
GC-rich sequence DNA-binding factor homolog candidat	3.0984
Villin	2.9808
3-phosphoglycerate dehydrogenase	2.9427
Olfactory receptor 202	2.9278
Discs, large homolog 5	2.9094
2'-phosphodiesterase	2.8426
Heat shock protein 1	2.7243
Similar to crooked neck protein	2.5873
Oxysterol binding protein like protein 9	2.5501
Mitochondrial ribosomal protein L50	2.2540
Proteasome (prosome, macropain) 26S subunit, non-ATl	2.2031
Coiled Coil domain containing 131	6.4372
WD repeat domain 50	4.9252
Spetex-2E protein	4.6574
Zinc Finger Protein 451	4.1537
aarF domain containing kinase 1(Adck1)	3.4641
AHNAK nucleoprotein	3.2688
Arginine/serine-rich coiled-coil 1	2.9404
HD domain containing 3 (Hdcc3)	2.7345
Myotubularin related protein 7	2.4370
NICE-5 protein	2.1272

	Change in Expression
Cellular/Ion Transport	
Pleckstrin	6.0575
Calcium binding and coiled coil domain 1	5.6489
Aquaporin-1	4.4128
Solute carrier family 6	4.4110
Exocyst complex component 3	3.9296
Protein-coupled receptor 19	3.8281
Solute carrier family 39	3.5028
Frequenin homolog	3.1881
Serine Hydrolase like	3.1718
Solute carrier family 14	3.0842
Translocator of inner mitochondrial membrane	2.7129
ATPase, Ca++ transporting, plasma membrane 2	2.4328
Transient receptor potential cation channel, subfamily M,	1.9917

Appendix L: Expression Levels of Down-Regulated Genes in Heterozygous MEFs upon UV Exposure

	Change in Expression
Cell Cycle	
CLIP-associating protein CLASP2 isoform a (Clasp2)	-2.253557
centromere protein P (CENPP)	
tousled-like kinase 1	-2.227575
DNA Damage/DNA Repair	
Rad51-like 3 (RAD51)	
Essential meiotic endonuclease (Eme2)	-2.188290593
excision repair cross-complementing rodent repair deficiency, complementation group 6 (Ercc6)	
Transcription/Translation	
General transcription factor II A, 1 isoform 1 (Gtf2a1)	-2.255575267
Polypyrimidine tract binding protein 2 (Ptbp2)	-2.348106
MIF4G domain containing (Mif4gd)	-2.63721535
	-2.346700133
Cell Signaling	
Phosphatidylinositol-4-phosphate 5-kinase, type II, alpha (Pip5k2a)	-2.235478867
Lymphocyte protein tyrosine kinase (Lck)	
Cellular Transport	
Complement component 3a receptor 1 (C3ar1)	-2.2936206
Membrane-spanning 4-domains, subfamily A, member 4B (Ms4a4b)	-2.23249735
Glutamate receptor, ionotropic, AMPA4 (alpha 4) (Gria4)	-2.1057106
	-3.1265202

	Change in Expression
Developmental	
Developing brain homeobox 1 (Dbx1)	-2.1851174
	-2.271258133
DNA Binding	
	-3.1221408
Thymocyte selection-associated HMG box (TOX)	
Epigenetics	
	-3.2187268
Ring finger protein 20	-2.44656925
	-2.108886433
Metabolism	
Neuraminidase 1 (NEU1)	
Atpase, class VI, type 11C isoform a (Atp11c)	-2.0738409
Phosphodiesterase 3B, cGMP-inhibited (Pde3b)	-2.2659343
DnaJ (Hsp40) homolog, subfamily C, member 1 (Dnajc1)	-2.4006736
Unknown Function	
Testis-specific LRR protein	-2.2464884
(Leucine rich repeat containing 18 (Lrrc18))	-2.520506933
Hypothetical protein LOC236312	
C21orf19-like protein	
Hypothetical protein LOC66132	-2.4551529
Zinc finger protein 655 isoform a (Zfp655)	-3.3053385
	-2.197512433

Appendix M: Expression Levels of Up-Regulated Genes in Heterozygous MEFs upon UV Exposure

Cell Cycle

Gene	Change in Expression
Cell division cell 25B; Cdc25B	2.5406
SCY1-like 1	2.2866
Protein phosphatase 2, regulatory subunit B", alpha; (PPP2R2A)	3.0918
Transcription factor ELYS; AT hook containing transcription factor 1 (Ahctf1)	2.2541

Apoptosis

Gene	Change in Expression
WW domain-containing oxidoreductase (Wwox) (Wox1)	2.9443
CASP2 and RIPK1 domain containing adaptor with death domain (Cradd) (RAIDD)	3.4588
Transducin-like enhancer of split 1; Groucho-Related Gene 1	3.0116
Tumor necrosis factor, alpha-induced protein 3 (A20)	2.0551
Notch gene homolog 2 (Notch2)	2.2404
bromodomain PHD finger transcription factor (Bptf); FETAL ALZHEIMER ANTIGEN	2.1736
forehead box O3a (Foxo3a)	

DNA Damage

Gene	Change in Expression
mitogen activated protein kinase kinase 5 (MAP2K5)	3.0688
Fanconi anemia, complementation group M (Fancm)	2.5016

Tumorigenesis

Gene	Change in Expression
deleted in bladder cancer chromosome region candidate 1 (DBC1)	2.3125
cadherin 6	
Rho-related BTB domain containing 1 (Rhobtb1)	

Epigenetics

Gene	Change in Expression
sal-like protein 3	2.8501
TOX high mobility group box family member 3 (Tox3)	2.7101
Cat eye syndrome critical region protein 2 isoform 9 (Cecr2)	3.3581
synovial sarcoma translocation, Chromosome 18 (Ss18)	3.8073

Transcriptional/Translational Regulation

Gene	Change in Expression
WW domain-containing protein 2	2.6092
avian musculoaponeurotic fibrosarcoma (v-maf) AS42 oncogene homolog	2.4479
phenylalanine-tRNA synthetase 2 (mitochondrial) (Fars2)	3.6890
WW domain-containing protein 4 (Wbp4)	2.0954
GLIS family zinc finger 3 (Glis3)	3.2719
cAMP responsive element binding protein 3 like-2 (Creb3l2)	5.0646
	2.7962

Cellular Signaling

Gene	Change in Expression
Estrogen related receptor, beta (Esrrb)	3.0437
Eukaryotic translation initiation factor 4 gamma, 3 (Eif4g3)	3.7131
Rap guanine nucleotide exchange factor (GEF) 6 (Rapgef6)	5.3918
Unc93 homolog B (Unc93b1)	4.8852
Transmembrane protein 32 (Tmem32)	3.1603
Bassoon protein (BSN; zinc finger protein 231 (ZNF231)	3.8107
RUN and FYVE domain-containing 2 (Rufy2)	2.1824
Nuclear receptor co-repressor 1 (Ncor1)	2.2149
Neurexophilin 2 (Nxph2)	2.2425
RNA-binding region containing protein 2 (Rnpc2) (Caper)	2.2436
Pleckstrin (Plek)	2.2737
Nuclear receptor subfamily 2, group F, member 2 isoform 2	2.2984
Activin receptor IIA (Acvr2a)	2.3460

Appendix M: Expression Levels of Up-Regulated Genes in Heterozygous MEFs upon UV Exposure Cont.

Change in Expression

Metabolism

Gene	Change in Expression
Gamma-aminobutyric acid (GABA-A) receptor, subunit gamma 2 isoform 1	3.1657
Glutathione reductase 1 (Gsr)	5.0787
Leucyl/cystinyl aminopeptidase (Lnpep) (IRAP)	2.2192
Fatty acid desaturase 3 (Fads)	2.5815
Mannosidase alpha class 2B member 2 (Man2b2)	2.8505
Phosphatidylinositol glycan, class A (Piga)	2.0607
ADP-ribosylation factor related protein 2 (Arl15)	2.3679
SH3-domain GRB2-like (endophilin) interacting protein 1 (SGIP1)	2.5040
Dipeptidylpeptidase 8 (Dpp8)	3.7469
Dual specificity phosphatase 27 (Dusp27)	3.7494
Xylosyltransferase I (Xylt1)	

Cellular Transport

Gene	Change in Expression
Protein phosphatase 1F (PP2C domain containing) (Ppm1f)	2.8581
Frequenin homolog (Freq)	2.7558
Myotubularin related protein 10 (Mtmr10)	2.8033
Oxysterol binding protein (Osbp)	2.6583
Ring finger protein 17 (Rnf17)	2.6772

Change in Expression

Developmental

Change in Expression	Gene
2.5693	Thrombospondin 2
2.6765	Frizzled 5 precursor (FZD5)
2.4543	T-cell factor 4 (Tcf4)
2.4122	Stathmin-like 2
2.2077	Odd Oz/ten-m homolog 3 (Odz3)
2.0879	Chemokine-like factor super family 3 (CKLFSF3)
2.0393	Transducin-like enhancer protein 3 isoform 1 (Tle3)
3.1163	ADAMTS-like 3 (Adamtsl3)
3.4002	Angiopoietin-like 2
3.0121	SWI/SNF-related, matrix associated actin dependent regulator of chromatin,
4.7743	subfamily a, containing DEAD/H box 1 (Smarcad1)

Miscellaneous Function

Change in Expression	Gene
2.2304	CDC42 effector protein (Rho GTPase binding) 4 (CDC42EP4) (binder of Rho GTPases)
2.3188	Pleckstrin homology domain containing, family F (with FYVE domain) member 1 (Plekhf1)
2.0461	Similar to high-mobility group box 3
2.1037	CD96 antigen (CD96)
3.0331	FERM, RhoGEF and pleckstrin domain protein 2 (FGD2)
5.3912	Ubiquitin specific protease 31 (Usp31)
3.0801	Kalirin, RhoGEF kinase (Kalrn)
3.4097	DCN1, defective in cullin neddylation 1, domain containing 2 isoform a (Dcun1d2)
3.3178	Villin 1 (Vil)

LITERATURE CITED

Abraham RT. (2001). Cell cycle checkpoint signaling through the ATM and ATR kinases. *Genes Dev.* **15**: 2177-2196.

Aguilar, F., Harris, C.C., Sun, T., Hollstein, M. and Cerutti, P. (1994) Geographic variation of p53 mutational profile in nonmalignant human liver. *Science* **264**: 1317-1319.

Allen T, van Tuyl M, Iyengar P, Jothy S, Post M, Tsao MS, Lobe CG. (2006). Grg1 acts as a lung-specific oncogene in a transgenic mouse model. *Cancer Res.* **66**: 1294-1301.

Ando K, Ozaki T, Yamamoto H, Furuya K, Hosoda M, Hayashi S, Fukuzawa M, Nakagawara A. (2004). Polo-like kinase 1 (Plk1) inhibits p53 function by physical interaction and phosphorylation. *J. Biol. Chem.* **279**: 25549-25561.

Azimzadeh J, Bornens M. (2007). Structure and duplication of the centrosome. *J. Cell Sci.* **120**: 2139-2142.

Avides MC, Tavares AA, Glover DM. (2001). Polo kinase and Asp are needed to promote the mitotic organizing activity of centrosomes. *Nat. Cell. Biol.* **3**: 421-424.

Bakkenist CJ, Kastan MB. (2003). DNA damage activates ATM through intermolecular autophosphorylation and dimmer dissociation. *Nature.* **421**: 499-506.

Bahe S, Stierhof YD, Wilkinson CJ, Leiss F, Nigg EA. (2005). Rootletin forms centriole-associated filaments and functions in centrosome cohesion. *J. Cell Biol.* **171**: 27-33.

Bahler J, Steever AB, Wheatly S, Wang YI, Pringle JR, Gould KL, McCollum D. (1998). Role of polo kinase and Mid1p in determining the site of cell division in fission yeast. *J. Cell Biol.* **143**: 1603-1616.

Bardin AJ, Amon A. (2001). Men and sin: what's the difference? *Nat. Rev. Mol. Cell Biol.* **2**: 815-826.

Bassermann F, Peschel C, Duyster J. (2005). Mitotic entry: a matter of oscillating destruction. *Cell Cycle* **11**: 1515-1517.

Bell S, Klein C, Muller L, Hansen S, Buchner J. (2002). p53 contains large unstructured regions in its native state. *J. Mol. Biol.* **322**: 917-927.

Berger KH, Yaffe MP. (1998). Prohibitin family members interact genetically with mitochondrial inheritance components in *Saccharomyces cerevisiae. Mol. Cell Biol.* **18**: 4043-4052.

Bettencourt-Dias M, Rodrigues-Martins A, Carpenter L, Riparbelli M, Lehmann L, Gatt MK, Carmo N, Balloux F, Callaini G, Glover DM. (2005). Sak/Plk4 is required for centriole duplication and flagella development. *Curr. Biol.* **15**: 2199-2207.

Bonni S, Ganuelas M, Petrinac S, Hudson JW. (2008). Human Plk4 phosphorylates Cdc25c. *Cell Cycle* **7**.

Bowser R, Giambrone A, Davies P. (1995). FAC1, a novel gene identified with the monoclonal antibody Alz50, is developmentally regulated in human brain. *Dev. Neurosci.* **17**: 20-37.

Brassac T, Castro A, Lorca T, Le Peuch C, Doree M, Labbe JC, Galas S. (2000). The polo-like kinase Plx1 prevents premature inactivation of the APC(Fizzy)-dependent pathway in the early Xenopus cell cycle. *Oncogene* **19**: 3782-3790.

Broggini M, Buraggi G, Brenna A, Riva L, Codegoni AM, Torri V, Lissoni AA,Mangioni C, D'Incalci M. (2000). Cell cycle-related phosphatases CDC25A and B expression correlates with survival in ovarian cancer patients. *Anticancer Res.* **20**: 4835-4840.

Brehm A, Miska EA, McCance DJ, Reid JL, Bannister AJ, Kouzarides T. (1998). Retinoblastoma protein recruits histone deactylase to repress transcription. *Nature.* **391**: 597-601.

Brigstock DR. (2003). The CCN family: a new stimulus package. *J. Endocrinol.* **178**: 169-175.

Bugler B, Quaranta M, Aressy B, Brezak MC, Prevost G, Ducommun B. (2006). Genotoxic-activated G2-M checkpoint exit is dependent on CDC25B phosphatase expression. *Mol. Cancer Ther.* **5**: 1446-1451.

Bunz F, Dutriaux A, Lengauer C, Waldman T, Zhou S, Brown JP, Sedivy JM, Kinzler KW, Vogelstein B. (1998). Requirement for p53 and p21 to sustain G2 arrest after DNA damage. *Science.* **282**: 1497-1501.

Burns TF, Fei P, Scata KA, Dicker DT, El-Diery WS. (2003). Silencing of the nole p53 target gene Snk/Plk2 leads to mitotic catastrophe in paclitaxel (taxol)-exposed cells. *Mol. Cell. Biol.* **23**: 5556-5571.

Campisi J. (2001). Cellular senescence as a tumor-suppressor mechanism. *Trends Cell Biol.* **11**: 27-31.

Cangi MG, Cukor B, Soung P, Signoretti S, Moreira G Jr, Ranashinge M, Cady B,Pagano M, Loda M. (2000). Role of the Cdc25A phosphatase in human breast cancer. *J. Clin. Invest.* **106:** 753-761.

Cann KL, Hicks GG. (2006). Absence of an immediate G1/S checkpoint in primary MEFs following γ-irradiation identifies a novel checkpoint switch. *Cell Cycle* **5:** 1823-1830.

Casenghi M, Meraldi P, Weinhart U, Duncan PI, Korner R, Nigg EA. (2003). Polo-like kinase 1 regulates Nlp, a centrosome protein involved in microtubule nucleation. *Dev. Cell* **5:** 113-125.

Cervello M, Giannitrapani L, Labbozzetta M, Notarbartolo M, D'Alessandro N, Lampiasi N, Azzolina A, Montalto G. (2004). Expression of WISPs and of their novel alternative variants in human hepatocellular carcinoma cells. *Ann N Y Acad Sci.* **1028:** 432-439.

Chase D, Golden A, Heidecker G, Ferris DK. (2000). Caenorhabditis elegans contains a third polo-like kinase gene. *DNA Seq.* **11:** 327-334.

Chen X, Cheung ST, So S, Fan ST, Barry C, Higgins J, Lai KM, Ji J, Dudoit S, Ng IO, Van De Rijn M, Botstein D, Brown PO. (2002). Gene expression patterns in human liver cancers. *Mol. Biol. Cell* **13:** 1929-1939.

Cho EA, Dressler GR. (1998). TCF-4 binds beta-catenin and is expressed in distinct regions of the embryonic brain and limbs. *Mech. Dev.* **77:** 9-18.

Clute P, Pines J. (1999). Temporal and spatial control of cyclin B1 destruction in metaphase. *Nat. Cell Biol.* **1:** 82-87.

Conn CW, Hennigan RF, Dai W, Sanchez Y, Stambrook PJ. (2000). Incomplete cytokinesis and induction of apoptosis by overexpression of the mammalian polo-like kinase, Plk3. *Cancer Res.* **60:** 6826-6831.

Dai W, Li Y, Ouyang B, Pan H, Reissmann P, Li J, Wiest J, Stambrook P, Gluckman JL, Noffsinger A, Bejarano P. (2000). PRK, a cell cycle gene localized to 8p21, is downregulated in head and neck cancer. *Genes Chromosome Cancer* **27:** 332-336.

Dai W, Liu T, Wang Q, Rao CV, Reddy BS. (2002). Down-regulation of PLK3 gene expression by types and amount of dietary fat in rat colon tumors. *Int. J. Oncol.* **20:** 121-126.

Dai W, Cogswell JP. (2003). Polo-like kinases and the microtubule organizing centre: targets for cancer therapies. *Prog. Cell Cycle Res.* **5:** 327-334.

Dameron KM, Volpert OV, Tainsky MA, Bouck N. (1994). Control of angiogenesis in fibroblasts by p53 regulation of thrombospondin-1. *Science.* **265**: 1582-1584.

Dawe HR, Farr H, Gull K. (2007). Centriole/basal body morphogenesis and migration during ciliogenesis in animal cells. *J. Cell Sci.* **120**: 7-15.

de Carcer G, Avides MDC, Lallena MJ, Glover DM, Gonzalez C. (2001). Requirement of Hsp90 for centrosomal function reflects its regulation of polo kinase stability. *EMBO* **11**: 2878-2884.

Dell'Orco RT, McClung JK, Jupe ER, Liu XT. (1996). Prohibitin and the senescent phenotype. *Exp. Gerontol.* **31**: 245-252.

Donohue PJ, Alberts GF, Guo Y, Winkles JA. (1994). A delayed-early gene activated by fibroblast growth factor-1 encodes a protein related to aldose reductase. *J. Biol. Chem.* **269**: 8604-8609.

Donohue PJ, Alberts GF, Guo Y, Winkles JA. (1995). Identification of targeted differential display of an immediate early gene encoding a putative serine/threonine kinase. *J. Biol. Chem.* **270**: 10351-7.

Duncan PI, Pollet N, Niehrs C, Nigg EA. (2001). Cloning and characterization of Plx2 and Plx3, two additional Polo-like kinases from Xenopus laevis. *Exp. Cell Res.* **270**: 78-87.

Duggan DJ. Bittner M, Chen Y, Meltzer P, Trent JM. (1999). Expression profiling using cDNA microarrays. *Nat. Genet.* **21**: 10-14.

Eckerdt F, Yuan J, Strebhardt K. (2005). Polo-like kinases and oncogenesis. *Oncogene* **24**: 267-276.

Efeyan A, Serrano M. (2007). p53: guardian of the genome and policeman of the oncogenes. *Cell Cycle.* **9**: 1006-1010.

Elia AE, Cantley LC, Yaffe MB. (2003). Proteomic screen finds pSer/pThr-binding domain localizing Plk1 to mitotic substrates. *Science* **299**:1228-31.

Elledge SJ. (1996). Cell cycle checkpoints: preventing an identity crisis. *Science* **274**: 1664-1672.

Farmer G, Friedlander P, Colgan J, Manley JL, Prives C. (1996). Transcriptional repression by p53 involves molecular interactions distinct from those with the TATA box binding protein. *Nucleic Acids Res.***24**: 4281–4288.

Feng Y, Hodge DR, Palmieri G, Chase DL, Longo DL, Ferris DK. Association of polo-like kinase with alpha-, beta-, and gamma-tubulins in a stable complex. *J. Biochem.* **339**: 435-442.

Fenton B, Glover DM. (1993). A conserved mitotic kinase active at late anaphase-telophase in syncytial Drosophila embryos. *Nature* **363**: 637-640.

Ferguson AM, White LS, Donovan PJ, Piwnica-Worms H. (2005). Normal cell cycle and checkpoint responses in mice and cells lacking Cdc25B and Cdc25C protein phosphatases. *Mol. Cell Biol.* **7**: 2853-2860.

Fletcher L, Cerneglia GJ, Nigg EA, Yen TJ, Muschel RJ. (2004). Inhibition of centrosome segregation after DNA damage: a role for NEK2. *Radiat. Res.* **162**: 128-135.

Fletcher L, Muschel R. (2006). The centrosome and the DNA damage induced checkpoint. *Cancer Lett.* **243**: 1-8.

Fode C, Motro B, Yousefi S, Heffernan M, Dennis JW. (1994). Sak, a murine protein-serine/threonine kinase that is related to the Drosophila polo kinase and involved in cell proliferation. *Proc. Natl. Acad. Sci.* **91**:6388-6392.

Fode C, Binkert C, Dennis JW. (1996). Constitutive expression of murine Sak-a suppresses cell growth and induces multinucleation. *Mol. Cell. Biol.* **16**: 4665-4672.

Freiderich E, Vancompernolle K, Louvard D, Vandekerchkove J. (1999). Villin function in the organization of the actin cytoskeleton. Correlation of in vivo effects to its biochemical activities in vitro. *J. Biol. Chem.* **274**: 26751-26760.

Fusaro G, Dasgupta P, Rastogi S, Joshi B, Chellappan S. (2003). Prohibitin induces the transcriptional activity of p53 and is exported from the nucleus upon apoptotic signaling. *J. Biol. Chem.* **278**: 47853-47861.

Gasparotto D, Maestro R, Piccinin S, Vukosavljevic T, Barzan L, Sulfaro S, Boiocchi M. (1997). Overexpression of CDC25A and CDC25B in head and neck cancers. *Cancer Res.***57**:2366-2368.

Gautier J, Solomon MJ, Booher RN, Bazan JF, Kirschner MW. (1991). Cdc25 is a specific tyrosine phosphatase that directly activates p34cdc2. *Cell* **67**: 197-211.

Glover DM. (2005). Polo kinase and preogression through M phase in *Drosophila*: a perspective from the spindle poles. *Oncogene* **24**: 230-237.

Golan A, Yudkovsky Y, Hershko A. (2002). The cyclin-ubiquitin ligas activity of cyclosome/APC is jointly activated by protein kinases Cdk1-cyclin B and Plk1. *J. Biol. Chem.* **277**: 15552-15557.

Golsteyn RM, Schultz SJ, Bartek J, Ziemiecki A, Reid T, Nigg EA. (1994). Cell cycle analysis and chromosomal localization of human Plk1, a putative homologue of the mitotic kinases Drosophila polo and Saccharomyces cerevisiae Cdc5. *J. Cell Sci.* **107**: 1509-1517.

Golsteyn RM, Mundt KE, Fry AM, Nigg EA. (1995). Cell cycle regulation of the activity and subcellular localization of Plk1, a human protein kinase implicated in mitotic spindle function. *J. Biol. Chem.* **129**: 1617-28.

Golsteyn RM, Lane HA, Mundt KE, Arnaud L, Nigg EA. (1996). The family of polo-like kinases *Prog Cell Cycle Res.* **2**: 107-114.

Gonzalez C, Sunkel CE, Glover DM. (1998). Interactions between mgr, asp, and polo: asp function modulated by polo and needed to maintain the poles of monopolar and bipolar spindles. *Chromosoma.* **107**: 452-460.

Gottlob K, Majewski N, Kennedy S, Kandel E, Robey RB, Hay N. (2001). Inhibition of early apoptotic events by Akt/PKB is dependent on the first committed step of glycolysis and mitochondrial hexokinase. *Genes & Dev.* **15**: 1406-1418.

Gruneberg U, Nigg EA. (2003). Regulation of cell division: stop the SIN! *Trends Cell Biol.* **13**: 159-162.

Habedanck R, Stierhof YD, Wilkinson CJ, Nigg EA. (2005). The polo kinase Plk4 functions in centriole duplication. *Nat. Cell. Biol.* **11**: 1140-46.

Hanisch A, Wehner A, Nigg EA, Sillje HH. (2006). Different Plk1 functions show distinct dependencies on Polo-Box domain-mediated targeting. *Mol. Biol. Cell* **17**: 448-451.

Hernandez S, Hernandez L, Bea S, Cazorla M, Fernandez PL, Nadal A, Muntané J, Mallofré C, Montserrat E, Cardesa A, Campo E. (1998). Cdc25 cell cycle-activating phosphatases and c-myc expression in human non-hodgkin's lymphomas. *Cancer Res.* **58**: 1762-1767.

Hirao A, Kong Y, Matsuoka S, Wakeham S, Ruland J. (2000). DNA damage-induced activation of p53 by the checkpoint kinase Chk2. *Science.* **287**: 1824-1827.

Holtrich U, Wolf G, Yuan J, Beretier-Hahn J, Karn T, Weiler M, Kauselmann G, Rehli M, Andreesen R, Kaufmann M, Kuhl D, Stebhardt K. (2000). Adhesion induced expression of the serine/threonine kinase Fnk in human macrophages. *Oncogene.* **19**: 4832-9.

Hu Y, Benedict MA, Wu D, Inohara N, Nunex G. (1998). Bcl-XL interacts with Apaf-1 and inhibits Apaf-1 dependent caspase-9 activation. *Proc. Natl. Acad. Sci.* **95**: 4386-4391.

Hubscher U, Maga G, Spadari S. (2002). Eukaryotic DNA polymerases. *Annu. Rev. Biochem.* **71**: 133-63.

Hudson JW, Chen LY, Fode C, Binkert C, Dennis JW. (2000). Sak kinase gene structure and transcriptional regulation. *Gene* **241**: 65-73.

Hudson JW, Kozarova A, Cheung P, Macmillan JC, Swallow CJ, Cross JC, Dennis JW. (2001). Late mitotic failure in mice lacking Sak, a polo-like kinase. *Curr. Biol.* **11**: 441-446.

Jang YL, Lin CY, Ma S, Erikson RL. (2002). Functional studies on the role of the C-terminal domain of mammalian polo-like kinase. *Proc. Natl. Acad. Sci.* **99**: 1984-1989.

Jiang N, Wang X, Jhanwar-Uniyal M, Darzynkiewicz Z, Dai W. (2006). Polo box domain of Plk3 functions as a centrosome localization signal, overexpression of which causes mitotic arrest, cytokinesis defects, and apoptosis. *J. Biol. Chem.* **281**: 10577-10582.

Jimenez J, Cid VJ, Cenamor R, Yuste M, Molero G, Nombela C, Sanchez M. (1998). Morphogenesis beyond cytokinetic arrest in Saccharomyces cerevisiae. *J. Cell Biol.* **143**: 1617-1634.

Jin S, Fan F, Fan W, Zhao H, Tong T, Blanck P, Alomo I, Rajasekaran B, Zhan Q. (2001). Transcription factors Oct-1 and NF-YA regulate the p53-independent induction of the GADD45 following DNA damage. *Oncogene* **20**: 2683-2690.

Jordan-Sciutto KL, Dragich JM, Rhodes JL, Bowser R. (1999). Fetal Alz-50 clone 1, a novel zinc finger protein, binds a specific DNA sequence and acts as a transcriptional regulator. *J. Biol. Chem.* **274**: 35262-35268.

Kauselmann G, Weiler M, Wulff P, Jessberger S, Konietzko U, Scafidi J, Staubli U, Bereiter-Hahn J, Strebhardt K, Kuhl D. (1999). The polo-like kinases Fnk and Snk associate with a Ca(2+)- and integrin-binding protein and are regulated dynamically with synaptic plasticity. *Embo J.* **18**: 5528-39.

Kharbanda S, Pandey P, Schofield L, Israels S, Roncinske R, Yoshia K, Bharti A, Yuan ZM, Saxena S, Weichselbaum R. (1997). Role of Bcl-xL as an inhibitor of cytosolic cytochrome C accumulation in DNA damage-induced apoptosis. *Proc. Natl. Acad. Sci.* **94**: 6939-6942.

Kennedy SG, Kandel ES, Cross TK, Hay N. (1999). Akt/protein kinase B inhibits cell death by preventing the release of cytochrome c from mitochondira. *Mol. Cell. Biol.* **19**: 5800-5810.

Kim JS, Shukla SD. (2006). Acute in vivo effect of ethanol (binge drinking) on histone H3 modifications in rat tissues. *Alcohol Alcohol.* **41**: 126-132.

Kleylein-Sohn J, Westendorf J, Le Clech, M Habedanck R, Stierhof YD, Nigg EA. (2007). Plk4-induced centriole biogenesis in human cells. *Dev. Cell.* **13**: 190-202.

Kneisel L, Strebhardt K, Bernd A, Wolter M, Binder A, Kaufmann R. (2002). Expression of polo-like kinase (PLK1) in thin melanomas: a novel marker of metastatic disease. *J. Cutan. Pathol.* **29**: 354-358.

Ko MA, Rosario CO, Hudson JW, Kulkarni S, Pollett A, Dennis JW, Swallow CJ. (2005). Plk4 haploinsufficiency causes mitotic infidelity and carcinogenesis. *Nat. Genetics.* **37**: 883-888.

Kohlhase J, Hausmann S, Stojmenovic G, Dixhens C, Bink K, Schulz-Schaeffer W, Altmann M, Engel W. (1999). SALL3, a new member of the human spalt-like gene family, maps to 18q23. *Genomics* **62**: 216-222.

Kotani S, Tugendreich S, Fujii M, Jorgenson PM, Watanabe N, Hoog C, Hieter P, Todokoro K. (1998). PKA and MPF-activated polo-like kinase regulate anaphase-promoting complex activity and mitosis progression. *Mol. Cell* **1**: 371-380.

Kristjansdottir K, Rudolph J. (2004). Cdc25 phosphatases and cancer. *Chem. Biol.* **11:** 1043-1051.

Kudo Y, Yasui W, Ue T, Yamamoto S, Yokozaki H, Nikai H, Tahara E. (1997). Overexpression of cyclin-dependent kinase-activating CDC25B phosphatase in human gastric carcinomas. *Jpn. J. Cancer Res.* **88:** 947-952.

Kumagai A, Dunphy WG. (1996). Purification and molecular cloning of Plx1, a Cdc25-regulatory kinase from Xenopus egg extracts. *Science* **273**: 1377-1380.

Kuzmichev A, Zhang Y, Erdjument-Bromage H, Tempst P, Reinberg D. (2002). Role of the Sin3-histone deacetylase complex in growth regulation by the candidate tumor suppressor p33(ING1). *Mol. Cell Biol.* **22**: 835-848.

Lam MH, Rosen JM. (2004). Chk1 versus Cdc25: chking one's levels of cellular proliferation. *Cell Cycle.* **11**: 1355-1357.

Lane H, Nigg EA. (1996). Antibody microinjection reveals an essential role for human polo-like kinase 1 (Plk1) in the functional maturation of mitotic centrosomes. **135**: 1701-1713.

Lau LF, Lam SC. (1999). The CCN family of angiogenic regulators: the integrin connection. *Exp. Cell. Res.* **248**: 44-57.

Lee HC, Kim M, Wands JR. (2006). Wnt/Frizzled signaling in hepatocellular carcinoma. *Front Biosci.* **11**: 1901-1915.

Lee KS, Park JE, Asano S, Park CJ. (2005). Yeast polo-like kinases: functionally conserved multitask mitotic regulators. *Oncogene.* **24**: 217-229.

Lee KS, Yuan YL, Kuriyama R, Erikson RL. (1995). Plk is a M-phase-specific protein kinase and interactswith a kinesin-like protein, CHO1/MKLP-1. *Mol. Cell Biol.* **15**: 7143-7151.

Leung GC, Hudson JW, Kozarova A, Davidson A, Dennis JW, Sicheri F. (2002). The Sak polo-box comprises a structural domain sufficient for mitotic subcellular localization. *Nat. Struct. Biol.* **9**: 719-24.

Leung GC, Hudson JW, Kozarova A, Davidson A, Dennis JW, Sicheri F. (2002). The Sak polo-box comprises a structural domain sufficient for mitotic subcellular localization. *Nature Structural Biology.* **9**: 719-724.

Li B, Ouyang B, Pan H, Reissmann PT, Slamon DJ, Arceci R, Lu L, Dai W. (1996). Prk, a cytokine-inducible human protein serine/threonine kinase whose expression appears to be down-regulated in lung carcinomas. *J. Biol. Chem.* **271**: 19402-19408.

Li J, Tan M, Li L, Pamarthy D, Lawrence TS, Sun Y. (2005). Sak, a new polo-like kinase, is transcriptionally repressed by p53 and induces apoptosis upon RNAi silencing. *Neoplasia.* **7**: 312-323.

Li JF, Liu LD, Ma SH, Che YC, Wang LC, Dong CH, Zhao HL, Liao Y, Li QH. (2004). HTRP--an immediate-early gene product induced by HSV1 infection in human embryo fibroblasts, is involved in cellular co-repressors. *J. Biochem.* **136**: 169-176.

Lipshutz RJ, Fodor SPA, Gingeras TR, Lockhart D. (1999). High density synthetic oligonucleotide arrays. *Nat. Genet.* **21**: 20-24.

Liu Y, Dehni J, Purcell KJ, Sokolow J, Carcangiu ML, Artavanis-Tsakonas A, Stifani S. (1996). Epithelial expression and chromosomal location of human TLE genes: implications for notch signaling and neoplasia. **31**: 58-64.

Lowe SW, Sheer CJ. (2003). Tumor suppression by Ink4a-Arf: progress and puzzles. *Curr. Opin. Genet. Dev.* **13**:77-83.

Lui F, Stanton JJ, Wu Z, Piwnica-Worms H. (1997). The human Myt1 kinase preferentially phosphorylates Cdc2 on threonine 14 and localizes to the endoplasmic reticulum and Golgi complex. *Mol. Cell Bio.* **17**: 571-83.

Liu X, Erikson RL. (2002). Activation of Cdc2/cyclin B and inhibition of centrosome amplification in cells depleted of Plk1 by siRNA. *Proc. Natl. Acad. Sci.* **99**: 8672-8676.

Liu X, Erikson RL. (2003). Polo-like kinase (Plk)1 depletion induces apoptosis in cancer cells. *Proc. Natl. Acad. Sci.* **100**: 5789-5794.

Liu X, Zhou T, Kuriyama R, Erikson RL. (2004). Molecular interactions of Polo-like-kinase 1 with the mitotic kinesin-like protein CHO1/MKLP-1. *J. Cell Sci.* **117**: 3233-3246.

Lowery DM, Lim D, Yaffe MB. (2005). Structure and function of polo-like kinases. *Oncogene* **24**: 248-259.

Macmillan, JC, Hudson, JW, Bull S, Dennis JW, Swallow CJ. (2001). Comparative expression of the mitotic regulators Sak and Plk in colorectal cancer. *Ann. Surg. Oncol.* **8**: 729-740.

Ma S, Charron J, Erikson RL. (2003). Role of Plk2 (Snk) in mouse development and cell proliferation. *Mol. Cell Biol.* **23**: 6936-6943.

Maehara K, Yamakoshi K, Ohtani N, Kubo Y, Takahashi A, Arase S, Jones N, Hara E. (2005). Reduction of total E2F/DP activity induces senescence-like cell cycle arrest in cancer cells lacking functional pRB and p53. *J. Cell Biol.* **168**: 553-560.

Matsuoka S, Huang M, and Elledge SJ. (1998). Linkage of ATM to cell cycle regulation by the Chk2 protein kinase. *Science* **282**, 1893-1897.

Matsuoka S, Rotman G, Ogawa A, Shiloh Y, Tamai K, Elledge SJ. (2000). Ataxia telangiectasia-mutated phosphorylates Chk2 in vivo and in vitro. *Proc. Natl. Acad. Sci.* **97**: 10389-10394.

Mayor T, Stierhof YD, Tanaka K, Fry AM, Nigg EA. (2000). The centrosomal protein C-Nap1 is required for cell cycle-regulated centrosome cohesion. *J. Cell Biol.* **147**: 1371-1378.

Martindell DM, Risebro CA, Smart N, Franco-Viseras M, Rosario CO, Swallow CJ, Dennis JW, Riley PR. (2007). Nucleolar release of Hand1 acts as a molecular switch to determine cell fate. *Nat. Cell. Biol.* **10**: 1131-41.

Matsumoto Y, Hayashi K, Nishida E. (1999). Cyclin-dependent kinase 2 (Cdk2) is required for centrosome duplication in mammalian cells. *Curr. Biol.* **9**: 429-432.

Matsuoka S, Rotman G, Ogawa A, Shiloh Y, Tamai K, Elledge SJ. (2000). Ataxia telangiectasia-mutated phosphorylates Chk2 in vivo and in vitro. *Proc. Natl. Acad. Sci.* **97**: 10389-10394.

McGowan CH, Russell P. (1993). Human Wee1 kinase inhibits cell division by phosphorylating p34cdc2 exclusively on Tyr15. *EMBO J.* **12**: 75-85.

Meijers-Heijboer H, Van den Ouweland A, Klijn J, Wasielewski M, de Snoo A, Oldenburg R, Hollestelle A, Houben A, Crepin E, van Veghel-Plandsoen M, Elstrodt F, van Duijn C, Bartels C, Meijers C, Schutte M, McGuffog L, Thompson D, Easton DF, Sodha N, Seal S, Barfoot R, Mangion J, Chang-Claude J, Eccles D, Eeles R, Evans DG, Houlston R, Murday V, Narod S, Peretz T, Peto J, Phelan C, Zhang HX, Szabo C, Devilee P, Goldgar D, Futreal PA, Nathanson KL, Weber BL, Rahman N & Stratton MR. (2002). Low-penetrance susceptibility to breast cancer due to CHEK2(*)1100delC in noncarriers of BRCA1 or BRCA2 mutations. *Nat. Genet.* **31**: 55-59.

Midorikawa Y, Tsutsumi S, Taniguchi H, Ishii M, Kobune Y, Kodama T, Makuuchi M, Aburatani H. (2002). Identification of genes associated with dedifferentiation of hepatocellular carcinoma with expression profiling analysis. *Jpn. J. Cancer Res.* **93**: 636-643.

Moshe Y, Boulaire J, Pagano M, Hershko A. (2004). Role of polo-like kinase in the degradation of early mitotic inhibitor 1, a regulator of the anaphase promoting complex/cyclosome. *Proc. Natl. Acad. Sci.* **101**: 7937-7942.

Moutinho-Santos T, Sampaio P, Amorim I, Costa M, Sunkel CE. (1999). In vivo localization of the mitotic polo kinase shows a highly dynamic association with the mitotic apparatus during early embryogenesis in *Drosophila. Biol. Cell* **91**: 585-596.

Mulvihill DP, Peterson J, Ohkura H, Glover DM Hagan IM. (1999). Plo1 kinase recruitment to the spindle pole body and its role in cell division in Schizosaccharomyces pombe. *Mol. Biol. Cell* **10**: 2771-2785.

Narita M, Nunez S, Heard E, Lin AW, Hearn SA, Spector DL, Hannon GJ, Lowe SW. (2003) Rb-mediated heterochromatin formation and silencing of E2F target genes during cellular senescence. *Cell* **113**: 703-716.

Nicholson KM, Anderson NG. (2002). The protein kinase B/Akt signaling pathway in human malignancy. *Cell. Signal.* **14**: 381-395.

Neef R, Preisinger C, Sutcliffe J, Kopajtich R, Nigg EA, Mayer TU, Barr FA. (2003). Phosphorylation of mitotic kinesin-like protein 2 by polo-like kinase 1 is required for cytokinesis. *J. Cell Biol.* **162**: 863-875.

Nigg EA. (2007). Centrsome duplication: of rules and licenses. *Trends Cell. Biol.* **17**: 215-221.

Niiya F, Tatsumoto T, Lee KS, Miki T. (2005). Phosphorylation of the cytokinesis regulator ECT2 at G2/M phase stimulates association of the mitotic kinase Plk1 and accumulation of GTP-bound RhoA. *Oncogene* **25**: 827-837.

Nishioka K, Doki Y, Shiozaki H, Yamamoto H, Tamura S, Yasuda T, Fujiwara Y, Yano M, Miyata H, Kishi K, Nakagawa H, Shamma A, Monden M. (2001). Clinical significance of CDC25A and CDC25B expression in squamous cell carcinomas of the oesophagus. *Br. J. Cancer* **85**: 412-421.

Ohkura H, Hagan IM, Glover DM. (1995). The conserved Schizosaccharomyces pombe kinase plo1, required to form a bipolar spindle, the actin ring, and septum, can drive septum formation in G_1 and G_2 cells. *Genes Dev.* **9**: 1059-1073.

Ouyang B, Pan H, Lu L, Li J, Stanbrook P, Li B, Dai W. (1997). Human Prk is a conserved protein serine/threonine kinase involved in regulating M phase functions. *J. Biol. Chem.* **272**: 28646-28651.

Ouyany B Wang Y Dai W. (1999). Caenorhabditis elegans contains structural homologs of human prk and plk. *DNA Seq.* **2**: 109-113.

Pabla N, Huang S, Mi QS, Daniel R, Dong Z. (2007). ATR-Chk2 signaling in p53 activation and DNA damage response during cisplatin-induced apoptosis. *J. Biol. Chem.* Manuscript in Press.

Pan G, O'Rourke K, Dixit VM. (1998). Caspase-9, Bcl-Xl, and Apaf-1 form a ternary complex. *J. Biol. Chem.* **273**: **5841**-5845.

Parrish M, Ott L, Lance-Jones C, Schuetz G, Schwaeger-Nickolenko A, Monaghan AP. (2004). Loss of the Sall3 gene leads to palate deficiency, abnormalities in cranial nerves, and perinatal lethality. *Mol. Cell Biol.* **24**: 7102-7112.

Pennica D, Swanson TA, Welsh JW, Roy MA, Lawrence DA, Lee J, Brush J, Taneyhill LA, Deuel B, Lew M, Watanabe C, Cohen RL, Melhem MF, Finley GG, Quirke P, Goddard AD, Hillan KJ, Gurney AL, Botstein D, Levine AJ. (1998). WISP genes are members of the connective tissue growth factor family that are up-regulated in wnt-1-transformed cells and aberrantly expressed in human colon tumors. *Proc Natl Acad Sci.* **95**: 14717–14722.

Polakis P. (1999). The oncogenic activation of beta-catenin. *Curr. Opin. Genet. Dev.* **9**: 15-21.

Qian YW, Erikson E, Li C, Maller JL. (1998). Activated polo-like kinase Plx1 is required at multiple points during mitosis in Xenopus laevis. *Mol. Cell Biol.* **18**: 4262-71.

Qian YW, Erikson E, Maller JL. (1999). Mitotic effects of a constitutively active mutant of the Xenopus polo-like kinase Plx1. *Mol. Cell Biol.* **19**: 8625-8632.

Qian YW, Erikson E, Taieb FE, Maller JL. (2001). The polo-like kinase Plx1 is required for activation of the phosphatase Cdc25C and cyclin B-Cdc2 in Xenopus oocytes. *Mol. Biol. Cell.* **12**: 1791-99

Rastogi S, Bharat J, Dasgupta P, Morris M, Wright K, Chellappan S. (2006). Prohibitin facilitates cellular senescence by recruiting specific corepressors to inhibit E2F target genes. *Mol. Cell Biol.* **26**: 4161-4171.

Ree AH, Bratland A, Nome RV, StokkeT, Fodstad O. (2003). Repression of mRNA for the PLK cell cycle gene after DNA damage requires BRCA1. *Oncogene* **22**: 8952-8955.

Reimann JD, Freed E, Hsu JY, Kramer ER, Peters JM, Jackson PK. (2001). Emi1 is a mitotic regulator that interacts with Cdc20 and inhibits the anaphase promoting complex. *Cell* **105**: 645-655.

Reynolds N, Ohkura H. (2003) Polo boxes form a single functional domain that mediates interactions with multiple proteins in fission yeast polo kinase. *J. Cell Sci.* **116**:1377-87.

Roshak AK, Capper EA, Imburgia C, Fornwald J, Scott G, Marshall LA. (2000).The human polo-like kinase, PLK, regulates cdc2/cyclin B through phosphorylation and activation of the cdc25C phosphatase. *Cell Signal* **12**:405-11.

Ross JF, Liu X, Dynlacht BD. (1999). Mechanism of transcriptional repression of E2F by the retinoblastoma tumor suppressor protein. *Mol. Cell* **3**: 195-205.

Sakchaisri K, Asano S, Yu LR, Shulewitz MJ, Park CJ, Park JE, Cho YW, Veenstra TD, Thorner J, Lee KS. (2004). Coupling morphogenesis to mitotic entry. *Proc. Natl. Acad. Sci.* **101**: 4124-4129.

Sampaio P, Rebollo E, Varmark H, Sunkel CE, Gonzalez C. (2001). Organized microtubule arrays in gamma-tubulin-depleted Drosophila spermatocytes. *Curr. Biol.* **11**: 1788-1793.

Schmitt E, Paquet C, Beauchemin M, Bertrand R. (2007). DNA-damage response network at the crossroads of cell-cycle checkpoints, cellular senescence and apoptosis. *J. Zhejiang Univ. Sci. B.* **8**: 377-397.

Seong YS, Kamijo K, Lee JS, Fernandez E, Kuriyama R, Miki T, Lee KS. (2002). A spindle checkpoint arrest and a cytokinesis failure by the dominant-negative polo-box domain of Plk1 in U2OS cells. *J. Biol. Chem.* **277**: 32282-93.

Shalon D, Smith SJ, Brown PO. (1996). A DNA microarray system for analyzing complex DNA samples using two-colour fluorescent probe hybridization. *Genome Res.* **7**: 639-645.

Shimizu-Yoshida Y, Sugiyama K, Rogounovitch T, Ohtsuru A, Namba H, Saenko V, Yamashita S. (2001). Radiation-inducible hSNK gene is transcriptionally regulated by p53 binding homology element in human thyroid cells. *Biochem. Biophys. Res. Commun.* **289**: 491-98.

Sibon OCM, Kelkar A, Lemstra W, Theurkauf WE. (2000). DNA replication/DNA damage-dependent centrosome inactivation in Drosophila embryos. *Nat. Cell Biol.* **2**: 90-95.

Silverstein RA, Ekwall K. (2005). Sin3: a flexible regulator of global gene expression and genome stability. *Curr. Genet.* **47**: 1-17.

Simizu S, Osada H. (2000). Mutations in the plk gene lead to instability of Plk protein in human tumour cell lines. *Nat. Cell Biol.* **2**: 852-854.

Simmons DL, Neel BG, Stevens R, Evett G, Erikson RL. (1992). Identification of an early-growth-response gene encoding a novel putative protein kinase. *Mol. Cell Biol.* **12**: 4164-9.

Smith P, Syed N, Crook T. (2006). Epigenetic inactivation implies a tumor suppressor function in hematologic malignancies for Polo-like kinase 2 but not Polo-like kinase 3. *Cell Cycle* **5**: 1262-1264.

Song S, Grenfell TZ, Garfield S, Erikson RL, Lee KS. (2000). Essential function of the polo box of Cdc5 in subcellular localization and induction of cytokinetic structures. *Mol. Cell Biol.* **20**: 286-298.

Southern E, Mir K, Shchepinov M. (1999). Molecular interactions on microarray. *Nat. Genet.* **21**: 5-9.

Stegmeier F, Visintin R, Amon A. (2002). Separase, polo kinase, the kinetochore protein Slk19, and Spo12 function in a network that controls Cdc14 localization during early anaphase. *Cell* **108**: 207-220.

Strachan GD, Ostrow LA, Jordan-Sciutto KL. (2005). Expression of the fetal Alz-50 clone 1 protein induces apoptotic cell death. *Biochem. Biophys. Res. Commun.* **336**: 490-495.

Strober BE, Dunaief JL, Goff SP. (1996). Functional interactions between the hBRM/hBRG1 transcriptional activators and the pRB family of proteins. *Mol. Cell Biol.* **16**: 1576-1583.

Swallow CJ, Ko MA, Siddiqui NU, Hudson JW, Dennis JW. (2005). Sak/Plk4 and mitotic fidelity. *Oncogene.* **24**: 306-312.

Su F, Overholtzer M, Besser D, Levine AJ. (2002). WISP-1 attenuates p53-mediated apoptosis in response to DNA damage through activation of the Akt kinase. *Genes Dev.* **16**: 46-57.

Sunkel, CE, Glover DM. (1988). Polo, a mitotic mutant of Drosophila displaying abnormal spindle poles. *J. Cell Sci.* **89**: 25-38.

Takemasa I, Yamamoto H, Sekimoto M, Ohue M, Noura S, Miyake Y, Matsumoto T,Aihara T, Tomita N, Tamaki Y, Sakita I, Kikkawa N, Matsuura N, Shiozaki H, Monden. (2000). Overexpression of CDC25B phosphatase as a novel marker of poor prognosis of human colorectal carcinoma. *Cancer Res.* **60**: 3043-3050.

Takekawa M, Saito H. (1998). A family of stress-inducible GADD45-like proteins mediate activation of the stress-responsive MTK1/MEKK4 MAPKKK. *Cell* **95**: 521-530.

Tanaka S, Sugimachi K, Saeki H, Kinoshita J, Ohga T, Shimada M, Maehara Y, Sugimachi K. (2001). A novel variant of *WISP1* lacking a Von Willebrand type C module overexpressed in scirrhous gastric carcinoma. *Oncogene.* **20**: 5525-5532.

Tanaka S, Sugimachi K, Kameyama T, Maehara S, Shirabe K, Shimada M, Wands JR, Maehara Y. (2003). Human WISP1v, a member of the CCN family, is associated with invasive cholangiocarcinoma. *Hepatology* **37**: 1122-1129.

Tang J, Erikson RL, Liu X. (2006). Checkpoint kinase1 (Chk1) is required for mitotic progression through negative regulation of polo-like kinase 1. *Proc. Natl. Acad. Sci.* **103**: 11964-69.

Toyoshima-Morimoto F, Taniguchi E, Nishida E. (2002). Plk1 promotes nuclear translocation of human Cdc25C during prophase. *EMBO Rep.* **3**: 341-8.

Tsou M-FB, Stearns T. Mechanism limiting centrosome duplication to once per cell cycle. *Nature* **442**: 947-957.

Tsvetkov L, Xu X, Li J, Stern DF. (2003). Polo-like kinase 1 and Chk2 interact and co-localize to centrosomes and the midbody. *J. Biol. Chem.* **278**: 8468-8475.

Vandel L, Nicolas E, Vaute O, Ferreira R, Ait-Si-Ali S, Trouche D. (2001). Transcriptional repression by the retinoblastoma protein through the recruitment of a histone methyltransferase. *Mol. Cell Biol.* **21**: 6484-6494.

Van de Weerdt BCM, Medema, RH. (2005). Polo-Like Kinases: A team in control of the division. *Cell Cycle.* **8**: 853-864.

Van Vugt MA, Smits VA, Klompmaker R, Medema RH. (2001). Inhibition of Polo-like kinase 1 by DNA damage occurs in an ATM- or ATR-dependent fashion. *J Biol. Chem.* **276**: 41650-60.

Van Vugt MA, Bras A, Medema RH. (2004) Polo-like kinase-1 controls recovery from a G2 DNA-damage-induced arrest in mammalian cells. *Mol. Cell* **15**: 799-811.

Volpert OV, Dameron KM, Bouck N. (1997) Sequential development of an angiogenic phenotype by human fibroblasts progressing to tumorigenicity. *Oncogene* **14**: 1495-1502.

Wakefield JG, Bonaccorsi S, Gatti M. (2001). The drosophila protein asp is involved in microtubule organization during spindle formation and cytokinesis. *J. Cell Biol.* **153**: 637-648.

Wang Q, Xie S, Chen J, Fukasawa K, Naik U, Traganos F, Darzynkiewicz Z, Jhanwar-Uniyal M, Dai W. (2002). Cell cycle arrest and apoptosis induced by human Polo-like kinase 3 is mediated through perturbation of microtubule integrity. *Mol. Cell. Biol.* **22**: 3450-3459.

Wang S, Nath N, Adlam M, Chellappan S. (1999). Prohibitin, a potential tumor suppressor, interacts with Rb and regulates E2F function. *Oncogene.* **18**: 3501-3510.

Wang S, Fusaro G, Padmanabhan J, Chellappan SP. (2002). Prohibitin co-localizes with Rb in the nucleus and recruits N-CoR and HDAC1 for transcriptional repression. *Oncogene.* **21**: 8388-8396.

Wang XW, Zhan Q, Coursen JD, Khan MA, Kontny HU, Yu L, Hollander MC, O'Conner PM, Fornace Jr AJ, Harris CC. (1999). GADD45 induction of G2/M cell cycle checkpoint. *Proc. Natl. Acad. Sci.* **96**: 3706-3711.

Warnke S, Kemmler S, Hames RS, Tsai, HL, Hoffmann-Rohrer U, Fry AM, Hoffmann I. (2004). Polo-like kinase-2 is required for centriole duplication in mammalian cells. *Curr. Biol.* **14**: 1200-1207.

Watanabe N, Arai H, Nishihara Y, Taniguchi M, Watanabe N, Hunter T, Osada H. (2004). M-phase kinases induce phospho-dependent ubiquitination of somatic Wee1 by SCFbeta-TrCP. *Proc. Natl. Acad. Sci.* **101**:4419-24.

Weichert W, Schmidt M, Gekeler V, Denkert C, Stephan C, Jung K, Loening S, Dietel M, Kristiansen G. (2004). Polo-like kinase 1 is overexpressed in prostate cancer and linked to higher tumor grades. *Prostate* **60**: 240-245.

Wolf G, Hildenbrand R, Schwar C, Grobholz R, Kaufmann M, Stutte HJ, Strebhardt K, Bleyl U. (2000). Polo-like kinase: a novel marker of proliferation: correlation with estrogen-receptor expression in human breast cancer. *Pathol. Res. Pract.* **196**: 753-759.

Wu W, Fan YH, Kemp BL, Walsh G, Mao L. (1998). Overexpression of cdc25A and cdc25B is frequent in primary non-small cell lung cancer but is not associated with overexpression of c-myc. *Cancer Res.* **58**: 4082-4085.

Xie D, Nakachi K, Wang H, Elashoff R, Koeffler HP. (2001). Elevated levels of connective tissue growth factor, WISP-1, and CYR61 in primary breast cancers associated with more advanced features. *Cancer Res.* **61**: 8917-8923.

Xie S, Wu H, Wang Q, Cogswell JP, Husain I, Conn C, Stambrook P, Jhanwar-Uniyal M, Dai W. (2001). Plk3 functionally links DNA damage to cell cycle arrest and apoptosis at least in part via the p53 pathway. *J. Biol. Chem.* **276**: 43305-43312.

Xie S, Xie B, Lee MY, Dai W. (2005). Regulation of cell cycle checkpoints by polo-like kinases. *Oncogene.* **24**: 277-86.

Xu L, Corcoran RB, Welsh JW, Pennica D, Levine AJ. (2000). Wisp1 is a Wnt1 and β-catenin responsive oncogene. *Genes Dev.* **14**: 585-595.

Yan X, Chua M, He J, So SK. (2008). Small interfering RNA targeting CDC25B inhibits liver tumor growth in vitro and in vivo. *Mol. Cancer* **7**: Manuscript in Press.

Yarm FR. (2002). Plk phosphorlylation regulates the microtubule stabilizing protein TCTP. *Mol. Cell Biol.* **22**: 6209-6221.

Zhan Q, Bae I, Kastan MB, Fornace Jr AJ. (1994). The p53- dependent gamma-ray response to GADD45. *Cancer Res.* **54**: 2755-2760.

Zhan Q, Fan S, Smith ML, Bae I, Yu K, Alamo Jr I, O'Conner PM, Fornace Jr AJ. (1996). Abrogation of p53 function affect gadd gene responses to DNA base-damaging agents and starvation. *DNA Cell Biol.* **15**: 805-815.

Zhan Q. (2005). Gadd45a, a p53- and BRCA1-regulated stress protein, in cellular response to DNA damage. *Mutat Res.* **569**: 133-143.

Zhang W, Fletcher L, Muschel RJ. (2005). The role of polo-like kinase in the inhibition of centrosome separation after ionizing radiation. *J. Biol. Chem.* **280**: 42994-42999.

Zhang Y, LeRoy G, Seelig HP, Lane WS, Reinberg D. (1998) The dermatomyositis-specific autoantigen Mi2 is a component of a complex containing histone deacetylase and nucleosome remodeling activities. *Cell* **95**: 279–289.

Zhang Y, Sun Z, Iratni R, Erdjument-Bromage H, Tempst P, Hampsey M, Reinberg D. (1998). SAP30, a novel protein conserved between human and yeast, is a component of a histone deacetylase complex. *Mol. Cell.* **1**: 1021-1031.

Zhao DH, Hong JJ, Guo SY, Yang RL, Yuan J, Wen CY, Zhou KY, Li CJ. (2004). Aberrant expression and function of TCF4 in the proliferation of hepatocellular carcinoma cell line BEL-7402. *Cell Res.* **14**: 74-80.

Zhou T, Aumais JP, Liu X, Yu-Lee LY, Erikson RL. (2003). A role for Plk1 phosphorylation of NudC in cytokinesis. *Dev. Cell* **5**: 127-138.

Zimmerman WC, Erikson RL. (2006). Polo-like kinase 3 is required for entry into S phase. *Proc. Natl. Acad. Sci.* **104**: 1847-1852.

VITA AUCTORIS

NAME: Alan James Morettin

PLACE OF BIRTH: Sault Ste. Marie, ON

YEAR OF BIRTH: 1980

EDUCATION: St. Mary's College, Sault Ste. Marie, Ontario
1994-1999
Lake Superior State University, Sault Ste. Marie, MI
1999-2003 B.Sc.
University of Windsor, Windsor, Ontario
2005-2008 M.Sc.